Title: Neural circuitry of dialects through social learning in Drosophila.

Authors: Balint Z Kacsoh, Julianna Bozler, Sassan Hodge, and Giovanni Bosco*

Affiliation:

Department of Molecular and Systems Biology, Geisel School of Medicine at Dartmouth, Hanover, NH, 03755, USA.

*Corresponding author: (GB) giovanni.bosco@dartmouth.edu

Running Title: Circuitry in Drosophila social learning.

Key Words

- *D. melanogaster*
- Learning and memory
- Long-term memory
- Behavior
- Neural circuitry
- Neurobiology
- Drosophila species
- Olfaction
- Vision
- Fan-shaped body

ABSTRACT

Drosophila species communicate the presence of parasitoid wasps to naïve individuals. This observation suggests a rudimentary Drosophila social structure. Communication between closely related species is efficient, while more distantly related species exhibit a dampened, partial communication. Partial communication between some species is enhanced following a period of cohabitation, suggesting that species-specific variations in communication "dialects" can be learned through social interactions. However, it remains unclear as to how the behavioral acquisition and how learning dialects is facilitated by distinct brain regions. In this study, we have identified six regions of the Drosophila brain essential for dialect learning, including the odorant receptor Or69a. Furthermore, we pinpoint subgroups of neurons such as motion detecting neurons in the optic lobe, layer 5 of the fan-shaped body, and the D glomerulus in the antennal lobe, where activation of each are necessary for dialect learning. These results demonstrate that Drosophila can display complex social behaviors with inputs to multiple regions of the Drosophila brain and unique subsets of neurons that must integrate olfactory, visual and motion cues.

INTRODUCTION

The ability to decipher, unravel, and react to environmental information is a phenomenon found throughout all life forms. Organisms benefit from receiving information regarding stressors and/or advantageous environmental conditions. From bacteria to plants and to mammals, information transfer can occur within and between species. Social communication is most extensively documented in more complex organisms such as mammals and birds. However, insects can also display a broad range of sociality. When one observes insect groups in nature, their

behavior readily reveals distinct planes of cooperation, communication, and social structure (Wilson, 1997). Eusocial insects provide insight to a high level of complex social structure. For example, one can observe honeybees gathering nectar from a flowerbed. While this might seem a rudimentary and relatively simple behavior, this forager was guided to this particular flower by nest mates' dance, which contains symbolic information about distance, direction, and food source quality (Beekman et al, 2006, Breed et al, 2004, Chittka & Geiger, 1995, Crist, 2004, Gould, 1974). Ants also demonstrate a highly complex social structure comprised of multiple castes and accompanying behavior (Hölldobler & Wilson, 2009, Wilson, 1983, Wilson, 1971). In some species, when a queen has recently been lost, worker ants begin to antenna-duel for the prize of becoming the new queen. The winner converts into a queen, acquires an extended lifespan, and becomes reproductively active by means of epigenetic changes(Yan et al, 2017). This queen contest is dependent on many social cues and interactions including winning the antenna duel, but also acceptance of winners and losers. Clearly, multiple signals must be shared among individual ants for a queen to suppress workers from becoming a queen, while, in the absence of a queen, different inputs allow for only one worker to become a queen.

Drosophila melanogaster, in conjunction with other Drosophila species, have provided insights into a wide array of biological processes, including the mechanisms of learning, memory, and other multifaceted behaviors (Bier, 2005, Helfand & Rogina, 2003). The once canonically "asocial" fruit fly can be utilized to study rudimentary social interactions, including social learning where information transfer occurs between two individuals (Battesti et al, 2012). Another fundamental study of sociality in Drosophila is the behavior and associated neural circuitry of mating (Lebreton et al, 2017a). Mating requires recognition of a receptive individual by visual and olfactory cues. Machine learning has been employed to demonstrate the ability of Drosophila to

use the visually distinct features of other individuals to determine identity within a group setting—an important finding supporting the possibility that a rudimentary social structure exists in Drosophila (Schneider et al, 2018). Oviposition site and food selection are also driven by social exchange mediated by olfactory cues and neural processing (Lin et al, 2015). Recent work has also demonstrated the importance of the communal aspect of the Drosophila lifecycle involving tumor-genesis, where Drosophila are able to discriminate between individuals at different stages of tumor progression and prefer social environments of flies without tumors (Dawson et al, 2018). It has also been suggested that social learning in Drosophila can lead to persistent mate-choice reminiscent of cultural transmission, and that such choices can in turn be inherited through social learning from one generation to the next (Danchin et al, 2018, Danchin et al, 2010). Thus, there is mounting experimental evidence that Drosophila could be useful as models for understanding genetic and neurophysiological mechanisms of social learning as well as evolution of social structures.

Adult Drosophila across the genus have been in an arms race against predators and have subsequently evolved complex immune and behavioral changes to protect their offspring from endoparasitoid wasps. These wasps can prey on immature stages of larvae of certain Drosophilid species (Bozler et al, 2017, Driessen et al, 1989, Edmondson & Wyburn, 1963, Fleury et al, 2004, Kacsoh & Schlenke, 2012, Kacsoh et al, 2014a, LaSalle, 1993, Mortimer et al, 2012, Mortimer et al, 2013, Rizki, 1957, RIZKI & RIZKI, 1959, Schlenke et al, 2007a, Wigglesworth, 1959). These behavioral changes include, but are not limited to, an altered food preference and reduced oviposition (egg-laying) (Kacsoh et al, 2018a, Kacsoh et al, 2018b, Kacsoh et al, 2013, Kacsoh et al, 2015a, Kacsoh et al, 2015c, Kacsoh et al, 2017, Lefevre et al, 2012). The wasp predator threat triggers social transference of information between experienced and naïve individuals. Wasp-

exposed teacher flies communicate the wasp threat to naïve flies through visual cues (Kacsoh et al, 2015c), followed by naïve student flies then depressing their own egg-laying rate. This communication can occur within a species, but it also occurs between related species. Closely related species demonstrate an efficient level of communication. A dampened, or partial communicative ability is observed when more distantly related species are paired (Kacsoh et al, 2018b). Very distantly related species lack the ability to communicate. Remarkably, the observed partial communication between some species is alleviated following a cohabitation period where an exchange of visual and olfactory signals is enabled. This observation is highly suggestive of natural variations in modes of communication, similar to the evolution of linguistic variations between species, termed "dialects" (Kacsoh et al, 2018b, Manak, 2018).

Each of the behaviors outlined above is achieved with a brain the size of a grain of sand, yet, these Drosophila demonstrate a remarkable level of neuronal plasticity influenced by life history and socialization (Avarguès-Weber et al, 2011, Chittka & Niven, 2009, Dyer, 2012, Dyer, 1996, Giurfa, 2003, Greggers & Menzel, 1993, Srinivasan, 2010, Zhang, 2012, Zhang et al, 2007). In ants, bees, and even Drosophila, we are privileged to not only see how complex societies evolve independently of humans, but also to dissect, with ever increasing clarity, the relationship between advanced social order, the forces of natural selection that shaped them, and the underlying neuro-genetic, epigenetic, and genetic mechanisms that guide these behaviors.

In this study we focus on neural circuitry of dialect learning in the Drosophila system: Interspecies dialect learning, unlike intraspecies social learning, is multi-modal, requiring, at minimum, olfactory, visual, sex-specific, temporal, neuronal, and ionotropic cues for successful dialect acquisition (Kacsoh et al, 2018b, Kacsoh et al, 2015c). Considering the ecological niches of Drosophila, where these insects do not exist in a monoculture, brings to the forefront the highly

social nature of these insects(Markow, 2015). Using this fly-fly social learning paradigm, we asked: (1) what neuronal groups are required for interspecies dialect learning; (2) what is the subset of neurons in a given neuronal structure that is necessary for the behavior; and (3) what is the subset of neurons in a given neuronal structure that is sufficient, when activated, to drive dialect learning.

RESULTS

DIALECT LEARNING IS GOVERNED BY MULTIPLE BRAIN REGIONS

In order to ascertain communication ability, we utilized the fly duplex. The fly duplex is an apparatus with two transparent acrylic compartments allowing one to test whether *D. ananassae* responds to seeing predators (acute response) and if exposed "teacher" female flies can communicate this threat to naïve unexposed *D. melanogaster* "student" female flies (Kacsoh et al, 2015c). The fly duplex allows flies to see other flies or wasps in the adjacent compartment, without direct contact, making communication exclusively visual (Figure 1 A). We place ten female and two male *D. ananassae* into one duplex compartment, with an adjacent compartment containing (or not for control) twenty female wasps. Following a 24-hour exposure, wasps are removed and acute response is measured by counting the number of eggs laid in the first 24-hour period in a blinded manner. Flies are shifted to a new duplex, with ten female and two male *D. melanogaster* naïve student flies in the adjacent compartment (Figure 1 A, see methods). Subsequent to a second 24-hour period, all flies are removed and the response of both teacher and student is measured by counting the number of eggs laid in a blinded manner (see methods). The 24-48-hour period measures memory of teachers having seen the wasps and students having learned from the teachers. As previously shown, using wild-type *D. anananassae*, we find both an acute response

and a memory response to the wasp in teacher flies and a partial learned response in naïve *D. melanogaster* student flies (Supplementary Figure 1, Supplementary File 1 for all raw egg counts and p values) (Kacsoh et al, 2018b, Kacsoh et al, 2015c, Lefevre et al, 2012, Lynch et al, 2016). We define partial communication as oviposition depression of students paired with wasp-exposed teachers being ~50-65% of unexposed flies and statistically non-significant from the ~50% oviposition rate. Next, we recapitulated a previous finding demonstrating the ability of *D. melanogaster* to enhance its communication ability with *D. ananassae* following a weeklong cohabitation termed "dialect learning" (Supplementary Figure 1) (Kacsoh et al, 2018b). We define this enhanced communication ability as egg-laying by students paired with wasp-exposed teachers being ~10-30% compared to unexposed and statistically different from ~50% oviposition rate. Using this paradigm, we wished to elucidate the neural circuitry that governs this complex behavior by individually deactivating defined subsets of neurons in an inducible fashion. Understanding dialect learning, storage, and retrieval requires a fundamental knowledge of the underlying neuronal circuits, which is currently unknown.

In order to identify brain regions that govern dialect learning, we utilized the FlyLight database, from which we selected GAL4 drivers that marked singular structures both strongly and ubiquitously (Jenett et al, 2012a). The FlyLight GAL4 lines were generated by insertion of defined fragments of genomic DNA that serve as a transcriptional enhancer. We selected 9 brain structures to analyze: the optic lobe, mushroom body, antennal lobe, lateral horn, fan-shaped body, ellipsoid body, prow, superior clamp, and the bulb (Couto et al, 2005a, Hsu & Bhandawat, 2016, Yu et al, 2013). If available, we obtained two unique driver lines matching our selection criteria. Using mCD8-GFP as a reporter, immunofluorescence reveals GFP expression constrained to these regions of interest, justifying these lines for further testing (Supplementary Figures 2-15 A-B).

Following identification of GAL4-driver lines marking unique brain structures, we utilized Gal4-mediated expression of the temperature sensitive *shibire*, UAS-shibire^{ts} (UAS-shi^{ts}) in order to inducibly deactivate defined subsets of motion sensing neurons during dialect training (Kitamoto, 2001). Dialect training was performed at either the restrictive (30ºC) or permissive (22ºC) temperatures, after which trained or naïve *D. melanogaster* were paired with either unexposed or wasp-exposed *D. ananassae* at the permissive temperature only (Figure 1 A). This experimental setup means that only during the dialect training period is there an activation of the UAS-shi^{ts} construct, and subsequent inactivation of a defined region of interest (Figure 1 B). Wild-type flies demonstrate normal dialect learning ability and untrained states when incubated at either 22ºC or 30ºC for one week, indicating temperature shifts alone during the cohabitation period do not adversely affect dialect learning (Supplementary Figure 1). Additionally, outcrossed UAS-shi^{ts} (UAS-shi^{ts}/+) demonstrate wild-type untrained and dialect-trained states at both the restrictive and permissive temperatures (Figure 1 C-D).

Previous results have demonstrated that visual system and mushroom body (MB) are required for dialect learning (Kacsoh et al, 2018b). This was demonstrated by dialect training (cohabitation) in the dark, resulting in no dialect learning. In addition, the GAL4 Gene-Switch system to transiently express tetanus toxin light chain (UAS-TeTx) specifically in the MB of *D. melanogaster* (to inhibit synaptic transmission during dialect training) also resulted in no dialect learning (Kacsoh et al, 2018b, Mao et al, 2004). Recent work has also highlighted direct neural pathways, which convey visual information from the optic lobe to the MB (Vogt et al, 2016). As a proof of concept of our experimental design, we tested two optic lobe and MB drivers in conjunction with UAS-shi^{ts}. Since previous observations indicated both MB and visual system function were essential for dialect learning, the expectation was that temperature induced

inactivation of both brain regions should recapitulate observations acquired with UAS-TeTx. When dialect training is performed at the restrictive temperature, both optic lobe and MB Gal4 lines driving expression of UAS-shi^{ts} result in perturbed dialect learning (Supplementary Figures 2-5). This was true for two unique Gal4 driver lines for each MB and optic lobe regions, while at the permissive temperature flies were exhibited wild-type dialect learning (Supplementary Figures 2-5). These results validate our experimental approach, further suggesting that dialect learning is in part governed by visual inputs and MB-dependent learning and memory circuitry (Aso et al, 2014, Takemura et al, 2017).

Using the approach where we utilize Gal4-mediated expression of UAS-shi^{ts}, we identify four additional brain regions that govern dialect learning, where we see perturbed dialect learning at the restrictive temperature: the antennal lobe (Supplementary Figure 6-7), lateral horn (Supplementary Figure 8), fan-shaped body (Supplementary Figure 9-10), and ellipsoid body (Supplementary Figure 11-12). We find three regions, the bulb (Supplementary Figure 13), prow (Supplementary Figure 14), and superior clamp (Supplementary Figure 15), whose activation is dispensable for dialect learning. Collectively, we identify 6 regions of the brain that require activation during dialect learning (Figure 1 E), and 3 regions that do not (Figure 1 F). The finding that 3 structures could be inactivated and still result in dialect learning suggests that inactivation of any brain structure is not sufficient to perturb dialect learning. This further suggests that the regions we did identify are important and are appropriate candidates for further circuit dissection.

DIALECT LEARNING IS PARTIALLY MEDIATED BY OR69A

Following the observation that the antennal lobe is required for dialect learning (Supplementary Figures 6-7), we wished to further dissect this brain region and identify a more

precise series of neurons and possible pheromone candidates involved in dialect learning. Previous data has demonstrated a role for *Orco* in dialect learning—specifically that *Orco* function is a necessary during dialect training (Kacsoh et al, 2018b). The majority of olfactory receptors in Drosophila require a co-receptor for wild-type function, including *Orco* (Or83b) for odorant receptors (Larsson et al, 2004). In nature, Drosophila can utilize volatiles to transmit information across both long and short distances (Greenfield, 1981, Wicker-Thomas, 2007, Wyatt, 2014, Wyatt, 2010). Given this observation, we wished to identify a more specific odorant receptor that is necessary for dialect learning and the accompanying glomerulus that is enervated.

The Drosophila olfactory system is comprised of four sensillum classes—antennal trichoids, antennal basiconics, antennal coeloconics, and palp basiconics. These detectors are present on the third antennal segment and the maxillary palp (Figure 2 A). Housed within these sensillar classes are olfactory sensory neurons (OSNs), of which there are approximately 1300, that project from sensilla to innervate the glomeruli of the antennal lobe (Figure 2 A) (Vosshall et al, 1999, Vosshall et al, 2000, Vosshall, 2001, Vosshall & Hansson, 2011). Olfactory glomeruli are morphologically conserved, spherical compartments of the olfactory system located in the antennal lobe. These 52 glomeruli are distinguishable by their chemosensory repertoire, position, and volume. Glomeruli receive information regarding olfactory detecting from responses originating from OSNs in the sensilla (Grabe et al, 2016). Individual OSNs express only one receptor gene in conjunction with the *Orco* co-receptor, providing specificity. Detected information is then subsequently relayed to other regions of the brain, i.e. to the mushroom body signaling to the lateral horn by projection neurons. OSNs are housed in each of the four sensilla classes (Fishilevich & Vosshall, 2005).

We utilized the current knowledge of the Drosophila olfactory system to identify potential olfactory receptor candidates that might be involved in dialect learning. In particular, we identify Or47b, Or65a, and Or69a as potential candidates, which have been demonstrated to play a role in other social interaction based assays (Lebreton et al, 2017b, Lone & Sharma, 2012, van Naters, Wynand van der Goes & Carlson, 2007). The glomeruli enervated by each of the Ors respective OSNs are also marked in both antennal lobe drivers we utilized previously, making them suitable candidates (Supplementary Figure 6-7).

The sensillum that houses the Or47b receptor enervates the VA1lm glomerulus of the Drosophila antennal lobe (Supplementary Figure 16 D, F) (Fishilevich & Vosshall, 2005). Previous studies have demonstrated that Or47b receptor and receptor neurons are necessary for social-sexual interactions, such as locomotor activity and nocturnal sex drive (Lone & Sharma, 2012). Or47b in males drives responses to virgin females, and in females drives responses to male cuticular extract (van Naters, Wynand van der Goes & Carlson, 2007). Given that both males and females are required in dialect learning (Kacsoh et al, 2018b), we hypothesized that Or47b would be a suitable candidate for testing. We find that flies mutant in Or47b ($Or47b^{-/-}$) and RNAi ($Or47b^{RNAi}$) expressing *D. melanogaster* targeting Or47b using an Or47b-GAL4 results in wild-type dialect learning, suggesting that dialect learning is not directly mediated by Or47b (Supplementary Figure 16 E, G).

The sensillum that houses the Or65a receptor enervates the DL3 glomerulus of the Drosophila antennal lobe (Figure 2 A, Supplementary Figure 16 H) (Fishilevich & Vosshall, 2005). Previous studies have demonstrated that the Or65a receptor and receptor neuron is involved in mate recognition. In particular, Or65a responds to 11-cis-Vaccenyl acetate (cVA), a male-specific lipid that is present on male genital material (van Naters, Wynand van der Goes & Carlson,

2007). cVA is utilized as both an attractant pheromone to an oviposition site as well as a means to dampen female mating receptivity following copulation (Datta et al, 2008, Kurtovic et al, 2007, Laturney & Billeter, 2016). We hypothesized that his complex interaction between males and females could be co-opted in dialect learning, including testing the possibility of involvement of the *fruitless* neural circuitry. We find that RNAi (Or65a^{RNAi}) expressing *D. melanogaster* targeting Or65a using an Or65a-GAL4 results in wild-type dialect learning, suggesting that dialect learning is not directly mediated by Or65a, and most likely not primarily mediated by the fruitless circuit (Supplementary Figure 16 I).

Or69a is expressed in the third antennal segment (Figure 2 C-D, Supplementary Figure 16 A). Or69a has been recently deorphanized and identified to be involved in long-range, species-specific pheromone detection as well as food detection (Lebreton et al, 2017b). This dual function likely evolved as there are two isoforms of Or69a—Or69aA and Or69aB (Lebreton et al, 2017b). The sensillum that houses the Or69a receptor enervates the D glomerulus of the Drosophila antennal lobe via the ab9A OSN (Figure 2 A-B) (Couto et al, 2005a, Fishilevich & Vosshall, 2005). The compounds detected by this receptor is the cuticular hydrocarbon *Z4-11A1* that acts as a species identifier in both sexes (i.e. *D. melanogaster* is attracted but *D. simulans* is repelled). Additionally, this receptor binds kairomonal terpenoids, such as linalool or terpineol, which are found in both fruit and yeast headspace, suggesting food and oviposition site detection (Lebreton et al, 2017b). We find that flies mutant in Or69a (Or69a$^{-/-}$) and RNAi (Or69a^{RNAi}) expressing *D. melanogaster* targeting Or69a using an Or69a-GAL4 results in perturbed dialect training (Figure 2 E-F). Outcrossed UAS and GAL4 lines demonstrate wild-type dialect learning (Supplementary Figure 16 B-C). This suggests that Or69a is an essential mediator of dialect learning.

Collectively, our more in-depth analysis into the role of antennal lobe neural circuitry and its associated olfactory receptors in dialect learning reveals the role of Or69a as an olfactory receptor involved in dialect learning during communal living. Or69a has been previously demonstrated to have a dual affinity for both sex and food odorants, in a species-specific manner. Our data provide further evidence of complex integration of pheromonal cues in Drosophila that involve integration of social and habitat derived cues. We also rule out Or47b and Or65a receptors, both previously demonstrated to be involved in other social interactions. We also identify the OSN that enervates the D glomerulus in the antennal lobe as part of the neural circuit governing dialect learning.

DIALECT LEARNING IS MEDIATED BY MOTION-DETECTING CIRCUITRY

Given our finding that the optic lobe is necessary for dialect learning, we wished to further dissect this brain region and identify a more precise neuron subset. In Drosophila, motion detection requires synaptic outputs of the R1-R6 photoreceptors. These photoreceptors project their axons into the first optic neuropil, known as the lamina. This projection forms a retinotopic map of visual space (Heisenberg & Buchner, 1977, Heisenberg & Wolf, 1979, Wardill et al, 2012, Yamaguchi et al, 2008). This map is comprised of 800 columnar elements, within which R1-R6 make synaptic connections with three projection neurons. These three neurons are the lamina monopolar neurons L1, L2, and L3, as well as a local interneuron, known as amc (Figure 3 A) (Meinertzhagen & O'neil, 1991, Rivera-Alba et al, 2011). Each of these neurons has been shown to respond to different types of inputs. The L1 neuron has been shown to provide input to a pathway that detects moving light edges, while the L2 neurons provides input into a pathway that detects moving dark edges(Clark et al, 2011, Joesch et al, 2010, Joesch et al, 2013). The L3 neuron is thought to inform

landmark orientation and spectral preference (Rister et al, 2007a). L1-L3 neurons represent all of the direct second order relays from R1-R6 into the medulla. Interestingly, L2 makes synaptic contacts with a third order monopolar cell, L4, which has been proposed to be involved in motion sensing, given its morphology and connectivity, though not definitively shown (Figure 3 A) (Braitenberg, 1970, Meinertzhagen & O'neil, 1991, Silies et al, 2013, Strausfeld & Campos-Ortega, 1973, Strausfeld & Campos-Ortega, 1977, Takemura et al, 2017, Zhu et al, 2009).

Previous data suggests that a moving visual cue, provided by wing movement, is detected by Drosophila in the dialect-training period (Kacsoh et al, 2018b). Given this observation, we wondered whether motion-detecting neurons in the optic lobe could be responsible for acquisition of visual information dialect learning. Therefore, we utilized Gal4-mediated expression of the temperature sensitive *shibire*, UAS-shibire^{ts} (UAS-shi^{ts}) in order to inducibly deactivate defined subsets of motion sensing neurons in the optic lobe during dialect training (Kitamoto, 2001). Paired controls were performed where dialect training was conducted at the permissive temperature. We utilized L1-, L2-, and L4-GAL4 lines with strong, but constrained, expression patterns (Figure 3 B, D, F, H and Supplementary Figures 17-20) (Fisher et al, 2015, Silies et al, 2013). Silencing of the L1 motion detecting neuron resulted in wild-type dialect learning, suggesting that activation of the L1 neurons are dispensable for this behavior (Figure 3 C). Silencing of the L2 motion detecting neuron resulted in the inability of *D. melanogaster* to learn the dialect, suggesting that L2 neurons are necessary for this behavior (Figure 3 E). L4 receives most of its synaptic inputs from L2, but is also interconnected with neighboring dorso- and ventroposterior cartridges (Meinertzhagen & O'neil, 1991, Rivera-Alba et al, 2011, Takemura et al, 2017). When we silenced the L4 motion detecting neurons, we find that the ability of *D. melanogaster* to learn the dialect is perturbed, suggesting that L4 neurons are necessary for this behavior (Figure 3 G). Following this result, we

tested a *splitL4-GAL4* line ($L4^{0980}$-VP16AD, $L4^{0987}$-GAL4DBD) (Figure 3 H, Supplementary Figure 20). When using the *splitL4* line in conjunction with UAS-shi^{ts}, we find that the ability of *D. melanogaster* to learn the dialect is perturbed, further solidifying the observation that L4 neuronal activation is necessary for dialect learning (Figure 3 I). This finding uncovers a novel role for the L4 neurons, which have been suggested to be involved in motion detection in spatial summation by anatomical experimentation, but L4 neurons have never been implicated in a specific behavioral paradigm(Silies et al, 2013). Untrained animals at the control and restrictive temperatures behave as wild-type (Supplementary Figure 21).

Given that the L2 and L4 neurons are necessary for dialect learning, we wondered whether they are also sufficient. To ask this question, we expressed a temperature sensitive transient receptor potential A1 (TRPA1)(Kang et al, 2012, Lamaze et al, 2017) channel via a Gal4-mediated expression, confining expression to either the L2 or L4 neurons. Using this construct, neurons can be activated at 30ºC, while the neurons are in their steady state at 22ºC (Supplementary Figure 22 A-B). Outcrossed TRPA1/+ behave as wild-type when trained at either 30ºC or 22ºC (Lamaze et al, 2017)(Supplementary Figure 22 C-D). We activated motion-detecting neurons during the dialect-training period while keeping flies in the dark as a means to test sufficiency (Figure 4 A). Flies were kept in the dark during the training period, but all other sensory stimuli are presumably engaged (i.e. olfactory and mechanosensory interactions). At the thermally inactive temperature (basal activity level), *D. melanogaster* are unable to learn the dialect in the dark, even though the other senses are still engaged (Figure 4 C,G,E), recapitulating previous experiments demonstrating the need for full spectrum light (Kacsoh et al, 2018b). Activation of the either the L1 or L2 motion detecting neuron results in no dialect training, suggesting that activation of these neurons is not sufficient to overcome the lack of visual cues in the dark to elicit dialect learning (Figure 4 B-C).

Surprisingly, we find that activation of the L4 motion detecting neurons results in the ability of *D. melanogaster* to learn the dialect even when in the dark (Figure 4 F-G). Untrained flies behave as wild-type, with no dialect acquisition, when kept at either temperature in the dark (Supplementary Figure 23 B). Given that senses other than visual cues are stimulated when training is performed in the dark, and that activation of the L4 neurons results in dialect learning in the dark experimental setup, we conclude that the activation of L4 neurons is sufficient for dialect learning, but only with respect to the visual circuit.

Collectively, our genetic analysis of the optic lobe neurocircuitry and its involvement in dialect learning reveals that the visual stimulus that is detected during dialect learning is primarily detected by the dark edge detecting L2 circuit that enervates the L4 neuron, both of which are necessary for dialect learning (Figures 3 and 4). When dialect training is performed in the dark, activation of the L4 neuron is sufficient for dialect learning (Figure 4).

DIALECT LEARNING IS MEDIATED BY REGION 5 OF THE FAN-SHAPED BODY

Given our observation that the fan-shaped body is necessary for dialect learning, we wished to further dissect this brain region and identify a more precise neuron subset. The fan-shaped body (FB) is located at a centralized region of the fly brain that is organized into multiple layers. As a member of the central complex(Hanesch et al, 1989), the FB is reported to be important for multiple functions, including control of locomotion(Strauss, 2002), visual feature recognition (Liu et al, 2006) and visual information processing (Weir & Dickinson, 2015), courtship maintenance (Sakai & Kitamoto, 2006), and sleep regulation(Berry et al, 2015, Donlea et al, 2011, Ueno et al, 2012). The FB has been also implicated in the regulation of electric- and heat-shock-induced innate avoidance and conditioned avoidance(Hu et al, 2018). The FB is composed of at least 9 layers(Hu

et al, 2018, Wolff et al, 2015). Given that one can probe distinct layers of the FB, we wondered whether the entire FB or distinct FB regions are involved in dialect learning.

We first focused on the entire FB, followed by subsets of FB neurons, by selecting three GAL4 lines from the FlyLight database (Jenett et al, 2012a). The lines were chosen based on covering either the entirety (39906) or a subset (50007, 40553, 38712) of the FB in addition to labeling few to no other regions of the brain. Using mCD8-GFP as a reporter, immunofluorescence reveals that all FB regions are labeled by 39906 (Figure 5 B, Supplementary Figure 24); regions 5, 8, 9 labeled by 50007 (Figure 5 D, Supplementary Figure 25); regions 2, 8, 9 by 40553 (Figure 5 F, Supplementary Figure 26); and regions 1, 4, 6 by 38712 (Figure 5 H, Supplementary Figure 27). We individually blocked the output of these neurons by expression of UAS-shibire^{ts} (UAS-shi^{ts}) at the restrictive temperature. We find that inactivation of the entire FB, or the sub-regions 5, 8, and 9 with the 50007 driver line, resulted in perturbed dialect learning at the restrictive temperature, but wild-type dialect learning at the permissive temperature (Figure 5 C, E). The untrained state is wild-type at both restrictive and permissive temperatures (Supplementary Figure 28 A-D). Inactivation of regions 2, 8 and 9 with the 40553 driver line and inactivation of regions 1, 4, and 6 with the 38712 driver line resulted in wild-type dialect learning in both the restrictive and permissive temperatures, and wild-type untrained states (Figure 5 G, I, Supplementary Figure 28 E-H). Taken together, we conclude that region 5 of the FB is necessary for dialect learning, whereas regions 1,2, 4, 6, 8, and 9 are dispensable.

Given that the FSB is necessary for dialect learning, specifically neurons in region 5, we wondered whether they are also sufficient. To ask this question, we expressed a temperature sensitive transient receptor potential A1 (TRPA1)(Kang et al, 2012, Lamaze et al, 2017) channel via a Gal4-mediated expression. To ascertain sufficiency of the FB, we altered the dialect learning

setup—we altered the function of time whereby dialect training was performed for either 24 hours or 72 hours (Figure 6 A). When using wild-type *D. melanogaster*, we find that 24 hours is not a sufficient length of training for dialect acquisition, while 72 hours is sufficient (Figure 6 B).

We utilized the temporal requirement of dialect learning to elucidate whether activation of FB neurons is sufficient to enhance dialect learning. Activation of the FB was achieved using UAS-TRPA1 for either 1 or 3 days, paired with thermally inactive/basal control, in order to see if activation can change the temporal requirement of dialect learning. We find that pan FB activation accelerates dialect learning; we observe that 1 day of training is sufficient at the activated temperature (Figure 6 D). At both the thermally inactive/basal and active temperatures for the TRPA1 protein, we observe wild-type dialect acquisition following a 3-day training regime (Figure 6 D, Supplementary Figure 29 A-B). When testing sub-regions, we find that activation of regions 5, 8, 9 produces accelerated dialect learning at the activated temperature following a 1-day regime, but activation of regions 2, 8, 9 and regions 1, 4, 6 do not produce an accelerated dialect learning output (Figure 6 E-J). All lines show wild-type dialect learning ability at both temperatures following a 3-day training regime (Figure 6 E-G, Supplementary Figure 29 C-H). Taken together, we conclude that activation of region 5 of the FB in the presence of *D. ananassae* via TRPA1 can enhance dialect learning by shortening the time required for dialect training.

DISCUSSION

In this study, we have elucidated the fundamental neural circuitry that governs dialect learning in Drosophila. When naïve *D. melanogaster* students are placed next to wasp-exposed *D. ananassae*, *D. melanogaster* students exhibit only partial communication ability. *D. melanogaster* can learn the dialect of *D. ananassae* after a period of cohabitation (dialect training), yielding inter-

species communication enhanced to levels normally observed among conspecifics. Using the FlyLight library, in conjunction with UAS-shi^{ts} to inducibly deactivate defined subsets of neurons during dialect training, we identify 6 distinct regions of the fly brain that are involved in dialect learning: the optic lobe, mushroom body, antennal lobe, ellipsoid body, fan-shaped body, and the lateral horn (Jenett et al, 2012a). Following identification of these regions, we further elucidated a neuronal subset in three distinct regions—the antennal lobe, optic lobe, and the fan-shaped body—that are necessary for dialect learning.

The current study has identified a novel role for an olfactory channel, Or69a, where twin Ors are simultaneously expressed in the same OSN population that sense species-specific pheromones and food odorants (Lebreton et al, 2017a)(Figure 2). The OSN enervates the D glomerulus in the antennal lobe, which we hypothesize signals to the lateral horn and MB through interneurons. A cluster of lateral horn neurons, termed P1, has been identified to collect olfactory and contact chemosensory signals and subsequently elicits male courtship, and might be involved (Pavlou & Goodwin, 2013). Projection neurons from the DA1 glomerulus respond to the male produced olfactory signal, cVA (Kohl et al, 2013). The question that arises for future work is how Or69a and projection neurons from its associated D glomerulus contribute excitatory input to the sexually dimorphic circuitry of the lateral horn (Couto et al, 2005b).

Previous studies have demonstrated the role of L1 and L2 motion detecting neurons as specialized for the detection of moving light and dark edges (Clark et al, 2011, Joesch et al, 2010). Additional work has identified the L4 neuron as involved in the connectome of motion recognition (Silies et al, 2013). The L4 neuron receives its main input from L2, but also receives functionally significant inputs from other neurons (Silies et al, 2013). Using genetic agents restricted to L2 and L4 neurons, we observe independent silencing of either neuron results in perturbed dialect

acquisition (Figure 3). When using activating agents, we find a role for L4 where activation of L4 in the absence of visual stimuli in *D. melanogaster* is sufficient for successful dialect training (Figure 4). Our results argue that L4 might have a specific role in motion detecting of specific Drosophila movements. This finding is consistent with previous studies that suggest that L4 neurons may play a role in spatial summation and pooling information about contrast changes in motion detection (Rister et al, 2007b, Rivera-Alba et al, 2011, Takemura et al, 2008, Takemura et al, 2011, Takemura et al, 2017). L2 and L4 neurons make a diverse range of connections in the medulla. Knowing this, our data raise the possibility that downstream motion computations are distributed among many different neuron types. These neurons may then further converge in deeper layers of the visual system. This additional connectivity may tune neurons to particular features (De Vries & Clandinin, 2012, Egelhaaf & Borst, 1992, Hausen, 1982, Krapp et al, 1998, Mu et al, 2012). These more downstream and specialized neurons could then inform specific outputs appropriate to the visual stimulus during dialect training. It will be interesting to investigate the connectivity of L2 and L4 to these downstream neurons and extract what feature information is being detected (Supplementary Movies 1-2).

The current work has also investigated the roles of the well-defined fly brain region, the FB, and several groups of FB neurons. Genetic manipulations were specifically targeted to FB neurons by using GAL4 lines 39906, 50007, 40553, and 38712 (Jenett et al, 2012b, Li et al, 2009). The results presented demonstrate that FB neurons are capable of mediating social interactions. We identified a subgroup of large-field FB neurons contained in ventral layer 5 of the FB. Outputs of layer 5 neurons are necessary for dialect learning (Supplementary Movies 3-4). Silencing this particular layer or the entire FB demonstrates perturbed dialect acquisition (Figure 5). Activating layer 5 or the entire FB results in an alteration of the temporal dynamics of dialect learning such

that flies can learn the dialect faster (Figure 6). As one of the distinct parts of the central complex in the fly brain (Hanesch et al, 1989), the FB is important for multiple functions, including locomotor control (Strauss, 2002), visual feature recognition and associated processing (Liu et al, 2006), courtship (Sakai & Kitamoto, 2006), sleep (Berry et al, 2015, Donlea et al, 2011, Ueno et al, 2012), and avoidance behaviors (Hu et al, 2018). Visual feature recognition and sleep primarily rely on dorsal FB layers, while avoidance behaviors largely rely on ventral and middle layers of FB. We identify a ventral layer of the FB involved in mediating social interactions during dialect learning. The current state of FB research suggests that different FB layers serve as hubs for distinct behavioral information.

Collectively, we present a model of dialect learning where inhibiting and activating synaptic transmission in certain brain regions results in perturbed or enhanced dialect learning, demonstrating a foundational neural circuit map of dialect learning (Figure 7, Supplementary Figure 30). Given the need for multiple sensory inputs, dialect learning is fundamentally different from the previously described teacher-student paradigms that utilizer only visual cue exchange as a means of information transfer (Kacsoh et al, 2015c). Additionally, we suggest that this study also points to previously unappreciated functions of the Drosophila MB in integrating information from olfactory and visual inputs, perhaps through the L4 motion detecting neuron in the optic lobe and the D glomerulus of the antennal lobe (Takemura et al, 2017).

Dialect learning between *D. melanogaster* and *D. ananassae* results in the ability of each species to more efficiently receive information about a common predator. Cognitive plasticity in conjunction with multiple circuits acts in unison to allow for dialect learning. This finding hints that adult behaviors may emerge only as a result of previous social experiences. Such experiences take place in nature, where relevant ecological pressures are ever present and multiple species co-

exist and compete for resources while simultaneously cooperate against common foes. Cognitive plasticity wields a real fitness benefit to the individual and the collective, where sharing of information directly, or by coincident bystanders, could result in behavioral immunity to pan-specific threats. Our observations also raise the interesting possibility that different species share information not just about common predators, and perhaps even rudimentary social learning neuronal circuitry can be co-opted to receive and integrate useful information from a variety of close and distantly related species.

We have only just arrived at the boundary between insect behavioral neuro-genetics, evolution and ecology, and sociobiology. The current study integrates the vast tool-box and the life history of the Drosophila model in an effort to dissect the neuro-circuitry governing the observation that the direct fitness of the *individual* not being the primary determinant of fitness in a natural setting, but rather the maximization of inclusive fitness. The sociobiology trait of a group is not determined by a group member's genetic fitness, but by the summed effects of all of the survival indices of the group. Collective wisdom in the group arises from poorly informed members, whose interactions with informed members are shaped by natural selection promoting cognitive plasticity and rudimentary sociality.

Materials and Methods

Insect Species/Strains

The *D. melanogaster* strain Canton-S (CS) was used as the wild-type strain and used for outcrosses. The Drosophila species *D. ananassase* and *D. virilis* were acquired from the Drosophila Species Stock Center (DSSC) at the University of California, San Diego, stock

numbers 14024-0371.13 and 15010-1051.87, respectively. *L1, L2, L4^{0987},* and *splitL4* GAL4 lines were kindly provided by Marion Silies (European Science Institute, Germany). The CD8-GFP line was kindly provided by Mani Ramaswami (Trinity College, Dublin Ireland). All stocks used in experiments are listed in Table S1 with stock numbers shown (when applicable).

Flies aged 3-6 days post-eclosion on fresh Drosophila media were used in all experiments. All flies were maintained at 22ºC (the permissive temperature of experiments described later) with approximately 30-45% humidity, with a 12:12 light:dark cycle at light intensity 16_7 with 30-55% humidity dependent on weather. Light intensity was measured using a Sekonic L-308DC light meter. The light meter utilized measures incident light and is set at shutter speed 120, sensitivity at iso8000, with a 1/10 step measurement value (f-stop). These are conditions used in previous studies (Kacsoh et al, 2018b, Kacsoh et al, 2015b, Kacsoh et al, 2015c, Kacsoh et al, 2017). All species and strains used were maintained in fly bottles (Genesse catalog number 32-130) containing 50 mL of standard Drosophila media. Bottles were supplemented with 3 Kimwipes rolled together and placed into the center of the food to promote pupation. Drosophila media was also scored to promote oviposition. Fly species stocks were kept separate to account for visual cues that could be conferred if the stocks were kept side-by-side.

We utilized the generalist Figitid larval endoparasitoid *Leptopilina heterotoma* (strain Lh14), that is known to infect a wide array of Drosophilids (Kacsoh & Schlenke, 2012, Kacsoh et al, 2014b, Schlenke et al, 2007b). *L. heterotoma* strain Lh14 originated from a single female collected in Winters, California in 2002. To propagate wasp stocks, we used adult *D. virilis*, which were placed in batches of 40 females and 15 males per vial (Genesse catalog number 32-116). The strain we used has been maintained on *D. virilis* since 2013. Adult flies are allowed to lay eggs in these standard Drosophila vials that contain 5 mL standard Drosophila media supplemented with

live yeast (approximately 25 granules) for 4-6 days. Flies were then replaced by adult wasps—15 female and 6 male wasps—for infections. Infection timing gives the wasps access to the L2 stage of *D. virilis* larvae. Vials that contain wasps are supplemented with approximately 500 µL of a 50% honey/water solution that is applied to the inside of the cotton vial plugs. The honey used was organic, raw and unfiltered. Wasps aged 3-7 days post eclosion were used for all infections and experiments. Wasps were never reused for experiments, nor were they used for stock propagation if used for experiments.

Fly Duplexes

We utilized the previously described fly duplex to examine teaching ability following dialect training (Kacsoh et al, 2018b, Kacsoh et al, 2015c). The fly duplexes were constructed (Desco, Norfolk, MA) by using three 25mm x 75mm pieces of acrylic that were adhered between two 75mm x 50mm x 3mm pieces of acrylic via clear acrylic sealant. This yields two compartments separated by one 3mm thick acrylic piece. Following sealant curing, each duplex is soaked in water and Sparkleen detergent (Fisherbrand™ catalog number 04-320-4) overnight, then soaked in distilled water overnight and finally air-dried.

For experiments using Fly Duplexes (teacher-student interaction), bead boxes (6 slot jewelers bead storage box watch part organizer sold by FindingKing) were used to accommodate 12 replicates of each treatment group. Compartments measure 32 x 114 mm with the tray in total measuring 21 x 12 x 3.5 mm. Each compartment holds 2 duplexes, and the tray holds a total of 12 duplexes (accounting for the 12 replicates). When setting up experiments, empty duplexes are placed into the bead box compartments. 50 mL standard Drosophila media in a standard Drosophila bottle (Genesse catalog number 32-130) is heated (Panasonic brand microwave) for 54

seconds. This heated media is then allowed to cool for 2 minutes on ice before being dispensed into the duplexes. Each duplex unit is filled with approximately 5 mL of the media and further allowed to cool until solidification. Food was scored to promote oviposition. We find that *D. ananassae* oviposition rate is extremely low in control conditions at 22ºC without scoring. The open end of the Fly Duplex is plugged with a cotton plug (Genesse catalog number 51-102B) to prevent insect escape. 10 female flies and 2 male flies are placed into one chamber of the Fly Duplex in the control, while 20 female Lh14 wasps are placed into the neighboring chamber in the experimental setting for 24 hours. After the 24-hour exposure, flies and wasps were removed by anesthetizing flies and wasps in the Fly Duplexes. Control flies undergo the same anesthetization protocol. Wasps are removed and replaced with 10 female and two male "student" flies. All flies are placed into new, clean duplexes for the second 24-hour period, containing 5 mL Drosophila media in a new bead box, prepared in the same manner as described for day 0 (wasp exposure period). Plugs used to keep insects in the duplexes are replaced every 24 hours to prevent odorant deposition on plugs that could influence behavior. The oviposition bead box from each treatment is also replaced 24 hours after the start of the experiment, and the second bead box is removed 48 hours after the start of the experiment. Fly egg counts from each bead box were made at the 0-24 and 24-48-hour time points in a blinded manner, where coding/decoding and counting are performed by two separate individuals. Used bead boxes and fly duplexes are soaked overnight in a 4% Sparkleen detergent solution (Fisherbrand™ catalog number 04-320-4), rinsed with distilled water, and allowed to air dry before subsequent use.

All experimental treatments as described above were run at 22ºC with a 12:12 light:dark cycle at light intensity 16_7, using twelve replicates at 40% humidity unless otherwise noted. Fly duplexes and bead boxes soaked with distilled water mixed with Sparkleen after every use for 4

hours at minimum and subsequently rinsed with distilled water and air-dried. All egg plates were coded and scoring was blind as the individual counting eggs was not aware of treatments or genotypes. Genotypes were numerically coded and not revealed until the conclusion of the experiment.

Dialect Exposure

Drosophila species were cohabitated during dialect training in standard Drosophila bottles (Genesee catalog number 32-130) containing 50 mL standard Drosophila media. Three Kimwipes were rolled together and placed into the center of the food. Three bottles were prepared per treatment. *D. melanogaster* and *D. ananassae* are incubated in each bottle with 100 female and 20 males of each species per bottle. Every two days, flies are placed into new bottles that prepared in the identical manner described above. Flies were cohabitation for approximately 168 hours (7 days), except where otherwise noted. This cohabitation takes place at either 30ºC or 22ºC depending on treatment parameters. Following cohabitation, flies are anesthetized and the two species are separated. *D. melanogaster* are then used as students to wasp or mock exposed *D. ananassae* teachers. This portion of the experiment always took place at 22ºC. For example, we cohabitated *D. melanogaster* and *D. ananassae* for one week at either 22ºC or 30ºC. Following the weeklong cohabitation, we separated the dialect-trained flies. Trained *D. melanogaster* were placed in duplexes next to *D. ananassae* either mock or wasp exposed at 22ºC.

For the one-day and three-day cohabitation experiments, batches of 3 bottles with 100 female and 20 males of each species were placed at 22ºC or 30ºC for 24 hours or 72 hours. Following the 24- or 72-hour cohabitation, flies were anesthetized and the two species were

separated. *D. melanogaster* are then used as students to wasp or mock exposed *D. ananassae* teachers.

All experimental, dialect training treatments were run either at 30ºC or 22ºC (as indicated in figures) with a 12:12 light:dark cycle at light intensity 16_7, using twelve replicates at 40% humidity unless otherwise noted. Light intensity was measured using a Sekonic L-308DC light meter. The light meter measures incident light and was set at shutter speed 120, sensitivity at iso8000, with a 1/10 step measurement value (f-stop). Additionally, all treatments were coded and scoring was blind as the individual counting eggs was not aware of treatments or genotypes. Coding and decoding was performed by a single individual, while counting was performed by another individual. All raw egg counts and corresponding p-values are provided in supplementary file 1.

Cross set-up

For experiments utilizing either UAS-shi^{ts} or UAS-TRPA1^{TS}, male flies containing tissue specific drivers were crossed to virgin female flies containing the UAS construct of interest. 20 female UAS virgin flies were mated to 10 males containing the selected hairpin. Crosses were performed in standard Drosophila fly bottles (Genesse catalog number 32-130) containing 50 mL of standard Drosophila media, supplemented with 10 granules of activated yeast. Crosses were kept at approximately 20ºC, with a 12:12 light:dark cycle at light intensity 16_7 with 30-45% humidity dependent on weather. Crosses were moved to new bottles every two days until oviposition rates declined, at which point the adults were disposed of. F1's were harvested upon eclosion and stored in standard Drosophila vials (Genesse catalog number 32-116) containing 5

mL Drosophila media with approximately 20 female and 5 male flies until utilized for experimentation.

Immunofluorescence

Drosophila brains containing genetically distinct GAL4 constructs driving a mCD8-GFP were dissected in a manner previously described(Kacsoh et al, 2015b, Kacsoh et al, 2015c). Flies expressing GAL4 in a tissue specific manner driving mCD8-GFP were placed in batches into standard vials (Genesee catalog number 32-116) of 20 females, 2 males. Three vials were prepared to produce three replicates to account for batch effects of expression. We observed no expression batch effects. Brains that were prepared for immunofluorescence were fixed in 4% methanol-free formaldehyde in PBS with 0.001% Triton-X for approximately five minutes. The samples were then washed in PBS with 0.1% Triton-X and placed into block solution for 2 hours (0.001% Triton-X solution 5% normal goat serum). Samples were then placed into a 1:10 dilution of nc82 antibody (Developmental Studies at Hybridoma Bank, University of Iowa, Registry ID AB 2314866) to 0.001% Triton-X overnight at 4ºC. Following the overnight primary stain, samples were washed in PBS with 0.1% Triton-X three times. Secondary Cy3 antibody (Jackson Immunoresearch) was then placed on samples in a 1:200 ratio in 0.001% Triton-X. Following secondary staining, samples were washed in PBS with 0.1% Triton-X three times. This was followed by a 10-minute nuclear stain with 4', 6-diamidino-2-phenylindole (DAPI) with three additional washes in PBS with 0.1% Triton-X before being mounted in vecta shield (vector laboratories catalog number: H-1000). Samples were then immediately imaged.

Imaging

A Zeiss LSM 880 with Airyscan Confocal microscope was used for brain imaging for all samples with the exception of Supplementary figure 8, where a Leica SP8 confocal microscope was used with Leica lighting image deconvolution. Image averaging of 16x during image capture was used for all images. Whole head images of antennal GFP expression were taken using Nikon E800 Epifluorescence microscope with Olympus DP software. For Supplementary Movies 1-4 and Supplementary Figure 30, a spectral confocal/super-resolution microscope LSM 880 with Airyscan was used.

Statistical analysis

Statistical tests on exposed v unexposed/teacher v student interactions were performed in Microsoft Excel. Welch's two-tailed t-tests were performed for data. P-values reported were calculated for comparisons between paired treatment-group and unexposed and are included in supplemental file 1.

Acknowledgements: We thank Mani Ramaswami, Marion Silies, FlyBase, the Vienna Drosophila Resource Center, and the Bloomington Drosophila Stock Center, for stocks. We acknowledge grants from Geisel School of Medicine at Dartmouth, the National Institute of Health Pioneer grant 1DP1MH110234 (GB), and the Defense Advanced Research Projects Agency grant HR0011-15-1-0002 (GB).

References:

Aso Y, Hattori D, Yu Y, Johnston RM, Iyer NA, Ngo TT, Dionne H, Abbott LF, Axel R, Tanimoto H, & Rubin GM (2014) The neuronal architecture of the mushroom body provides a logic for associative learning. *Elife* **3**: e04577

Avarguès-Weber A, Deisig N, & Giurfa M (2011) Visual cognition in social insects. *Annu Rev Entomol* **56**: 423-443

Battesti M, Moreno C, Joly D, & Mery F (2012) Spread of social information and dynamics of social transmission within Drosophila groups. *Current Biology* **22**: 309-313

Beekman M, Fathke RL, & Seeley TD (2006) How does an informed minority of scouts guide a honeybee swarm as it flies to its new home? *Anim Behav* **71**: 161-171

Berry JA, Cervantes-Sandoval I, Chakraborty M, & Davis RL (2015) Sleep facilitates memory by blocking dopamine neuron-mediated forgetting. *Cell* **161**: 1656-1667

Bier E (2005) Drosophila, the golden bug, emerges as a tool for human genetics. *Nature Reviews Genetics* **6**: 9-23

Bozler J, Kacsoh BZ, & Bosco G (2017) Nematocytes: Discovery and characterization of a novel anculeate hemocyte in Drosophila falleni and Drosophila phalerata. *PloS one* **12**: e0188133

Braitenberg V (1970) Order and orientation of elements in the visual system of the fly. *Kybernetik* **7**: 235-242

Breed MD, Guzmán-Novoa E, & Hunt GJ3 (2004) Defensive behavior of honey bees: organization, genetics, and comparisons with other bees. *Annual Reviews in Entomology* **49**: 271-298

Chittka L & Geiger K (1995) Can honey bees count landmarks? *Anim Behav* **49**: 159-164

Chittka L & Niven J (2009) Are bigger brains better? *Current biology* **19**: R995-R1008

Clark DA, Bursztyn L, Horowitz MA, Schnitzer MJ, & Clandinin TR (2011) Defining the computational structure of the motion detector in Drosophila. *Neuron* **70**: 1165-1177

Couto A, Alenius M, & Dickson BJ (2005a) Molecular, anatomical, and functional organization of the Drosophila olfactory system. *Current Biology* **15**: 1535-1547

Couto A, Alenius M, & Dickson BJ (2005b) Molecular, anatomical, and functional organization of the Drosophila olfactory system. *Current Biology* **15**: 1535-1547

Crist E (2004) Can an insect speak? The case of the honeybee dance language. *Soc Stud Sci* **34**: 7-43

Danchin ÉG, Blanchet S, Mery F, & Wagner RH (2010) Do invertebrates have culture? *Communicative & integrative biology* **3**: 303-305

Danchin E, Nöbel S, Pocheville A, Dagaeff A, Demay L, Alphand M, Ranty-Roby S, van Renssen L, Monier M, & Gazagne E (2018) Cultural flies: Conformist social learning in fruitflies predicts long-lasting mate-choice traditions. *Science* **362**: 1025-1030

Datta SR, Vasconcelos ML, Ruta V, Luo S, Wong A, Demir E, Flores J, Balonze K, Dickson BJ, & Axel R (2008) The Drosophila pheromone cVA activates a sexually dimorphic neural circuit. *Nature* **452**: 473

Dawson EH, Bailly TPM, Dos Santos J, Moreno C, Devilliers M, Maroni B, Sueur C, Casali A, Ujvari B, Thomas F, Montagne J, & Mery F (2018) **Social environment mediates cancer progression in *Drosophila***. *Nature communications* **9**

De Vries SE & Clandinin TR (2012) Loom-sensitive neurons link computation to action in the Drosophila visual system. *Current Biology* **22**: 353-362

Donlea JM, Thimgan MS, Suzuki Y, Gottschalk L, & Shaw PJ (2011) Inducing sleep by remote control facilitates memory consolidation in Drosophila. *Science* **332**: 1571-1576

Driessen G, Hemerik L, & Van Alphen JJ (1989) Drosophila species, breeding in the stinkhorn (Phallus impudicus Pers.) and their larval parasitoids. *Neth J Zool* **40**: 409-427

Dyer AG (2012) The mysterious cognitive abilities of bees: why models of visual processing need to consider experience and individual differences in animal performance. *J Exp Biol* **215**: 387-395

Dyer F (1996) Spatial memory and navigation by honeybees on the scale of the foraging range. *J Exp Biol* **199**: 147-154

Edmondson P & Wyburn J (1963) The Erythrocyte Life-span, Red Cell Mass and Plasma Volume of Normal Guinea-pigs as Determined by the Use of 51Chromium, 32Phosphorus Labelled Di-isopropyl Fluorophosphonate and 131Iodine Labelled Human Serum Albumin. *Br J Exp Pathol* **44**: 72

Egelhaaf M & Borst A (1992) Are there separate ON and OFF channels in fly motion vision? *Vis Neurosci* **8**: 151-164

Fisher YE, Leong JC, Sporar K, Ketkar MD, Gohl DM, Clandinin TR, & Silies M (2015) A class of visual neurons with wide-field properties is required for local motion detection. *Current Biology* **25**: 3178-3189

Fishilevich E & Vosshall LB (2005) Genetic and functional subdivision of the Drosophila antennal lobe. *Current Biology* **15**: 1548-1553

Fleury F, Ris N, Allemand R, Fouillet P, Carton Y, Boulétreau M (2004) Ecological and genetic interactions in Drosophila-parasitoids communities: a case study with D. melanogaster, D. simulans and

their common Leptopilina parasitoids in south-eastern France. In *Drosophila melanogaster, Drosophila simulans: So Similar, So Different,* Anonymous pp 181-194. Springer

Giurfa M (2003) Cognitive neuroethology: dissecting non-elemental learning in a honeybee brain. *Curr Opin Neurobiol* **13**: 726-735

Gould JL (1974) Honey bee communication. *Nature*

Grabe V, Baschwitz A, Dweck HK, Lavista-Llanos S, Hansson BS, & Sachse S (2016) Elucidating the neuronal architecture of olfactory glomeruli in the Drosophila antennal lobe. *Cell reports* **16**: 3401-3413

Greenfield MD (1981) Moth sex pheromones: an evolutionary perspective. *The Florida Entomologist* **64**: 4-17

Greggers U & Menzel R (1993) Memory dynamics and foraging strategies of honeybees. *Behav Ecol Sociobiol* **32**: 17-29

Hanesch U, Fischbach K, & Heisenberg M (1989) Neuronal architecture of the central complex in Drosophila melanogaster. *Cell Tissue Res* **257**: 343-366

Hausen K (1982) Motion sensitive interneurons in the optomotor system of the fly. *Biol Cybern* **45**: 143-156

Heisenberg M & Buchner E (1977) The role of retinula cell types in visual behavior ofDrosophila melanogaster. *Journal of comparative physiology* **117**: 127-162

Heisenberg M & Wolf R (1979) On the fine structure of yaw torque in visual flight orientation ofDrosophila melanogaster. *Journal of comparative physiology* **130**: 113-130

Helfand SL & Rogina B (2003) Genetics of aging in the fruit fly, Drosophila melanogaster. *Annu Rev Genet* **37**: 329-348

Hölldobler B & Wilson EO (2009) The superorganism.

Hsu CT & Bhandawat V (2016) Organization of descending neurons in Drosophila melanogaster. *Scientific reports* **6**: 20259

Hu W, Peng Y, Sun J, Zhang F, Zhang X, Wang L, Li Q, & Zhong Y (2018) Fan-Shaped Body Neurons in the Drosophila Brain Regulate Both Innate and Conditioned Nociceptive Avoidance. *Cell reports* **24**: 1573-1584

Jenett A, Rubin GM, Ngo T, Shepherd D, Murphy C, Dionne H, Pfeiffer BD, Cavallaro A, Hall D, & Jeter J (2012a) A GAL4-driver line resource for Drosophila neurobiology. *Cell reports* **2**: 991-1001

Jenett A, Rubin GM, Ngo T, Shepherd D, Murphy C, Dionne H, Pfeiffer BD, Cavallaro A, Hall D, & Jeter J (2012b) A GAL4-driver line resource for Drosophila neurobiology. *Cell reports* **2**: 991-1001

Joesch M, Schnell B, Raghu SV, Reiff DF, & Borst A (2010) ON and OFF pathways in Drosophila motion vision. *Nature* **468**: 300

Joesch M, Weber F, Eichner H, & Borst A (2013) Functional specialization of parallel motion detection circuits in the fly. *J Neurosci* **33**: 902-905

Kacsoh BZ, Barton S, Jiang Y, Zhou N, Mooney SD, Friedberg I, Radivojac P, Greene CS, & Bosco G (2018a) New Drosophila long-term memory genes revealed by assessing computational function prediction methods. *bioRxiv*: 414565

Kacsoh BZ, Bozler J, & Bosco G (2018b) Drosophila species learn dialects through communal living. *PLoS genetics* **14**: e1007430

Kacsoh BZ, Bozler J, & Schlenke TA (2014a) A role for nematocytes in the cellular immune response of the Drosophilid Zaprionus indianus. *Parasitology* **141**: 697-715

Kacsoh BZ, Bozler J, & Schlenke TA (2014b) A role for nematocytes in the cellular immune response of the Drosophilid Zaprionus indianus. *Parasitology* **141**: 697-715

Kacsoh BZ & Schlenke TA (2012) High hemocyte load is associated with increased resistance against parasitoids in Drosophila suzukii, a relative of D. melanogaster. *PloS one* **7**: e34721

Kacsoh BZ, Bozler J, Hodge S, Ramaswami M, & Bosco G (2015a) A novel paradigm for nonassociative long-term memory in Drosophila: predator-induced changes in oviposition behavior. *Genetics* **199**: 1143-1157

Kacsoh BZ, Bozler J, Hodge S, Ramaswami M, & Bosco G (2015b) A novel paradigm for nonassociative long-term memory in Drosophila: predator-induced changes in oviposition behavior. *Genetics* **199**: 1143-1157

Kacsoh BZ, Bozler J, Ramaswami M, & Bosco G (2015c) Social communication of predator-induced changes in Drosophila behavior and germ line physiology. *Elife* **4**: 10.7554/eLife.07423

Kacsoh BZ, Greene CS, & Bosco G (2017) Machine Learning Analysis Identifies DrosophilaGrunge/Atrophin as an Important Learning and Memory Gene Required for Memory Retention and Social Learning. *G3 (Bethesda)*

Kacsoh BZ, Lynch ZR, Mortimer NT, & Schlenke TA (2013) Fruit flies medicate offspring after seeing parasites. *Science* **339**: 947-950

Kang K, Panzano VC, Chang EC, Ni L, Dainis AM, Jenkins AM, Regna K, Muskavitch MA, & Garrity PA (2012) Modulation of TRPA1 thermal sensitivity enables sensory discrimination in Drosophila. *Nature* **481**: 76

Kitamoto T (2001) Conditional modification of behavior in Drosophila by targeted expression of a temperature-sensitive shibire allele in defined neurons. *J Neurobiol* **47**: 81-92

Kohl J, Ostrovsky AD, Frechter S, & Jefferis GS (2013) A bidirectional circuit switch reroutes pheromone signals in male and female brains. *Cell* **155**: 1610-1623

Krapp HG, Hengstenberg B, & Hengstenberg R (1998) Dendritic structure and receptive-field organization of optic flow processing interneurons in the fly. *J Neurophysiol* **79**: 1902-1917

Kurtovic A, Widmer A, & Dickson BJ (2007) A single class of olfactory neurons mediates behavioural responses to a Drosophila sex pheromone. *Nature* **446**: 542

Lamaze A, Öztürk-Çolak A, Fischer R, Peschel N, Koh K, & Jepson JE (2017) Regulation of sleep plasticity by a thermo-sensitive circuit in Drosophila. *Scientific reports* **7**: 40304

Larsson MC, Domingos AI, Jones WD, Chiappe ME, Amrein H, & Vosshall LB (2004) Or83b encodes a broadly expressed odorant receptor essential for Drosophila olfaction. *Neuron* **43**: 703-714

LaSalle J (1993) Parasitic Hymenoptera, biological control and biodiversity. *Hymenoptera and Biodiversity*.: 197-215

Laturney M & Billeter J (2016) Drosophila melanogaster females restore their attractiveness after mating by removing male anti-aphrodisiac pheromones. *Nature communications* **7**: 12322

Lebreton S, Borrero-Echeverry F, Gonzalez F, Solum M, Wallin EA, Hedenström E, Hansson BS, Gustavsson A, Bengtsson M, & Birgersson G (2017a) A Drosophila female pheromone elicits species-specific long-range attraction via an olfactory channel with dual specificity for sex and food. *BMC biology* **15**: 88

Lebreton S, Borrero-Echeverry F, Gonzalez F, Solum M, Wallin EA, Hedenström E, Hansson BS, Gustavsson A, Bengtsson M, & Birgersson G (2017b) A Drosophila female pheromone elicits species-specific long-range attraction via an olfactory channel with dual specificity for sex and food. *BMC biology* **15**: 88

Lefevre T, de Roode JC, Kacsoh BZ, & Schlenke TA (2012) Defence strategies against a parasitoid wasp in Drosophila: fight or flight? *Biol Lett* **8**: 230-233

Li W, Pan Y, Wang Z, Gong H, Gong Z, & Liu L (2009) Morphological characterization of single fan-shaped body neurons in Drosophila melanogaster. *Cell Tissue Res* **336**: 509-519

Lin CC, Prokop-Prigge KA, Preti G, & Potter CJ (2015) Food odors trigger Drosophila males to deposit a pheromone that guides aggregation and female oviposition decisions. *Elife* **4**: 10.7554/eLife.08688

Liu G, Seiler H, Wen A, Zars T, Ito K, Wolf R, Heisenberg M, & Liu L (2006) Distinct memory traces for two visual features in the Drosophila brain. *Nature* **439**: 551

Lone SR & Sharma VK (2012) Or47b receptor neurons mediate sociosexual interactions in the fruit fly Drosophila melanogaster. *J Biol Rhythms* **27**: 107-116

Lynch ZR, Schlenke TA, & Roode J (2016) Evolution of behavioural and cellular defences against parasitoid wasps in the Drosophila melanogaster subgroup. *J Evol Biol*

Manak JR (2018) Multiculturalism is good for flies, too. *PLoS genetics* **14**: e1007480

Mao Z, Roman G, Zong L, & Davis RL (2004) Pharmacogenetic rescue in time and space of the rutabaga memory impairment by using Gene-Switch. *Proc Natl Acad Sci U S A* **101**: 198-203

Markow TA (2015) The secret lives of Drosophila flies. *Elife* **4**: 10.7554/eLife.06793

Meinertzhagen IA & O'neil S (1991) Synaptic organization of columnar elements in the lamina of the wild type in Drosophila melanogaster. *J Comp Neurol* **305**: 232-263

Mortimer NT, Kacsoh BZ, Keebaugh ES, & Schlenke TA (2012) Mgat1-dependent N-glycosylation of membrane components primes Drosophila melanogaster blood cells for the cellular encapsulation response. *PLoS pathogens* **8**: e1002819

Mortimer NT, Goecks J, Kacsoh BZ, Mobley JA, Bowersock GJ, Taylor J, & Schlenke TA (2013) Parasitoid wasp venom SERCA regulates Drosophila calcium levels and inhibits cellular immunity. *Proc Natl Acad Sci U S A* **110**: 9427-9432

Mu L, Ito K, Bacon JP, & Strausfeld NJ (2012) Optic glomeruli and their inputs in Drosophila share an organizational ground pattern with the antennal lobes. *J Neurosci* **32**: 6061-6071

Pavlou HJ & Goodwin SF (2013) Courtship behavior in Drosophila melanogaster: towards a 'courtship connectome'. *Curr Opin Neurobiol* **23**: 76-83

Rister J, Pauls D, Schnell B, Ting C, Lee C, Sinakevitch I, Morante J, Strausfeld NJ, Ito K, & Heisenberg M (2007a) Dissection of the peripheral motion channel in the visual system of Drosophila melanogaster. *Neuron* **56**: 155-170

Rister J, Pauls D, Schnell B, Ting C, Lee C, Sinakevitch I, Morante J, Strausfeld NJ, Ito K, & Heisenberg M (2007b) Dissection of the peripheral motion channel in the visual system of Drosophila melanogaster. *Neuron* **56**: 155-170

Rivera-Alba M, Vitaladevuni SN, Mishchenko Y, Lu Z, Takemura S, Scheffer L, Meinertzhagen IA, Chklovskii DB, & de Polavieja GG (2011) Wiring economy and volume exclusion determine neuronal placement in the Drosophila brain. *Current Biology* **21**: 2000-2005

Rizki M (1957) Alterations in the haemocyte population of Drosophila melanogaster. *J Morphol* **100**: 437-458

RIZKI MT & RIZKI RM (1959) Functional significance of the crystal cells in the larva of Drosophila melanogaster. *J Biophys Biochem Cytol* **5**: 235-240

Sakai T & Kitamoto T (2006) Differential roles of two major brain structures, mushroom bodies and central complex, for Drosophila male courtship behavior. *J Neurobiol* **66**: 821-834

Schlenke TA, Morales J, Govind S, & Clark AG (2007a) Contrasting infection strategies in generalist and specialist wasp parasitoids of Drosophila melanogaster. *PLoS Pathog* **3**: e158

Schlenke TA, Morales J, Govind S, & Clark AG (2007b) Contrasting infection strategies in generalist and specialist wasp parasitoids of Drosophila melanogaster. *PLoS pathogens* **3**: e158

Schneider J, Murali N, Taylor G, & Levine J (2018) Can Drosophila melanogaster tell Who's Who? *bioRxiv*: 342857

Silies M, Gohl DM, Fisher YE, Freifeld L, Clark DA, & Clandinin TR (2013) Modular use of peripheral input channels tunes motion-detecting circuitry. *Neuron* **79**: 111-127

Srinivasan MV (2010) Honey bees as a model for vision, perception, and cognition. *Annu Rev Entomol* **55**: 267-284

Strausfeld N & Campos-Ortega J (1973) The L4 monopolar neurone: a substrate for lateral interaction in the visual system of the flymusca domestica (L). *Brain Res* **59**: 97-117

Strausfeld NJ & Campos-Ortega JA (1977) Vision in insects: pathways possibly underlying neural adaptation and lateral inhibition. *Science* **195**: 894-897

Strauss R (2002) The central complex and the genetic dissection of locomotor behaviour. *Curr Opin Neurobiol* **12**: 633-638

Takemura S, Lu Z, & Meinertzhagen IA (2008) Synaptic circuits of the Drosophila optic lobe: the input terminals to the medulla. *J Comp Neurol* **509**: 493-513

Takemura S, Karuppudurai T, Ting C, Lu Z, Lee C, & Meinertzhagen IA (2011) Cholinergic circuits integrate neighboring visual signals in a Drosophila motion detection pathway. *Current biology* **21**: 2077-2084

Takemura SY, Aso Y, Hige T, Wong A, Lu Z, Xu CS, Rivlin PK, Hess H, Zhao T, Parag T, Berg S, Huang G, Katz W, Olbris DJ, Plaza S, Umayam L, Aniceto R, Chang LA, Lauchie S, Ogundeyi O et al (2017) A connectome of a learning and memory center in the adult Drosophila brain. *Elife* **6**: 10.7554/eLife.26975

Ueno T, Tomita J, Tanimoto H, Endo K, Ito K, Kume S, & Kume K (2012) Identification of a dopamine pathway that regulates sleep and arousal in Drosophila. *Nat Neurosci* **15**: 1516

van Naters, Wynand van der Goes & Carlson JR (2007) Receptors and neurons for fly odors in Drosophila. *Current biology* **17**: 606-612

Vogt K, Aso Y, Hige T, Knapek S, Ichinose T, Friedrich AB, Turner GC, Rubin GM, & Tanimoto H (2016) Direct neural pathways convey distinct visual information to Drosophila mushroom bodies. *Elife* **5**: 10.7554/eLife.14009

Vosshall LB (2001) The molecular logic of olfaction in Drosophila. *Chem Senses* **26**: 207-213

Vosshall LB, Amrein H, Morozov PS, Rzhetsky A, & Axel R (1999) A spatial map of olfactory receptor expression in the Drosophila antenna. *Cell* **96**: 725-736

Vosshall LB & Hansson BS (2011) A unified nomenclature system for the insect olfactory coreceptor. *Chem Senses* **36**: 497-498

Vosshall LB, Wong AM, & Axel R (2000) An olfactory sensory map in the fly brain. *Cell* **102**: 147-159

Wardill TJ, List O, Li X, Dongre S, McCulloch M, Ting CY, O'Kane CJ, Tang S, Lee CH, Hardie RC, & Juusola M (2012) Multiple spectral inputs improve motion discrimination in the Drosophila visual system. *Science* **336**: 925-931

Weir PT & Dickinson MH (2015) Functional divisions for visual processing in the central brain of flying Drosophila. *Proc Natl Acad Sci U S A* **112**: E5523-32

Wicker-Thomas C (2007) Pheromonal communication involved in courtship behavior in Diptera. *J Insect Physiol* **53**: 1089-1100

Wigglesworth V (1959) Insect blood cells. *Annu Rev Entomol* **4**: 1-16

Wilson DS (1997) The Wisdom of the Hive: The Social Physiology of Honey Bee Colonies By Thomas D. Seeley. *Perspect Biol Med* **40**: 304-306

Wilson EO (1983) Caste and division of labor in leaf-cutter ants (Hymenoptera: Formicidae: Atta). *Behav Ecol Sociobiol* **14**: 47-54

Wilson E (1971) The Insect Societies Belknap Press of Harvard University Press. *Cambridge, MA*

Wolff T, Iyer NA, & Rubin GM (2015) Neuroarchitecture and neuroanatomy of the Drosophila central complex: A GAL4-based dissection of protocerebral bridge neurons and circuits. *J Comp Neurol* **523**: 997-1037

Wyatt T (2014) Pheromones and Animal Behaviour. 2nd.

Wyatt TD (2010) Pheromones and signature mixtures: defining species-wide signals and variable cues for identity in both invertebrates and vertebrates. *Journal of Comparative Physiology A* **196**: 685-700

Yamaguchi S, Wolf R, Desplan C, & Heisenberg M (2008) Motion vision is independent of color in Drosophila. *Proc Natl Acad Sci U S A* **105**: 4910-4915

Yan H, Opachaloemphan C, Mancini G, Yang H, Gallitto M, Mlejnek J, Leibholz A, Haight K, Ghaninia M, & Huo L (2017) An engineered orco mutation produces aberrant social behavior and defective neural development in ants. *Cell* **170**: 736-747. e9

Yu H, Awasaki T, Schroeder MD, Long F, Yang JS, He Y, Ding P, Kao J, Wu GY, & Peng H (2013) Clonal development and organization of the adult Drosophila central brain. *Current Biology* **23**: 633-643

Zhang S (2012) Visually guided decision making in foraging honeybees. *Frontiers in neuroscience* **6**: 88

Zhang K, Guo JZ, Peng Y, Xi W, & Guo A (2007) Dopamine-mushroom body circuit regulates saliency-based decision-making in Drosophila. *Science* **316**: 1901-1904

Zhu Y, Nern A, Zipursky SL, & Frye MA (2009) Peripheral visual circuits functionally segregate motion and phototaxis behaviors in the fly. *Current Biology* **19**: 613-619

FIGURE LEGENDS

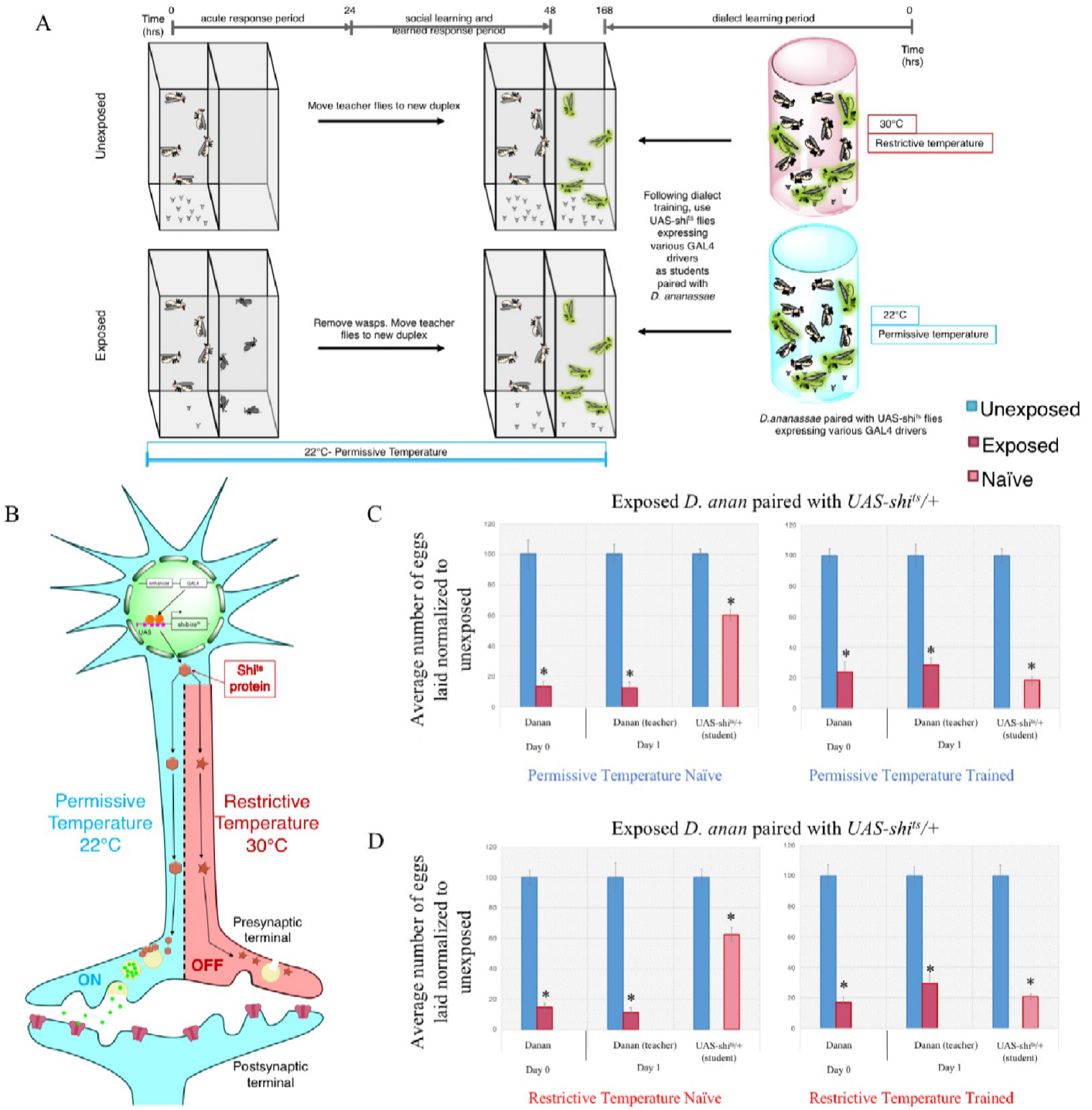
A
Time (hrs)
0
acute response period
24
social learning and learned response period
48
168
dialect learning period
0
Time (hrs)
Unexposed
Exposed
Move teacher flies to new duplex
Remove wasps. Move teacher flies to new duplex
Following dialect training, use UAS-shi^{ts} flies expressing various GAL4 drivers as students paired with D. ananassae
30°C
Restrictive temperature
22°C
Permissive temperature
D.ananassae paired with UAS-shi^{ts} flies expressing various GAL4 drivers
22°C- Permissive Temperature
Unexposed
Exposed
Naïve
B
Shi^{ts} protein
Permissive Temperature 22°C
Restrictive Temperature 30°C
Presynaptic terminal
ON
OFF
Postsynaptic terminal
C
Exposed D. anan paired with UAS-shi^{ts}/+
Average number of eggs laid normalized to unexposed
Danan
Danan (teacher)
UAS-shi^{ts}/+ (student)
Day 0
Day 1
Permissive Temperature Naïve
Permissive Temperature Trained
D
Exposed D. anan paired with UAS-shi^{ts}/+
Restrictive Temperature Naïve
Restrictive Temperature Trained
E
F
D
M
L
V

Figure 1. Dialect learning is governed by multiple brain regions revealed by UAS-shits.

(A) Standard experimental design using UAS-shibire (UAS-shits) in conjunction with various GAL4 drivers. Dialect learning is performed at either the permissive (22°C) or restrictive (30°C) temperature, while the wasp exposure and social learning period is performed exclusively at the permissive temperature. (B) Schematic of the UAS-shits expression in neurons, where the restrictive temperature turns off the neurons of interest and the permissive temperature does not affect these neurons. (C) Percentage of eggs laid by exposed flies normalized to eggs laid by unexposed flies is shown. UAS-shits outcrossed to *Canton S* trained by *D. ananassae* at either the permissive temperature (C) or the restrictive temperature (D) show wild-type dialect acquisition in both the naïve and trained states. Error bars represent standard error (n = 12 biological replicates) (*$p < 0.05$). (E) Brain regions identified as involved in dialect learning—the optic lobe (blue), mushroom body (orange), antennal lobe (teal), lateral horn (green), fan-shaped body (red), and ellipsoid body (light green). (F) Brain regions identified as being dispensable for dialect learning—the prow (light green), bulb (yellow), and superior clamp (purple).

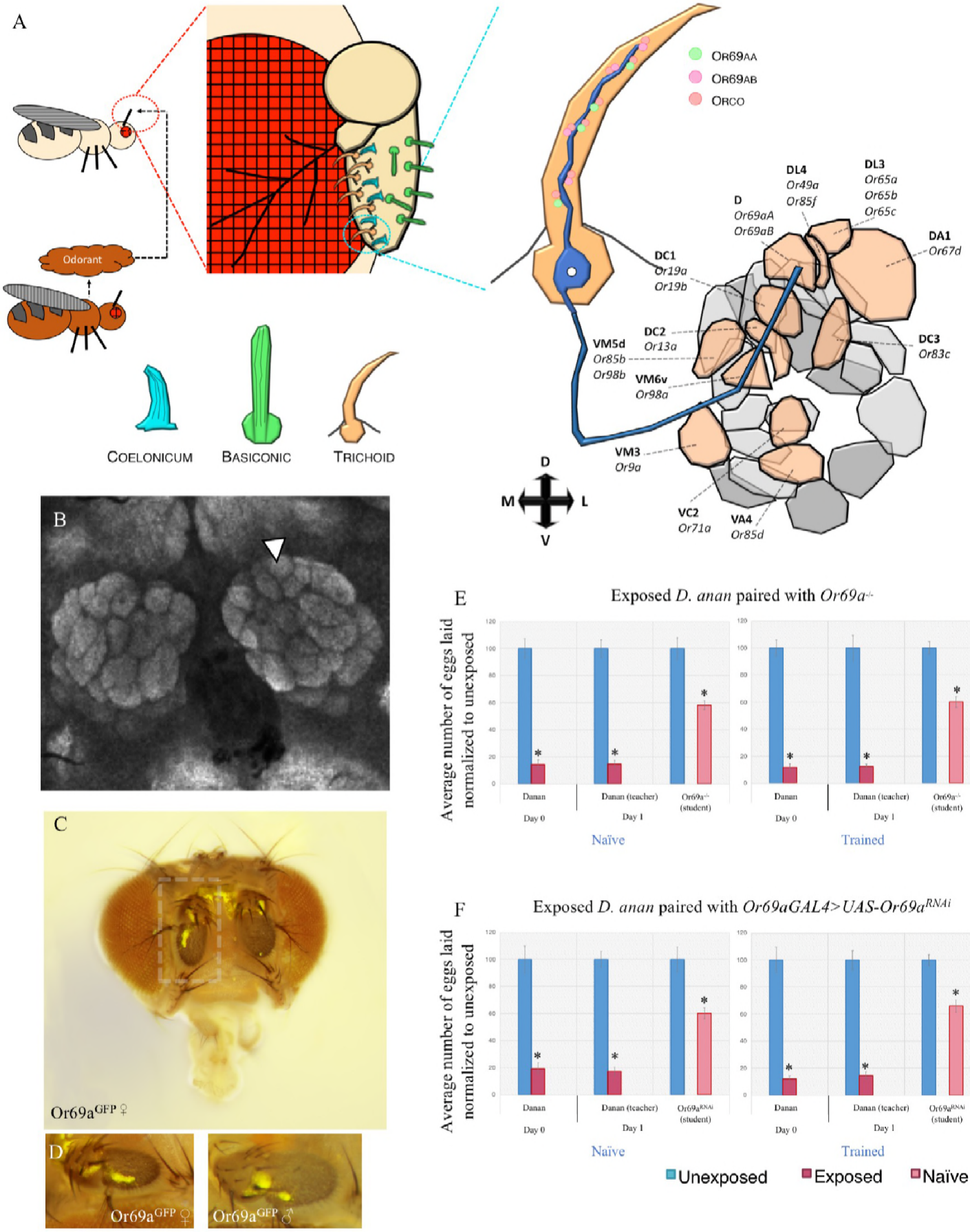
A
Odorant
Or69aA
Or69aB
Orco
DL4
Or49a
Or85f
DL3
Or65a
Or65b
Or65c
D
Or69aA
Or69aB
DA1
Or67d
DC1
Or19a
Or19b
DC2
Or13a
DC3
Or83c
VM5d
Or85b
Or98b
VM6v
Or98a
VM3
Or9a
VC2
Or71a
VA4
Or85d
D
M
L
V
Coelonicum
Basiconic
Trichoid
B
C
Or69a^{GFP} ♀
D
Or69a^{GFP} ♀
Or69a^{GFP} ♂
E
Exposed D. anan paired with Or69a$^{-/-}$
Average number of eggs laid normalized to unexposed
Danan
Danan (teacher)
Or69a$^{-/-}$ (student)
Day 0
Day 1
Naïve
Trained
F
Exposed D. anan paired with Or69aGAL4>UAS-Or69a^{RNAi}
Or69a^{RNAi} (student)
Unexposed
Exposed
Naïve

Figure 2. Dialect learning mediated by the odorant receptor Or69a.

(A) Schematic of Drosophila antenna which has three various olfactory detecting centers: coelonicum, basiconic, and trichoid. Or69a is highlighted in the closeup and its enervation of the D glomerulus in the antenna lobe is highlighted. Glomeruli in the same focal plane are colored orange, while glomeruli in a different focal plane are colored shades of grey. (B) The Drosophila antennal lobe with the D glomerulus indicated with an arrowhead. Nc82 staining shown in grey. (C-D) Expression of Or69a using the $Or69a^{GFP}$ construct highlighting expression in the antenna. Represented in (C) is a female fly head, while (D) represents magnified antennae (shown in box) of both female and male flies expressing $Or69a^{GFP}$. (E) Percentage of eggs laid by exposed flies normalized to eggs laid by unexposed flies is shown. $Or69a^{-/-}$ show wild-type naïve behavior, but are unable to learn the dialect from *D. ananassae* following training. (F) $Or69a^{GAL4}$ driving $Or69a^{RNAi}$ shows wild-type naïve behavior, but is unable to learn the dialect from *D. ananassae* following training. Error bars represent standard error (n = 12 biological replicates) (*$p < 0.05$).

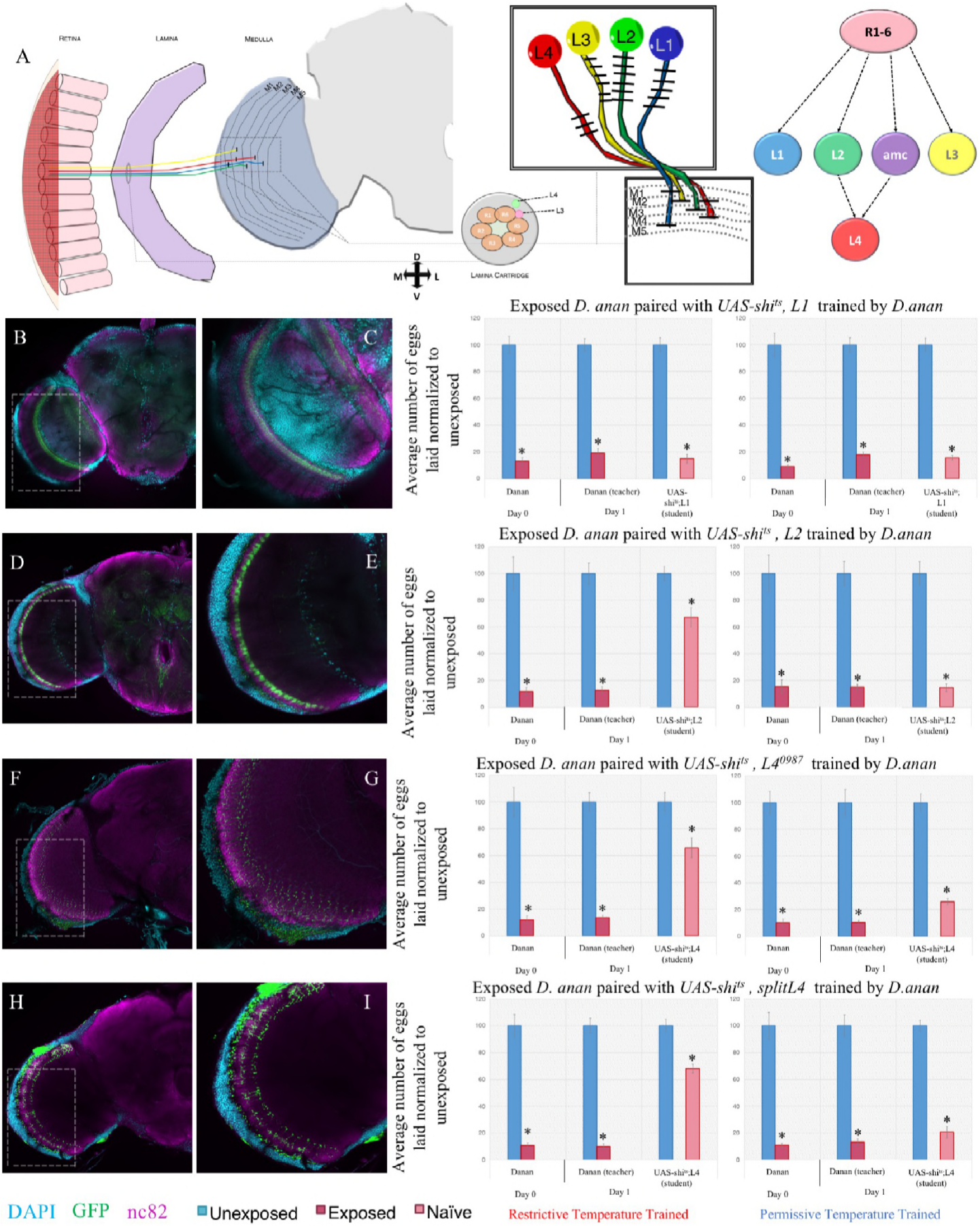
A
RETINA
LAMINA
MEDULLA
M1
M2
M3
M4
M5
L4
L3
L2
L1
R1-6
L1
L2
amc
L3
L4
LAMINA CARTRIDGE
D
M
L
V
B
C
D
E
F
G
H
I
Exposed D. anan paired with UAS-shi^ts, L1 trained by D.anan
Exposed D. anan paired with UAS-shi^ts , L2 trained by D.anan
Exposed D. anan paired with UAS-shi^ts , L4^0987 trained by D.anan
Exposed D. anan paired with UAS-shi^ts , splitL4 trained by D.anan
Average number of eggs laid normalized to unexposed
Danan
Danan (teacher)
UAS-shi^ts;L1 (student)
UAS-shi^ts;L2 (student)
UAS-shi^ts;L4 (student)
Day 0
Day 1
DAPI
GFP
nc82
Unexposed
Exposed
Naïve
Restrictive Temperature Trained
Permissive Temperature Trained

Figure 3. Motion detecting neurons in the optic lobe are required for dialect learning.

(A) Schematic of Drosophila visual system. The optic lobe is shown highlighting the L1, L2, L3, and L4 neurons. One lamina cartridge and one medulla column are magnified to show the dendritic and axonal arborization patterns. The photoreceptors R1-R6 make synaptic connections with the L1, L2, L3, and the amc interneurons. L4 receives most inputs from L2 and amc. Dialect learning is performed at either the permissive (22°C) or restrictive (30°C) temperature, while the wasp exposure and social learning period is performed exclusively at the permissive temperature. Naïve states are shown in figure S 19. (B) Confocal image of adult brain where L1-GAL4 is driving UAS-CD8-GFP, stained with nc82 (magenta) and DAPI (teal). A magnification is shown of boxed area. See also, figure S 17. (C) UAS-shits crossed to L1-GAL4 trained by *D. ananassae* at the permissive temperature shows wild-type trained state and at the restrictive temperature shows wild-type acquisition in the trained state. (D) Confocal image of adult brain where L2-GAL4 is driving UAS-CD8-GFP, stained with nc82 (magenta) and DAPI (teal). A magnification is shown of boxed area. See also, figure S 18. (E) UAS-shits crossed to L2-GAL4 trained by *D. ananassae* at the permissive temperature shows wild-type trained state, but at the restrictive temperature shows defective acquisition in the trained state. (F) Confocal image of adult brain where $L4^{0987}$-GAL4 is driving UAS-CD8-GFP, stained with nc82 (magenta) and DAPI (teal). A magnification is shown of boxed area. See also, figure S 19. (G) UAS-shits crossed to $L4^{0987}$-GAL4 trained by *D. ananassae* at the permissive temperature shows wild-type trained state, but at the restrictive temperature shows defective acquisition in the trained state. (H) Confocal image of adult brain where splitL4-GAL4 is driving UAS-CD8-GFP, stained with nc82 (magenta) and DAPI (teal). A magnification is shown of boxed area. See also, figure S 20. (I) UAS-shits crossed to splitL4-GAL4 trained by *D. ananassae* at the permissive temperature shows wild-type trained state, but at the restrictive temperature shows defective acquisition in the trained state. Error bars represent standard error (n = 12 biological replicates) (*$p < 0.05$).

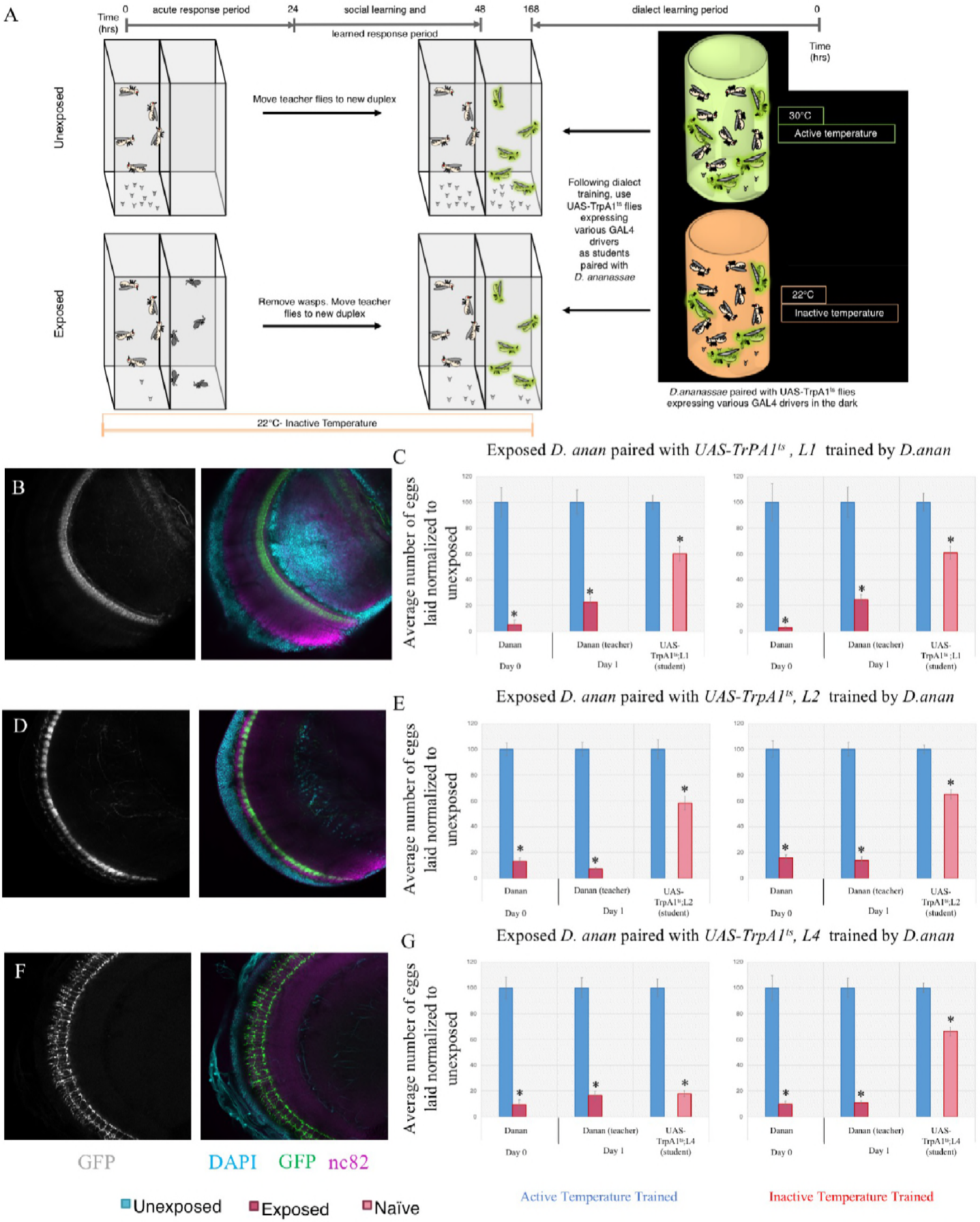
A
Time (hrs)
0
acute response period
24
social learning and
learned response period
48
168
dialect learning period
0
Unexposed
Exposed
Move teacher flies to new duplex
Remove wasps. Move teacher flies to new duplex
22°C- Inactive Temperature
Following dialect training, use UAS-TrpA1ts flies expressing various GAL4 drivers as students paired with D. ananassae
30°C
Active temperature
22°C
Inactive temperature
D.ananassae paired with UAS-TrpA1ts flies expressing various GAL4 drivers in the dark
B
C
Exposed D. anan paired with UAS-TrPA1ts , L1 trained by D.anan
Average number of eggs laid normalized to unexposed
Danan
Danan (teacher)
UAS-TrpA1ts;L1 (student)
Day 0
Day 1
D
E
Exposed D. anan paired with UAS-TrpA1ts, L2 trained by D.anan
UAS-TrpA1ts;L2 (student)
F
G
Exposed D. anan paired with UAS-TrpA1ts, L4 trained by D.anan
UAS-TrpA1ts;L4 (student)
GFP
DAPI GFP nc82
Unexposed
Exposed
Naïve
Active Temperature Trained
Inactive Temperature Trained

Figure 4. Motion detecting neurons in the optic lobe are sufficient for dialect learning.

(A) Experimental design using UAS-TrpA1^{ts} in conjunction with various GAL4 drivers to test the role of motion detecting neurons in the optic lobe. Dialect learning is performed at either the active (30°C) or inactive (22°C) temperature exclusively in the dark, while the wasp exposure and social learning period is performed exclusively at the restrictive temperature. Naïve states are shown in figure S 21. (B) Confocal image of adult brain where L1-GAL4 is driving UAS-CD8-GFP, shown in white. A merged color image, showing staining with nc82 (magenta) and DAPI (teal) is also shown. (C) UAS-TrpA1^{ts} crossed to *L1-GAL4* trained by *D. ananassae* at the activation temperature shows no acquisition of the dialect and no acquisition at the inactive temperature, which demonstrates the need for full spectrum light and that L1 neurons are not sufficient to drive the behavior. (D) Confocal image of adult brain where L2-GAL4 is driving UAS-CD8-GFP, shown in white. A merged color image, showing staining with nc82 (magenta) and DAPI (teal) is also shown. (E) UAS-TrpA1^{ts} crossed to *L2-GAL4* trained by *D. ananassae* at the activation temperature shows no acquisition of the dialect and no acquisition at the inactive temperature, which demonstrates the need for full spectrum light and that L2 neurons are not sufficient to drive the behavior. (F) Confocal image of adult brain where L4^{0987}-GAL4 is driving UAS-CD8-GFP, shown in white. A merged color image, showing staining with nc82 (magenta) and DAPI (teal) is also shown. (G) UAS-TrpA1^{ts} crossed to *L4^{0987}-GAL4* trained by *D. ananassae* at the activation temperature shows acquisition of the dialect, but not at the inactive temperature, which demonstrates the need for full spectrum light. Error bars represent standard error (n = 12 biological replicates) (*$p < 0.05$).

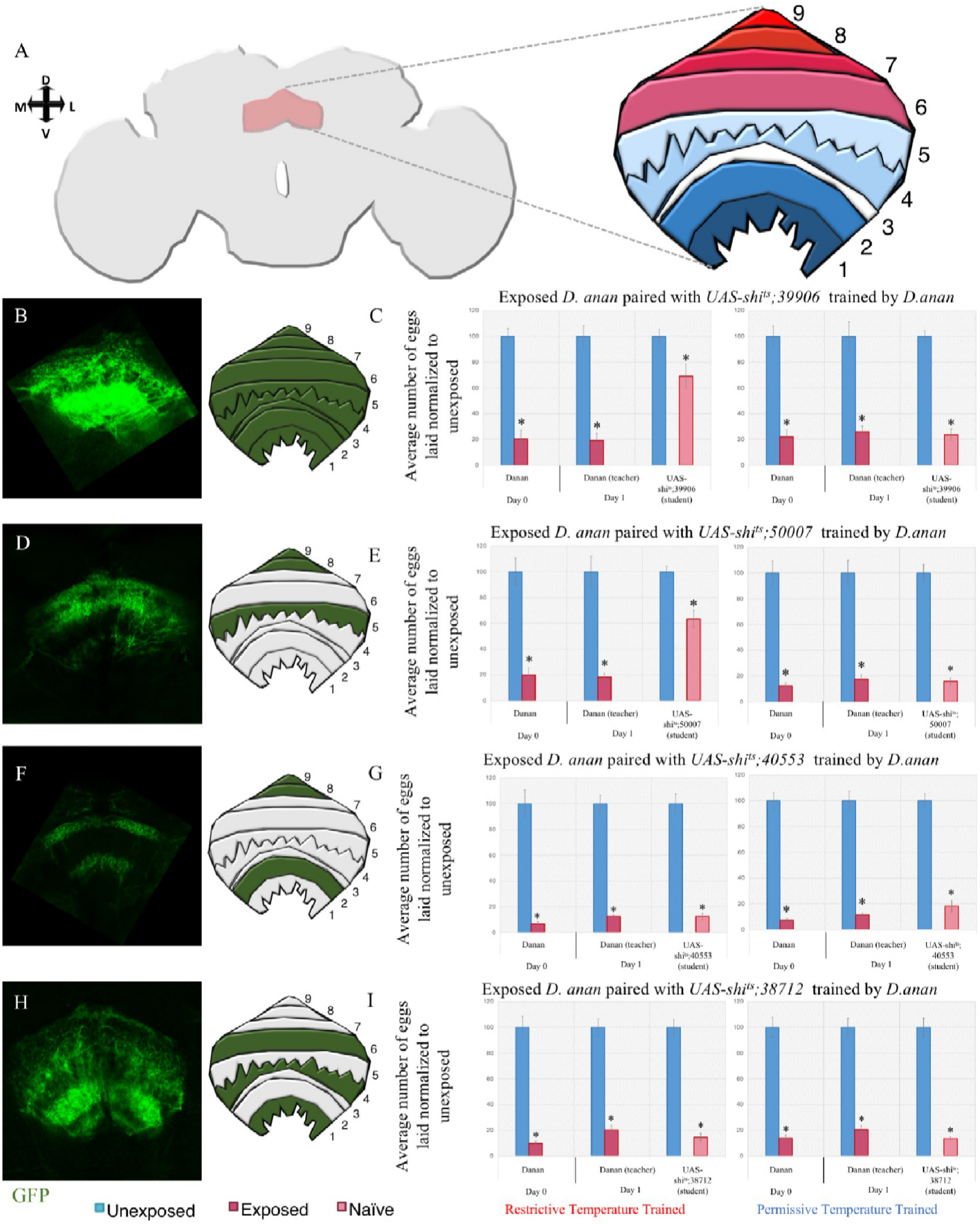
A
D
M
L
V
9
8
7
6
5
4
3
2
1
B
C
Exposed D. anan paired with UAS-shi^ts;39906 trained by D.anan
Average number of eggs laid normalized to unexposed
Danan
Danan (teacher)
UAS-shi^ts;39906 (student)
Day 0
Day 1
D
E
Exposed D. anan paired with UAS-shi^ts;50007 trained by D.anan
UAS-shi^ts;50007 (student)
F
G
Exposed D. anan paired with UAS-shi^ts;40553 trained by D.anan
UAS-shi^ts;40553 (student)
H
I
Exposed D. anan paired with UAS-shi^ts;38712 trained by D.anan
UAS-shi^ts;38712 (student)
GFP
Unexposed
Exposed
Naïve
Restrictive Temperature Trained
Permissive Temperature Trained

Figure 5. Region 5 of the fan-shaped body is necessary for dialect learning.

(A) Schematic of the Drosophila fan-shaped body (FSB) with the various regions (1-9) highlighted. (B) Expression pattern and schematic of the *39906* FSB driver shows pan-FSB marking. See also, figure S 24. Percentage of eggs laid by exposed flies normalized to eggs laid by unexposed flies is shown at the permissive (22°C) or restrictive (30°C) temperature. (C) UAS-shi^{ts} crossed to *39906* trained by *D. ananassae* at the permissive temperature shows wild-type trained state, but at the restrictive temperature shows defective acquisition in the trained state. (D) Expression pattern and schematic of the *50007* FSB driver shows FSB marking in regions 5,8, and 9. See also, figure S 25. (E) UAS-shi^{ts} crossed to *50007* trained by *D. ananassae* at the permissive temperature shows wild-type trained state, but at the restrictive temperature shows defective acquisition in the trained state. (F) Expression pattern and schematic of the *40553* FSB driver shows FSB marking in regions 2,8, and 9. See also, figure S 26. (G) UAS-shi^{ts} crossed to *40553* trained by *D. ananassae* at the permissive and the restrictive temperatures shows wild-type trained state. Naïve states are shown in figure S 25. (H) Expression pattern and schematic of the *38712* FSB driver shows FSB marking in regions 2,8, and 9. See also, figure S 27. (I) UAS-shi^{ts} crossed to *38712* trained by *D. ananassae* at the permissive and the restrictive temperatures shows wild-type trained state. All untrained states are shown in figure S 28. Error bars represent standard error (n = 12 biological replicates) (*$p < 0.05$).

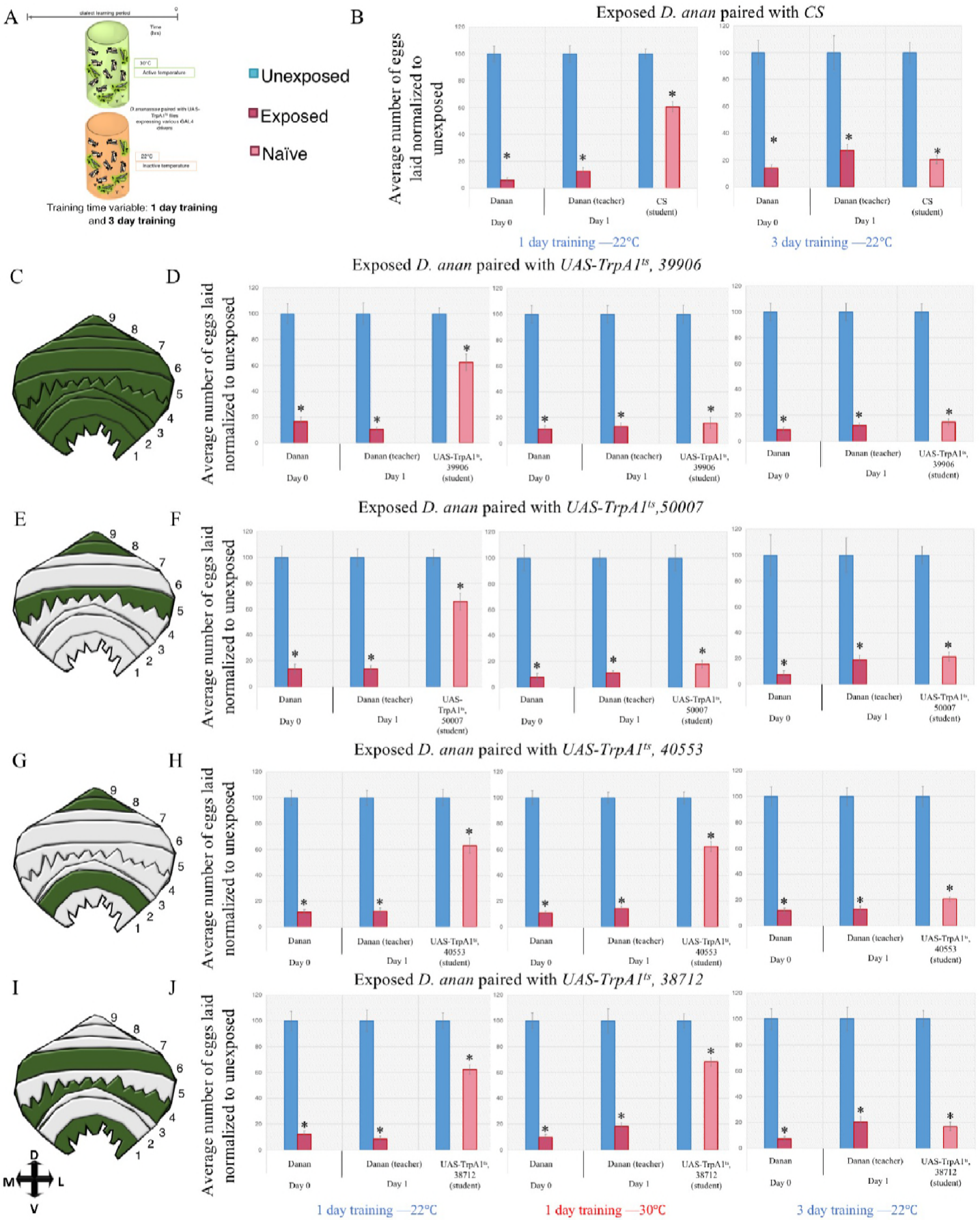
A
B
Training time variable: 1 day training and 3 day training
Unexposed
Exposed
Naïve
Exposed D. anan paired with CS
Average number of eggs laid normalized to unexposed
Danan
Danan (teacher)
CS (student)
Day 0
Day 1
1 day training —22°C
3 day training —22°C
C
D
Exposed D. anan paired with UAS-TrpA1ts, 39906
UAS-TrpA1ts, 39906 (student)
E
F
Exposed D. anan paired with UAS-TrpA1ts,50007
UAS-TrpA1ts, 50007 (student)
G
H
Exposed D. anan paired with UAS-TrpA1ts, 40553
UAS-TrpA1ts, 40553 (student)
I
J
Exposed D. anan paired with UAS-TrpA1ts, 38712
UAS-TrpA1ts, 38712 (student)
1 day training —22°C
1 day training —30°C
3 day training —22°C
D
M
L
V

Figure 6. Region 5 of the fan-shaped body is sufficient for dialect learning.

(A) Schematic of experimental variant introduced to standard dialect training setup—training is either 1 or 3 days at either the active (30°C) or inactive (22°C) temperature. Percentage of eggs laid by exposed flies normalized to eggs laid by unexposed flies is shown. (B) *Wild-type* flies are unable to learn the dialect from *D. ananassae* after 1 day of training but are able to learn after 3 days of training at 22°C. (C) Schematic of the *39906* fan-shaped body (FSB) driver shows FSB marking in all regions. (D) UAS-TrpA1^{ts} crossed to *39906* trained by *D. ananassae* at the inactive temperature shows wild-type phenotype. 1 day of training at the active temperature is sufficient to allow for dialect acquisition suggesting that this region of the FSB is sufficient to drive dialect learning. 3 days of training at the inactive temperature shows wild-type dialect acquisition. (E) Schematic of the *50007* FSB driver shows FSB marking in regions 5,8, and 9. (F) UAS-TrpA1^{ts} crossed to *50007* trained by *D. ananassae* at the inactive temperature shows wild-type phenotype. 1 day of training at the active temperature is sufficient to allow for dialect acquisition suggesting that this region of the FSB is sufficient to drive dialect learning. 3 days of training at the inactive temperature shows wild-type dialect acquisition. (G) Schematic of the *40553* FSB driver shows FSB marking in regions 2,8, and 9. (H) UAS-TrpA1^{ts} crossed to *40553* trained by *D. ananassae* at the inactive temperature shows wild-type phenotype. 1 day of training at the active temperature is not sufficient to allow for dialect acquisition suggesting that this region of the FSB is not sufficient to drive dialect learning. 3 days of training at the inactive temperature shows wild-type dialect acquisition. (I) Schematic of the *38712* FSB driver shows FSB marking in regions 2,8, and 9. (J) UAS-TrpA1^{ts} crossed to *38712* trained by *D. ananassae* at the permissive and the restrictive temperatures shows wild-type trained state. 3-day training period at active (30°C) is shown in figure S 29 for each genotype. Error bars represent standard error (n = 12 biological replicates) (*$p < 0.05$).

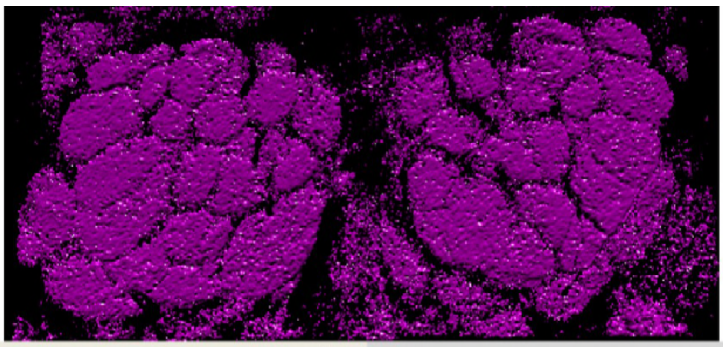

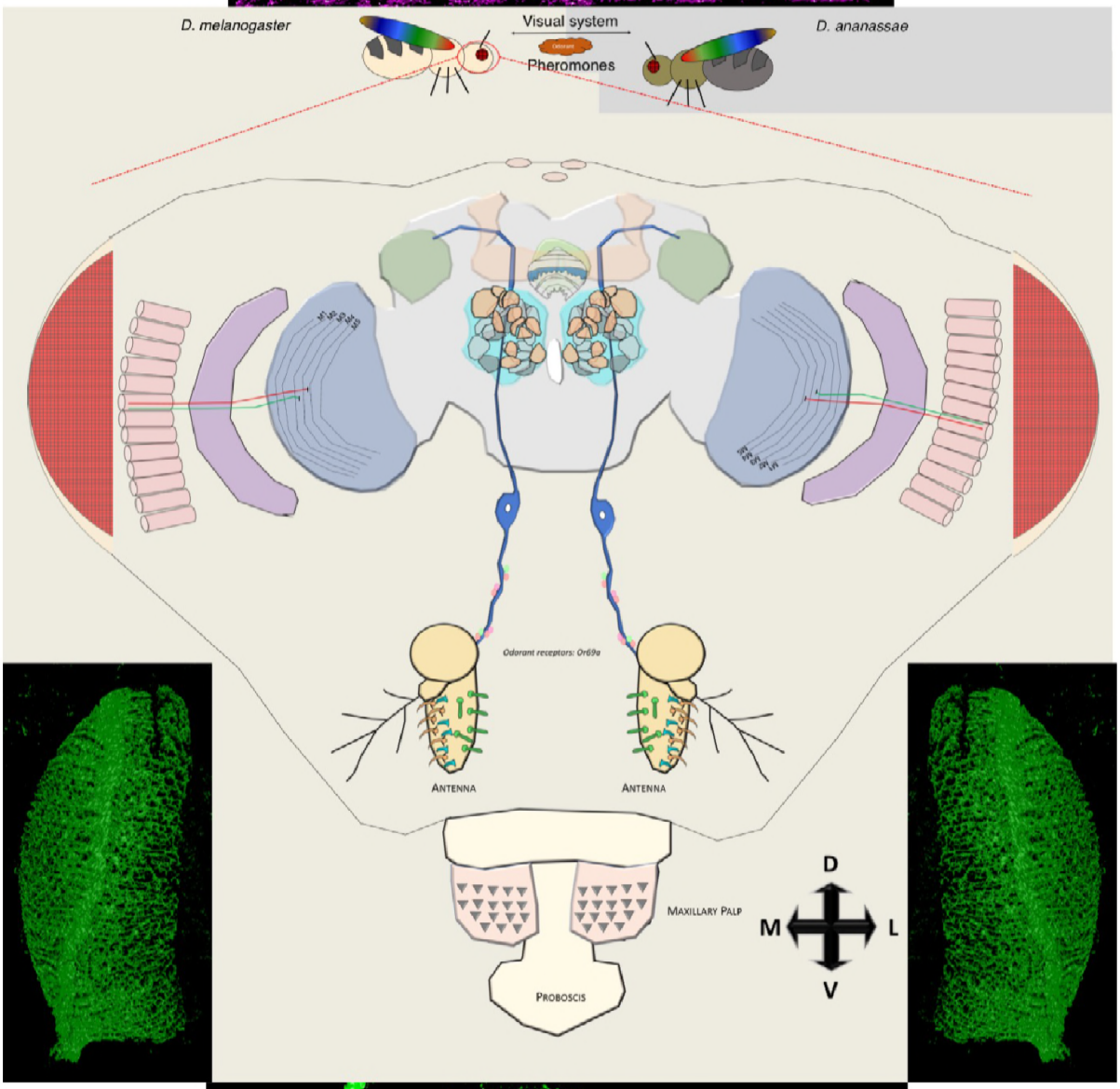
D. melanogaster
Visual system
Pheromones
D. ananassae
Odorant receptors: Or69a
Antenna
Antenna
Maxillary Palp
Proboscis
D
M
L
V

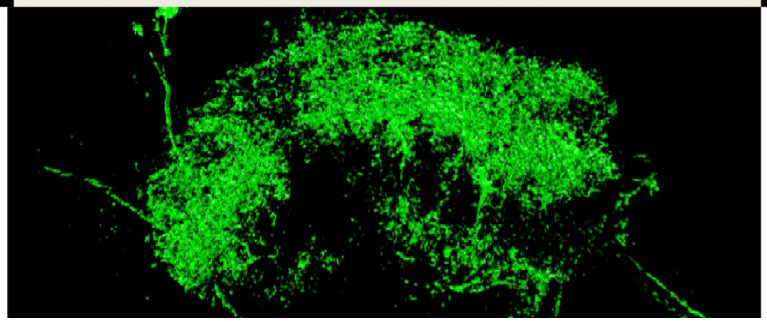

Figure 7. Model for the neural circuitry of dialect learning in Drosophila.

Interspecies communication and dialect learning is dependent on the presence of multiple cues between *D. melanogaster* and *D. ananassae*. These cues are, in part, olfactory, visual, and ionotropic in nature. In *D. melanogaster*, we have identified multiple brain regions and neurons that contribute to the dialect learning. Regions we identified to be involved in dialect learning—the optic lobe (blue), mushroom body (orange), antennal lobe (teal), lateral horn (green), fan-shaped body (green/white), and ellipsoid body (light green). For the antennal lobe, we identify the D glomerulus, innervated by *Or69a* olfactory receptor neuron (ORN). For the fan-shaped body, we identify region 5 as necessary and sufficient for dialect learning. For the optic lobe we identify the motion detecting circuit as necessary by isolation of the L4 neurons. Flanking the model, super resolution microscopy with a 3D render is provided of the key regions of the fly brain that were investigated—region 5 of the fan-shaped body, the L4 neurons, and the antennal lobe. Super resolution images without the 3D render are located in Supplementary Figure 30.

SUPPLEMENTARY FIGURE LEGENDS

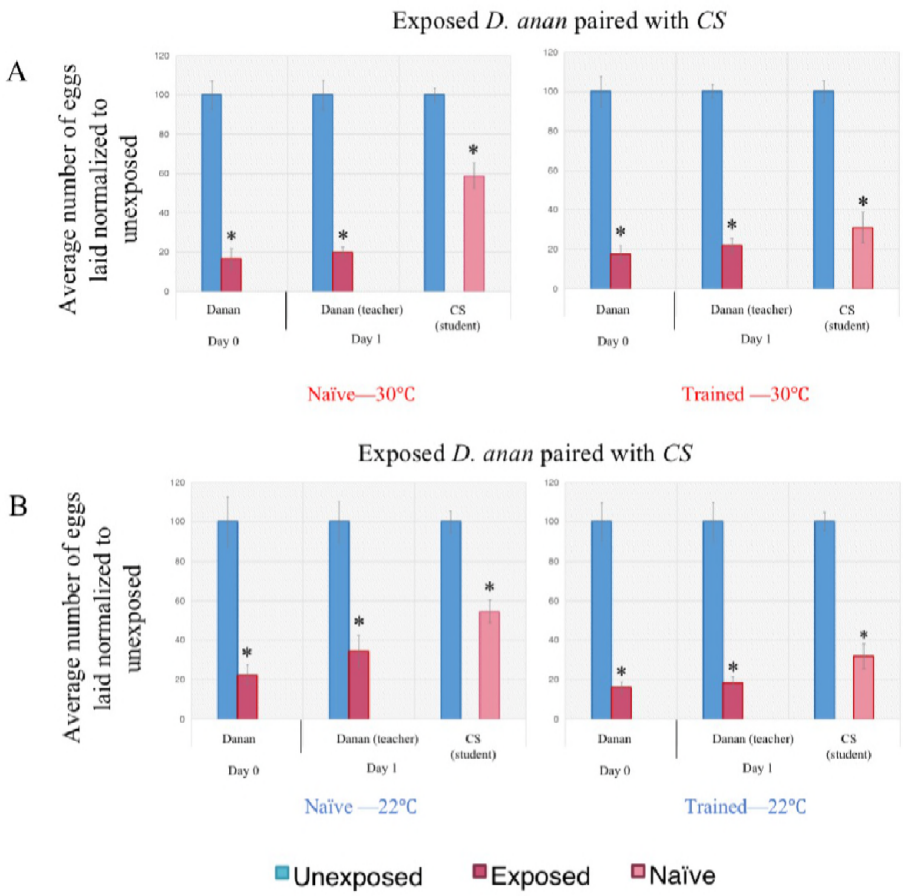
A
Exposed D. anan paired with CS
Average number of eggs laid normalized to unexposed
Danan
Danan (teacher)
CS (student)
Day 0
Day 1
Naïve—30°C
Trained —30°C
B
Exposed D. anan paired with CS
Naïve —22°C
Trained—22°C
Unexposed
Exposed
Naïve

Supplementary Figure 1. Wild-type *D. melanogaster* can be trained by *D. ananassae* at either 22°C or 30°C.

Dialect learning is performed at either the permissive (22°C) or restrictive (30°C) temperature, while the wasp exposure and social learning period is performed exclusively at the permissive temperature. Percentage of eggs laid by exposed flies normalized to eggs laid by unexposed flies is shown. *Canton S* naïve and trained states by *D. ananassae* at either 30°C (A) or 22°C (B) show wild-type dialect acquisition. Error bars represent standard error (n = 12 biological replicates) (*$p < 0.05$).

A

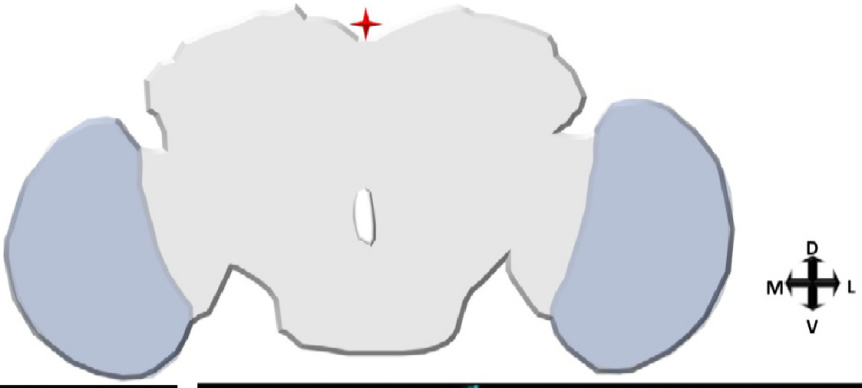
D
M
L
V

B

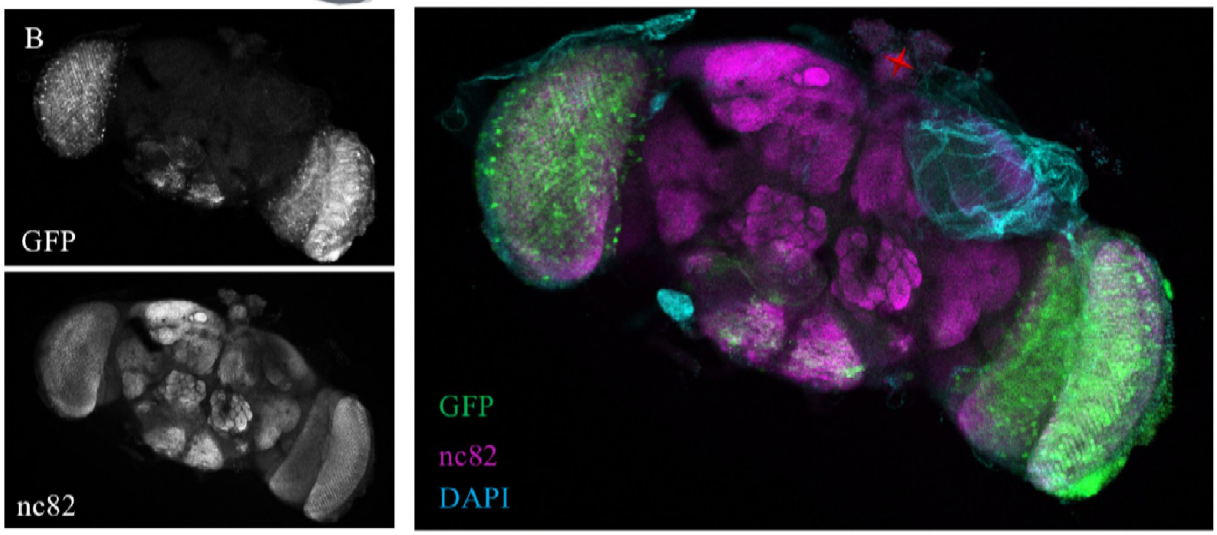
GFP
nc82
GFP
nc82
DAPI

C

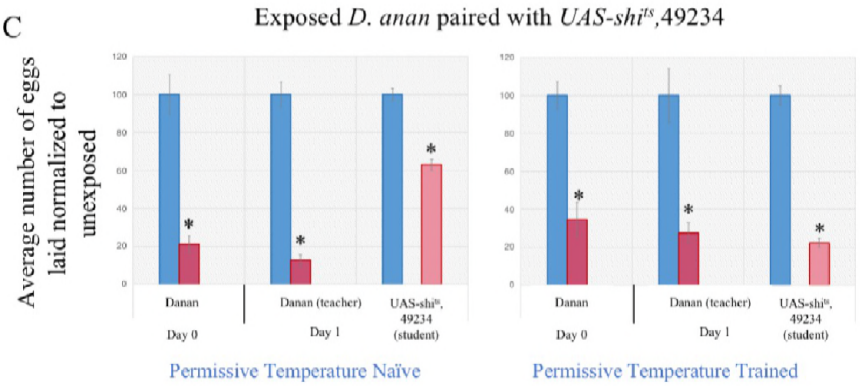
Exposed D. anan paired with UAS-shi^ts,49234
Average number of eggs laid normalized to unexposed
120
100
80
60
40
20
0
*
Danan
Day 0
Danan (teacher)
Day 1
UAS-shi^ts, 49234 (student)
Permissive Temperature Naïve
Permissive Temperature Trained

D

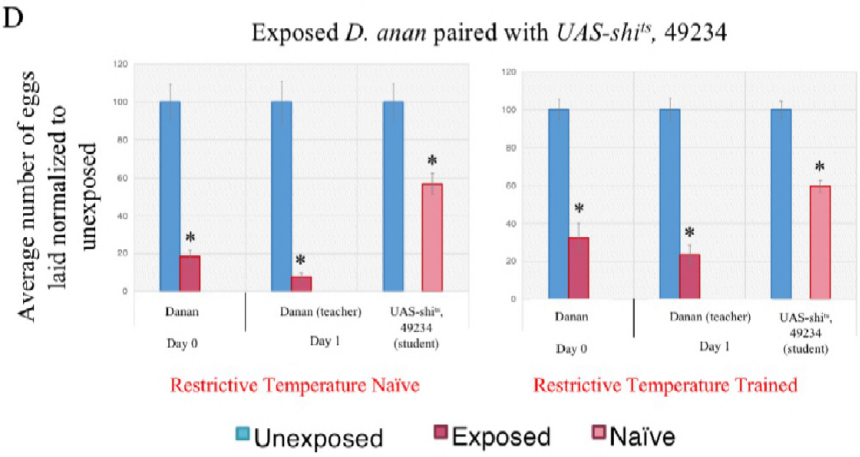
Exposed D. anan paired with UAS-shi^ts, 49234
Average number of eggs laid normalized to unexposed
120
100
80
60
40
20
0
*
Danan
Day 0
Danan (teacher)
Day 1
UAS-shi^ts, 49234 (student)
Restrictive Temperature Naïve
Restrictive Temperature Trained
Unexposed
Exposed
Naïve

Supplementary Figure 2. The optic lobe is required for dialect learning shown with 49234 driver.

(A) Cartoon schematic of the region of interest. (B) Confocal image of adult brain where 49234-GAL4 is driving UAS-CD8-GFP, stained with nc82 (magenta) and DAPI (teal). Fly light intensity/distribution score is 5/2 and was the only region of the brain identified. Percentage of eggs laid by exposed flies normalized to eggs laid by unexposed flies is shown. UAS-shi^{ts} crossed to 49234-GAL4 trained by *D. ananassae* at the permissive temperature shows wild-type trained state (C), but at the restrictive temperature shows defective acquisition in the trained state (D). Error bars represent standard error (n = 12 biological replicates) (*$p < 0.05$).

A

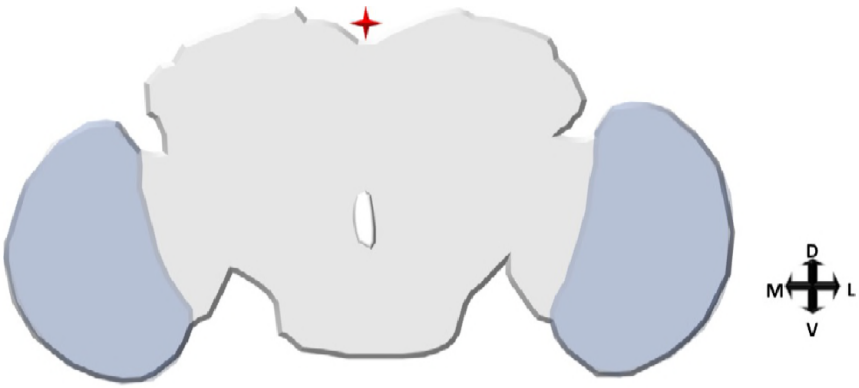
D
M
L
V

B

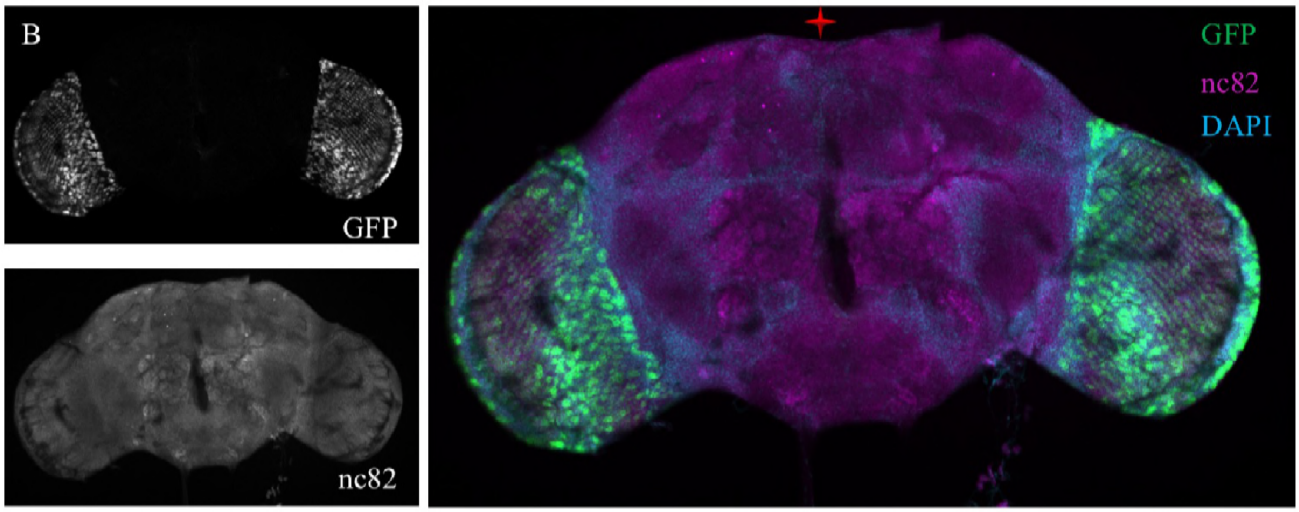
GFP
nc82
GFP
nc82
DAPI

C

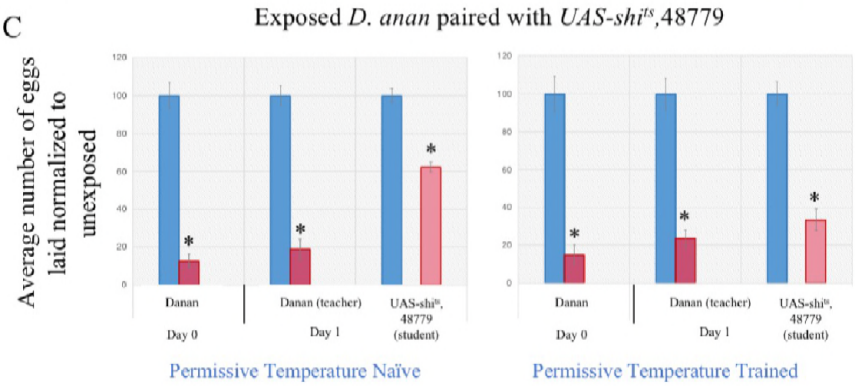
Exposed D. anan paired with UAS-shi^ts,48779
Average number of eggs laid normalized to unexposed
120
100
80
60
40
20
0
*
Danan
Day 0
Danan (teacher)
Day 1
UAS-shi^ts, 48779 (student)
Permissive Temperature Naïve
Permissive Temperature Trained

D

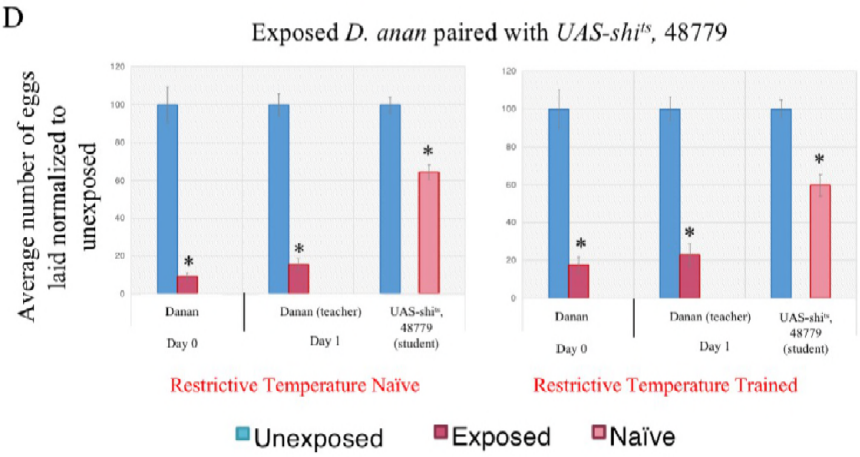
Exposed D. anan paired with UAS-shi^ts, 48779
Average number of eggs laid normalized to unexposed
120
100
80
60
40
20
0
*
Danan
Day 0
Danan (teacher)
Day 1
UAS-shi^ts, 48779 (student)
Restrictive Temperature Naïve
Restrictive Temperature Trained
Unexposed
Exposed
Naïve

Supplementary Figure 3. The optic lobe is required for dialect learning shown with 48779 driver.

(A) Cartoon schematic of the region of interest. (B) Confocal image of adult brain where 48779-GAL4 is driving UAS-CD8-GFP, stained with nc82 (magenta) and DAPI (teal). Fly light intensity/distribution score is 5/2 and was the only region of the brain identified. Percentage of eggs laid by exposed flies normalized to eggs laid by unexposed flies is shown. UAS-shi^{ts} crossed to 48779-GAL4 trained by *D. ananassae* at the permissive temperature shows wild-type trained state (C), but at the restrictive temperature shows defective acquisition in the trained state (D). Error bars represent standard error (n = 12 biological replicates) (*$p < 0.05$).

A

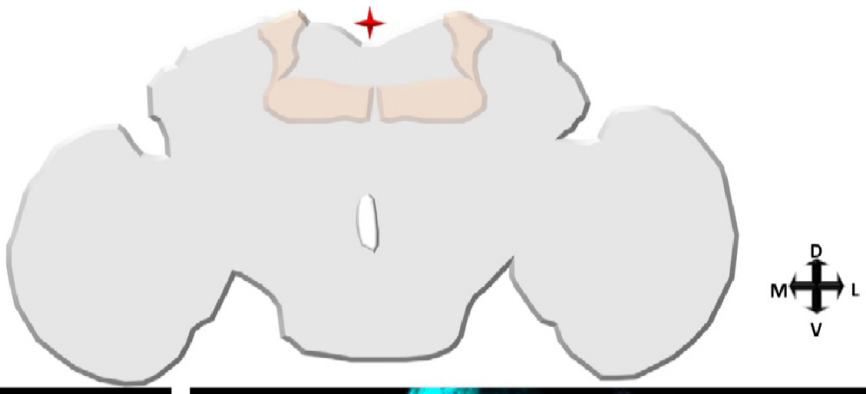
D
M
L
V

B

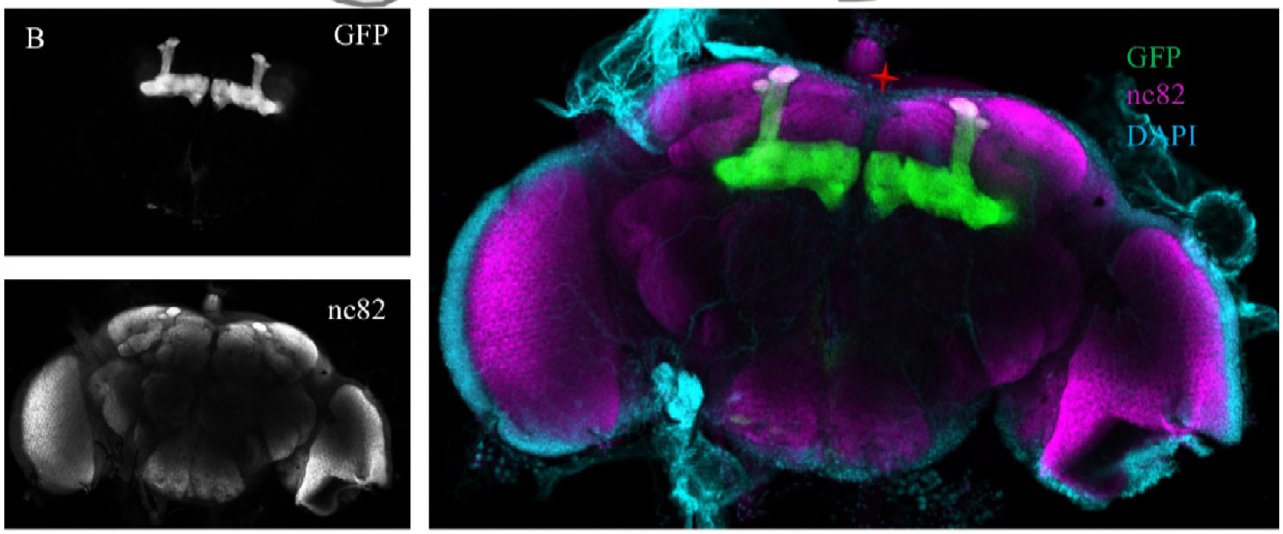
GFP
nc82
GFP
nc82
DAPI

C

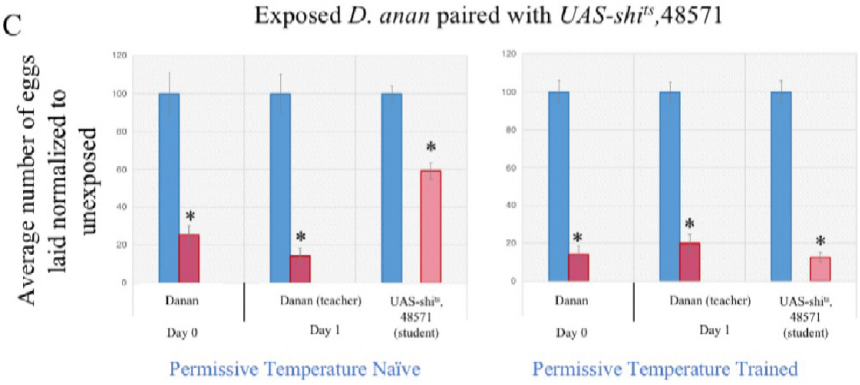
Exposed D. anan paired with UAS-shi^ts,48571
Average number of eggs laid normalized to unexposed
120
100
80
60
40
20
0
*
Danan
Day 0
Danan (teacher)
Day 1
UAS-shi^ts, 48571 (student)
Permissive Temperature Naïve
Permissive Temperature Trained

D

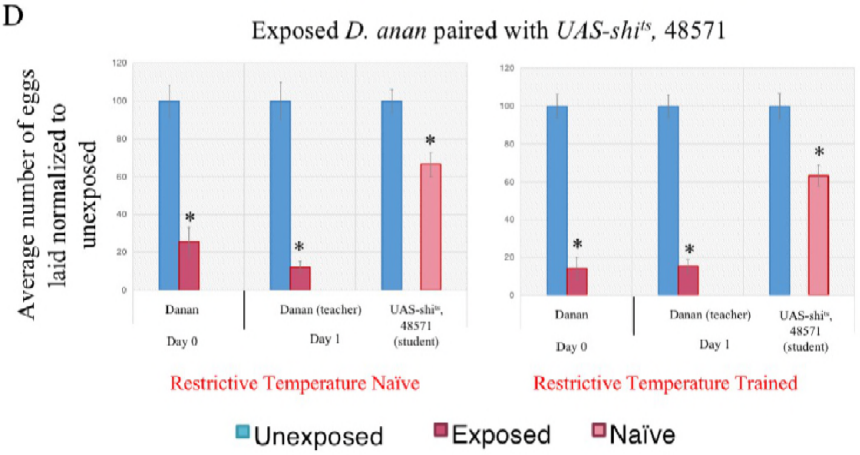
Exposed D. anan paired with UAS-shi^ts, 48571
Average number of eggs laid normalized to unexposed
120
100
80
60
40
20
0
*
Danan
Day 0
Danan (teacher)
Day 1
UAS-shi^ts, 48571 (student)
Restrictive Temperature Naïve
Restrictive Temperature Trained
Unexposed
Exposed
Naïve

Supplementary Figure 4. The mushroom body is required for dialect learning shown with 48571 driver.

(A) Cartoon schematic of the region of interest. (B) Confocal image of adult brain where 48571-GAL4 is driving UAS-CD8-GFP, stained with nc82 (magenta) and DAPI (teal). Fly light intensity/distribution score is 5/4 and was the only region of the brain identified. Percentage of eggs laid by exposed flies normalized to eggs laid by unexposed flies is shown. UAS-shi^{ts} crossed to 48571-GAL4 trained by *D. ananassae* at the permissive temperature shows wild-type trained state (C), but at the restrictive temperature shows defective acquisition in the trained state (D). Error bars represent standard error (n = 12 biological replicates) (*$p < 0.05$).

A

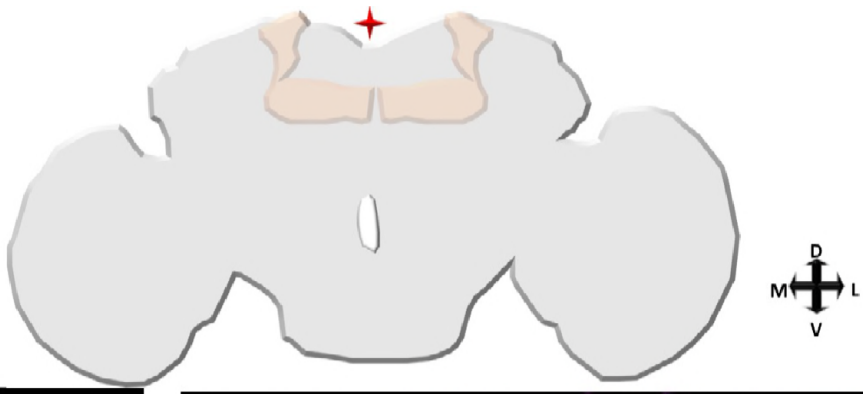
D
M
L
V

B

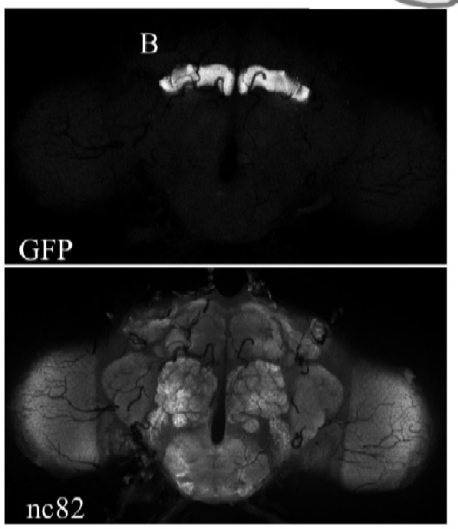
GFP
nc82

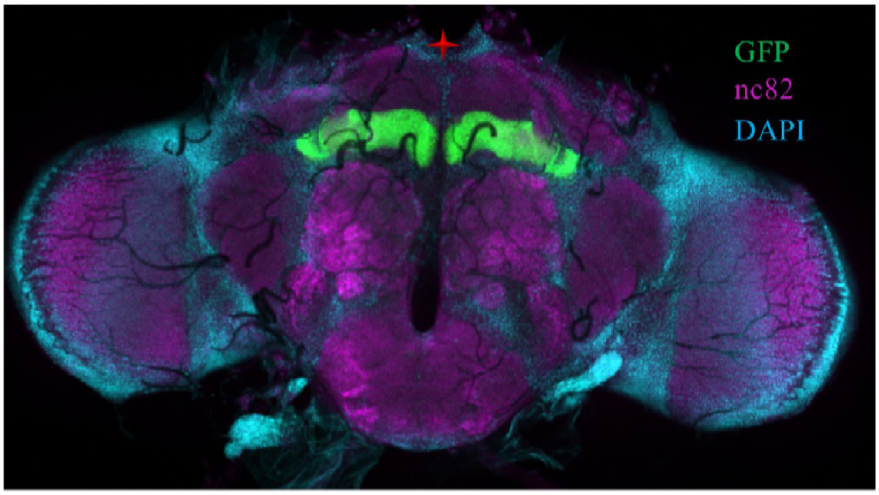
GFP
nc82
DAPI

C

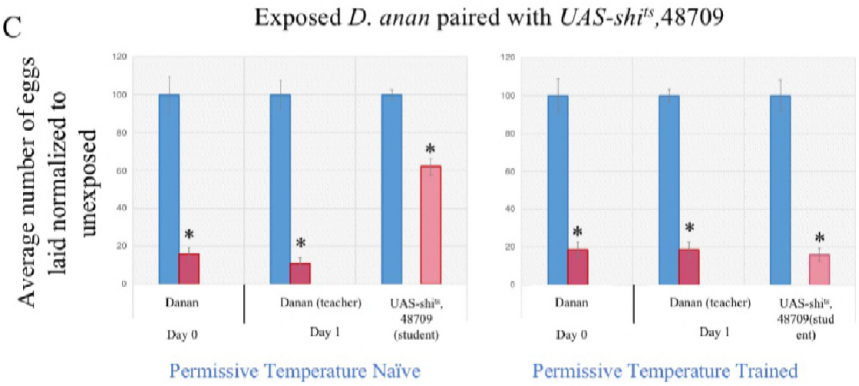
Exposed D. anan paired with UAS-shi^{ts},48709
Average number of eggs laid normalized to unexposed
120
100
80
60
40
20
0
*
Danan
Day 0
Danan (teacher)
Day 1
UAS-shi^{ts}, 48709 (student)
Permissive Temperature Naïve
Permissive Temperature Trained

D

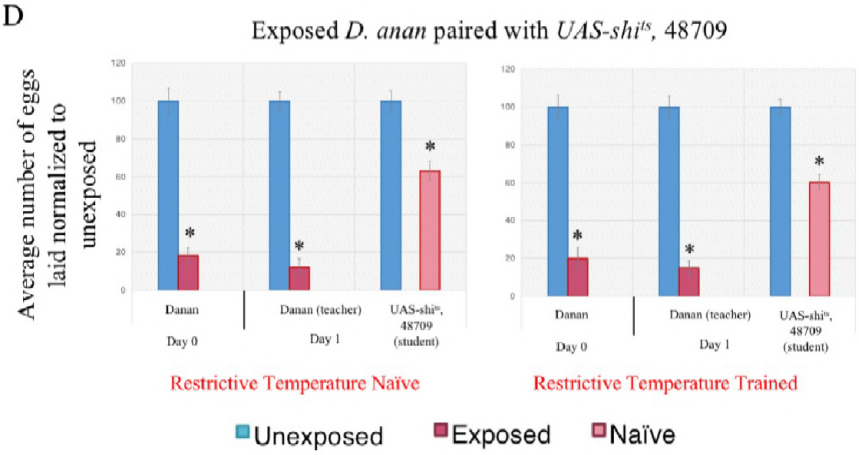
Exposed D. anan paired with UAS-shi^{ts}, 48709
Average number of eggs laid normalized to unexposed
120
100
80
60
40
20
0
*
Danan
Day 0
Danan (teacher)
Day 1
UAS-shi^{ts}, 48709 (student)
Restrictive Temperature Naïve
Restrictive Temperature Trained
Unexposed
Exposed
Naïve

Supplementary Figure 5. The mushroom body is required for dialect learning shown with 48709 driver.

(A) Cartoon schematic of the region of interest. (B) Confocal image of adult brain where 48709-GAL4 is driving UAS-CD8-GFP, stained with nc82 (magenta) and DAPI (teal). Percentage of eggs laid by exposed flies normalized to eggs laid by unexposed flies is shown. UAS-shi^{ts} crossed to 48709-GAL4 trained by *D. ananassae* at the permissive temperature shows wild-type trained state (C), but at the restrictive temperature shows defective acquisition in the trained state (D). Error bars represent standard error (n = 12 biological replicates) (*$p < 0.05$).

A

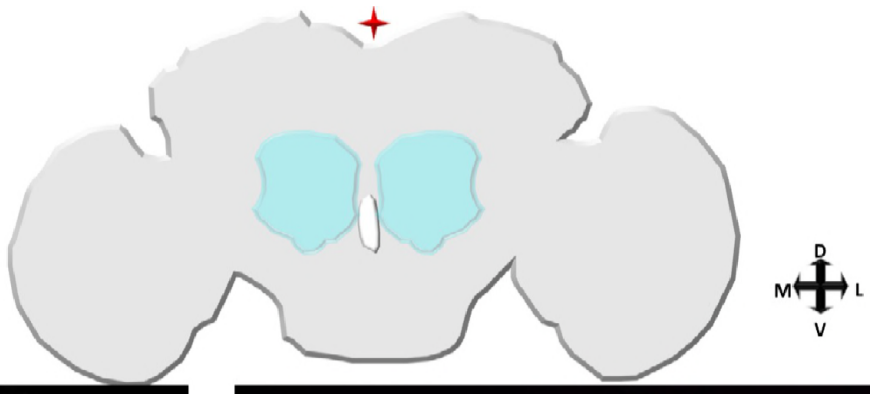
D
M
L
V

B

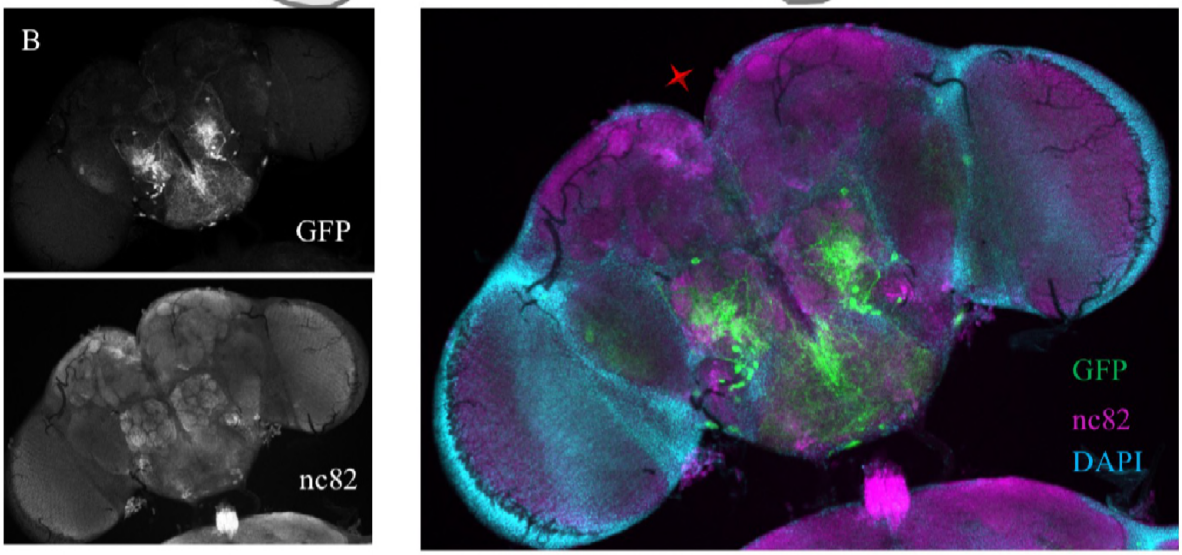
GFP
nc82
GFP
nc82
DAPI

C

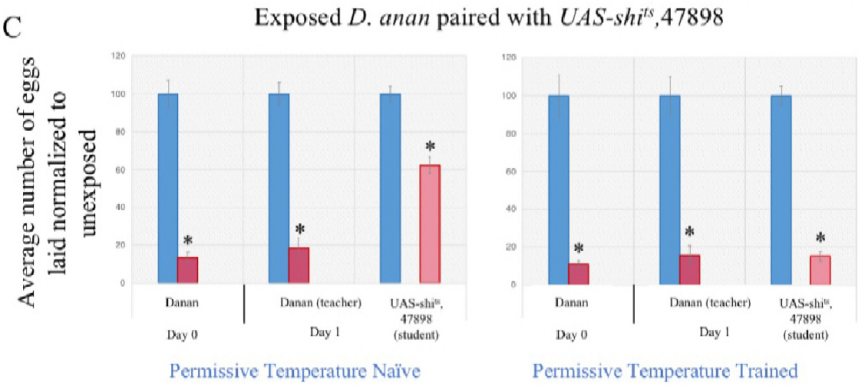
Exposed D. anan paired with UAS-shi^ts,47898
Average number of eggs laid normalized to unexposed
Danan
Day 0
Danan (teacher)
Day 1
UAS-shi^ts, 47898 (student)
Permissive Temperature Naïve
Permissive Temperature Trained

D

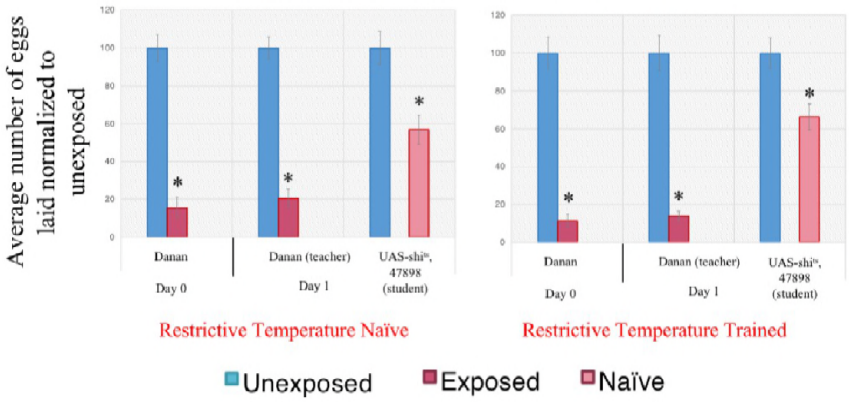
Exposed D. anan paired with UAS-shi^ts, 47898
Average number of eggs laid normalized to unexposed
Danan
Day 0
Danan (teacher)
Day 1
UAS-shi^ts, 47898 (student)
Restrictive Temperature Naïve
Restrictive Temperature Trained
Unexposed
Exposed
Naïve

Supplementary Figure 6. The antennal lobe is required for dialect learning shown with 47898 driver.

(A) Cartoon schematic of the region of interest. (B) Confocal image of adult brain where 47898-GAL4 is driving UAS-CD8-GFP, stained with nc82 (magenta) and DAPI (teal). Fly light intensity/distribution score is 4/4 and was the only region of the brain identified. Percentage of eggs laid by exposed flies normalized to eggs laid by unexposed flies is shown. UAS-shi^{ts} crossed to 47898-GAL4 trained by *D. ananassae* at the permissive temperature shows wild-type trained state (C), but at the restrictive temperature shows defective acquisition in the trained state (D). Error bars represent standard error (n = 12 biological replicates) (*$p < 0.05$).

A

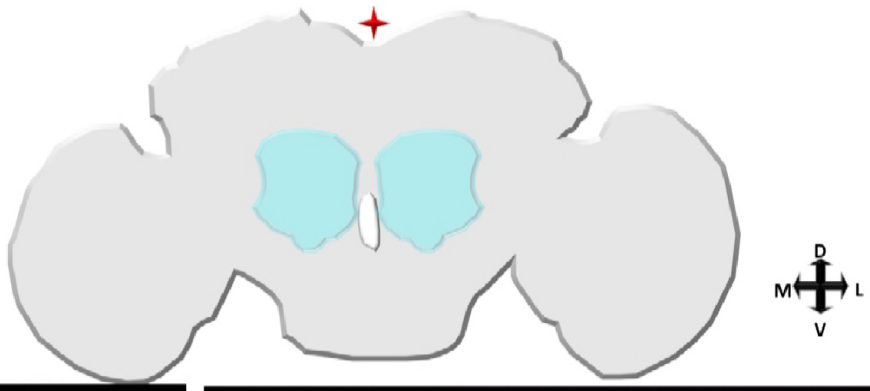
D
M
L
V

B

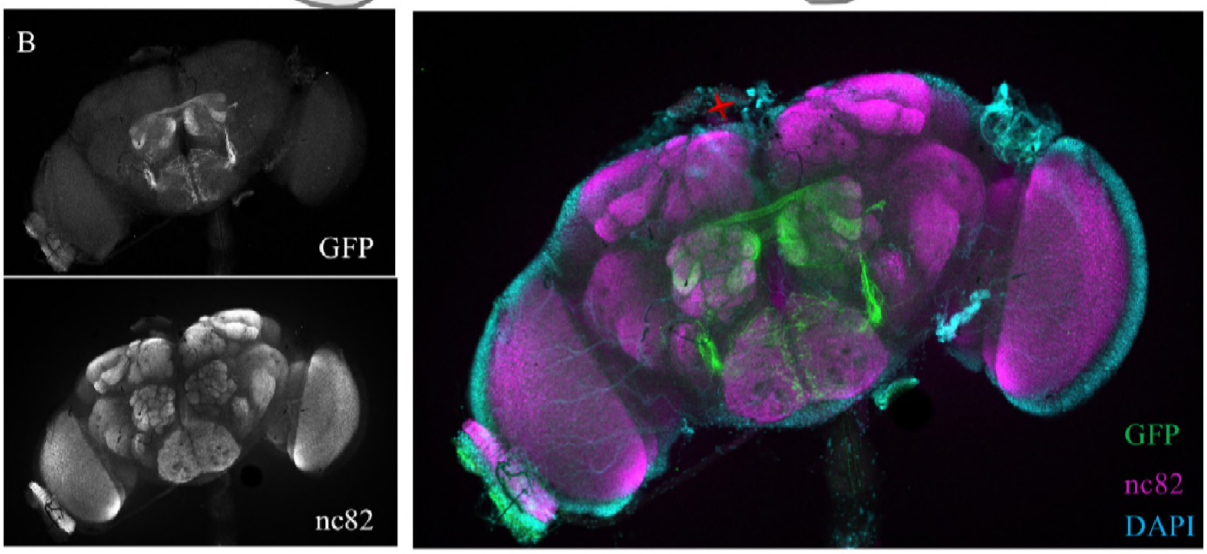
GFP
nc82
GFP
nc82
DAPI

C

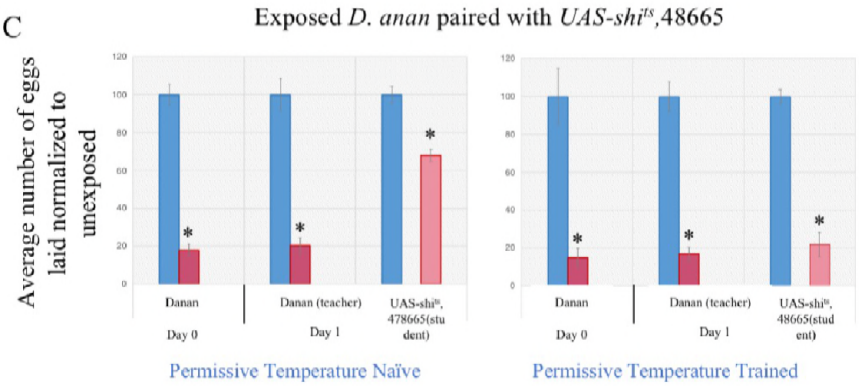
Exposed D. anan paired with UAS-shi^ts,48665
Average number of eggs laid normalized to unexposed
120
100
80
60
40
20
0
*
Danan
Day 0
Danan (teacher)
Day 1
UAS-shi^ts, 478665(student)
UAS-shi^ts, 48665(student)
Permissive Temperature Naïve
Permissive Temperature Trained

D

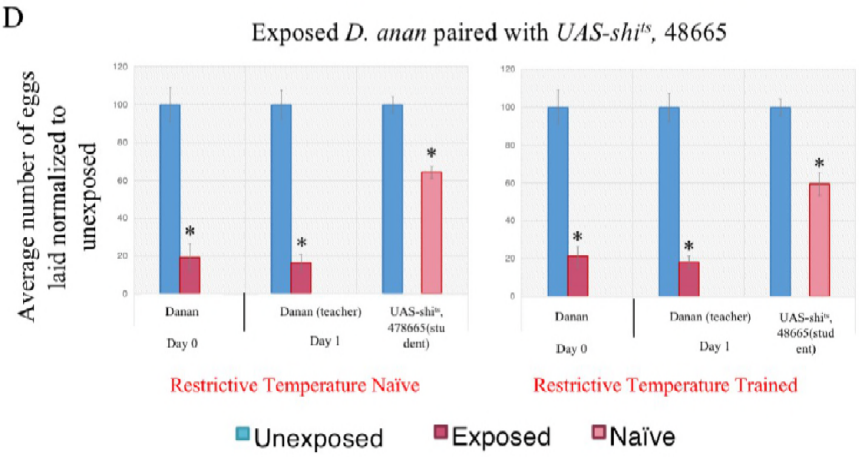
Exposed D. anan paired with UAS-shi^ts, 48665
Average number of eggs laid normalized to unexposed
120
100
80
60
40
20
0
*
Danan
Day 0
Danan (teacher)
Day 1
UAS-shi^ts, 478665(student)
UAS-shi^ts, 48665(student)
Restrictive Temperature Naïve
Restrictive Temperature Trained
Unexposed
Exposed
Naïve

Supplementary Figure 7. The antennal lobe is required for dialect learning shown with 48665 driver.

(A) Cartoon schematic of the region of interest. (B) Confocal image of adult brain where 48665-GAL4 is driving UAS-CD8-GFP, stained with nc82 (magenta) and DAPI (teal). Fly light intensity/distribution score is 5/5 and was the only region of the brain identified. Percentage of eggs laid by exposed flies normalized to eggs laid by unexposed flies is shown. UAS-shi^{ts} crossed to 48665-GAL4 trained by *D. ananassae* at the permissive temperature shows wild-type trained state (C), but at the restrictive temperature shows defective acquisition in the trained state (D). Error bars represent standard error (n = 12 biological replicates) (*$p < 0.05$).

A

D
M
L
V

B

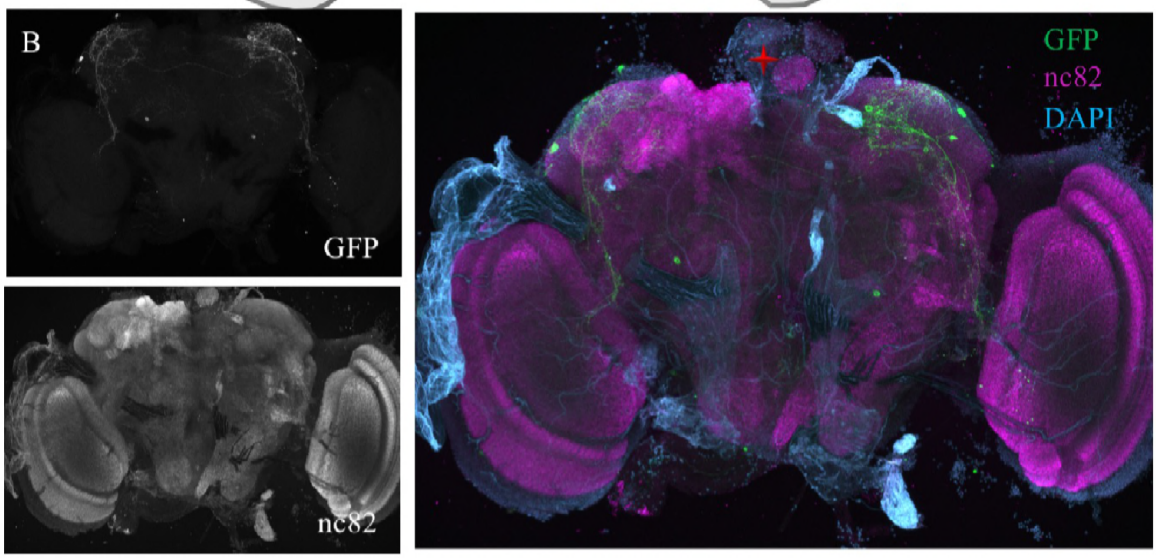
GFP
nc82
GFP
nc82
DAPI

C

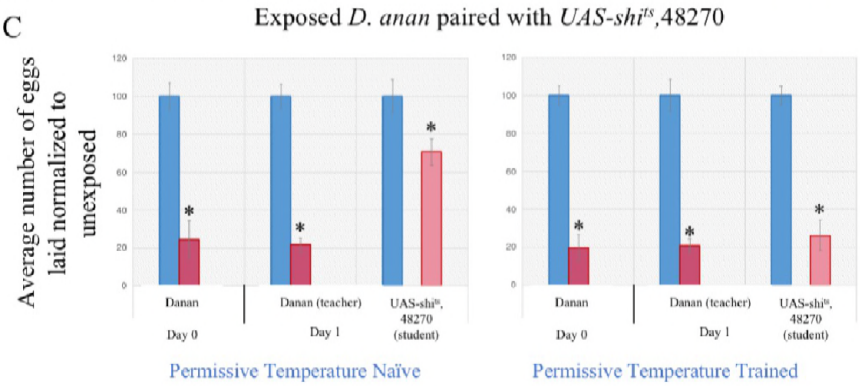
Exposed D. anan paired with UAS-shi^ts,48270
Average number of eggs laid normalized to unexposed
120
100
80
60
40
20
0
*
Danan
Day 0
Danan (teacher)
Day 1
UAS-shi^ts, 48270 (student)
Permissive Temperature Naïve
Permissive Temperature Trained

D

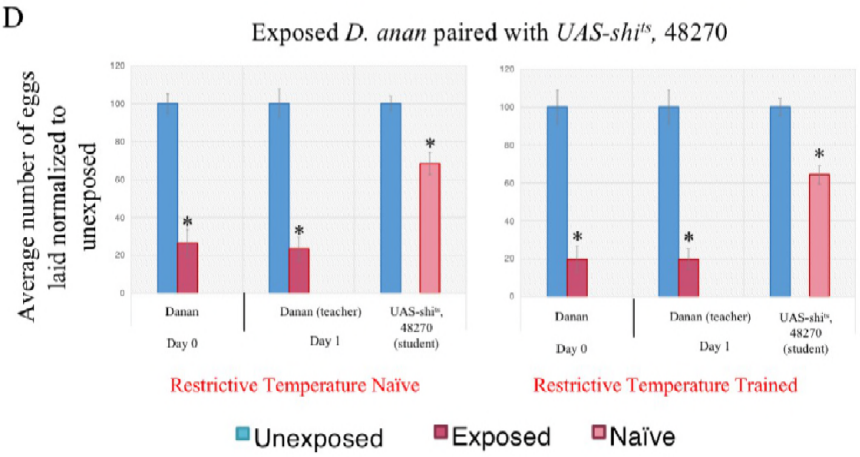
Exposed D. anan paired with UAS-shi^ts, 48270
Average number of eggs laid normalized to unexposed
120
100
80
60
40
20
0
*
Danan
Day 0
Danan (teacher)
Day 1
UAS-shi^ts, 48270 (student)
Restrictive Temperature Naïve
Restrictive Temperature Trained
Unexposed
Exposed
Naïve

Supplementary Figure 8. The lateral horn is required for dialect learning shown with 48270 driver.

(A) Cartoon schematic of the region of interest. (B) Confocal image of adult brain where 48270-GAL4 is driving UAS-CD8-GFP, stained with nc82 (magenta) and DAPI (teal). Fly light intensity/distribution score is 2/2 and was the only region of the brain identified. Percentage of eggs laid by exposed flies normalized to eggs laid by unexposed flies is shown. UAS-shi^{ts} crossed to 48270-GAL4 trained by *D. ananassae* at the permissive temperature shows wild-type trained state (C), but at the restrictive temperature shows defective acquisition in the trained state (D). Error bars represent standard error (n = 12 biological replicates) (*$p < 0.05$).

A

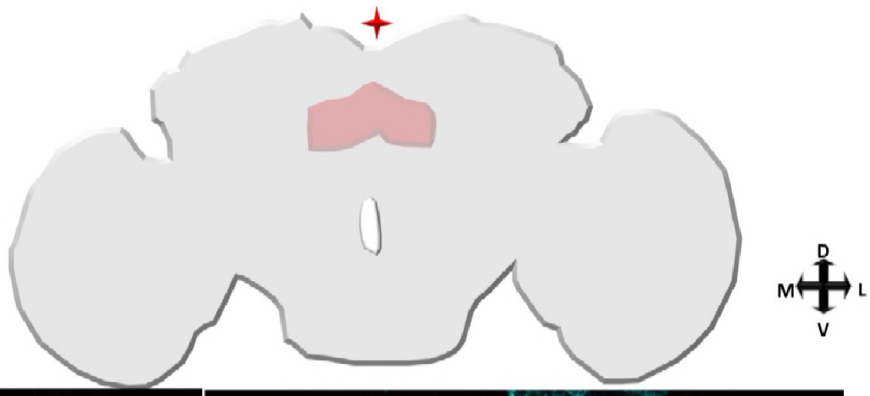
D
M
L
V

B

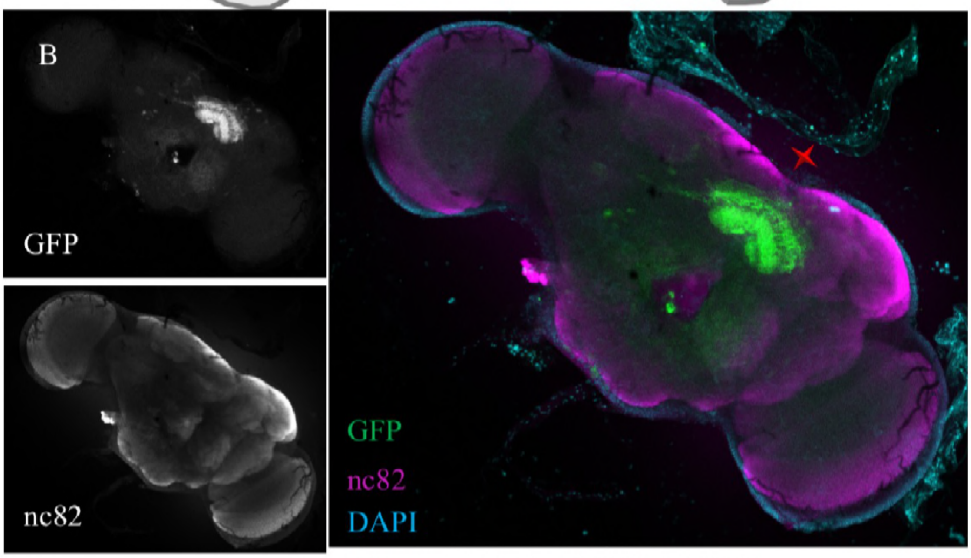
GFP
nc82
GFP
nc82
DAPI

C

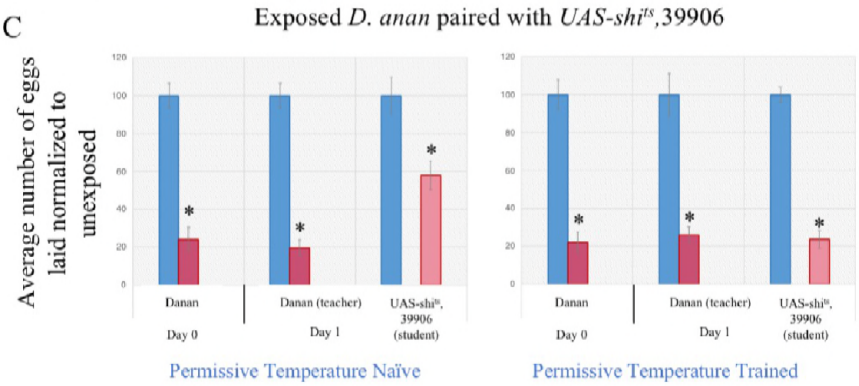
Exposed D. anan paired with UAS-shi^{ts},39906
Average number of eggs laid normalized to unexposed
120
100
80
60
40
20
0
*
Danan
Day 0
Danan (teacher)
Day 1
UAS-shi^{ts}, 39906 (student)
Permissive Temperature Naïve
Permissive Temperature Trained

D

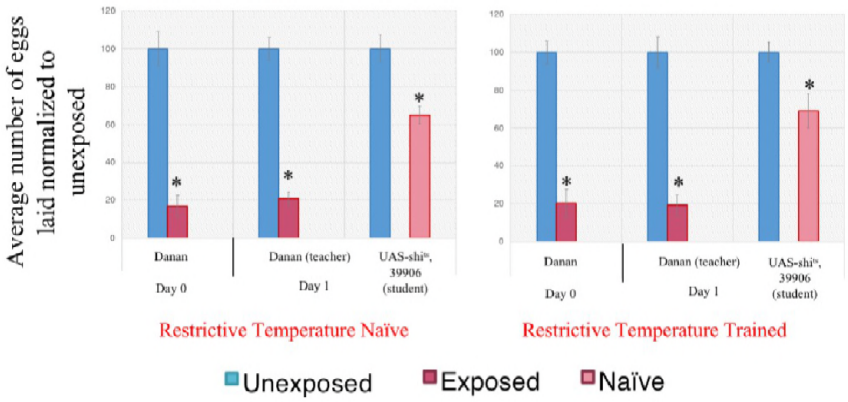
Exposed D. anan paired with UAS-shi^{ts}, 39906
Average number of eggs laid normalized to unexposed
120
100
80
60
40
20
0
*
Danan
Day 0
Danan (teacher)
Day 1
UAS-shi^{ts}, 39906 (student)
Restrictive Temperature Naïve
Restrictive Temperature Trained
Unexposed
Exposed
Naïve

Supplementary Figure 9. The fan-shaped body is required for dialect learning shown with 39906 driver.

(A) Cartoon schematic of the region of interest. (B) Confocal image of adult brain where 39906-GAL4 is driving UAS-CD8-GFP, stained with nc82 (magenta) and DAPI (teal). Fly light intensity/distribution score is 5/3 and was the only region of the brain identified. Percentage of eggs laid by exposed flies normalized to eggs laid by unexposed flies is shown. UAS-shi^{ts} crossed to 39906-GAL4 trained by *D. ananassae* at the permissive temperature shows wild-type trained state (C), but at the restrictive temperature shows defective acquisition in the trained state (D). Error bars represent standard error (n = 12 biological replicates) (*$p < 0.05$).

A

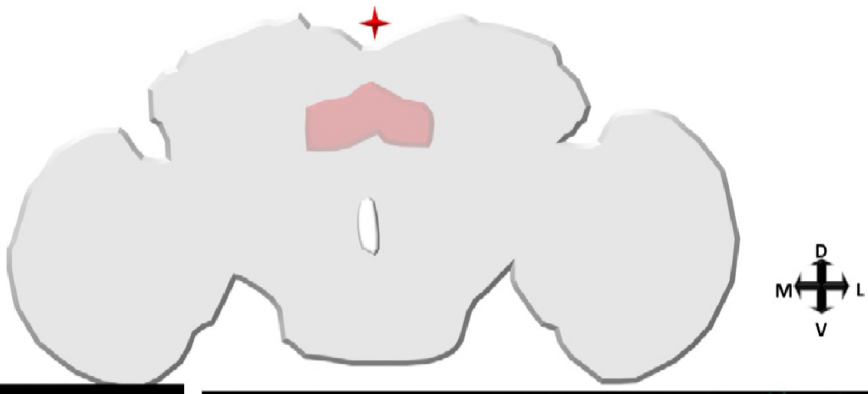
D
M
L
V

B

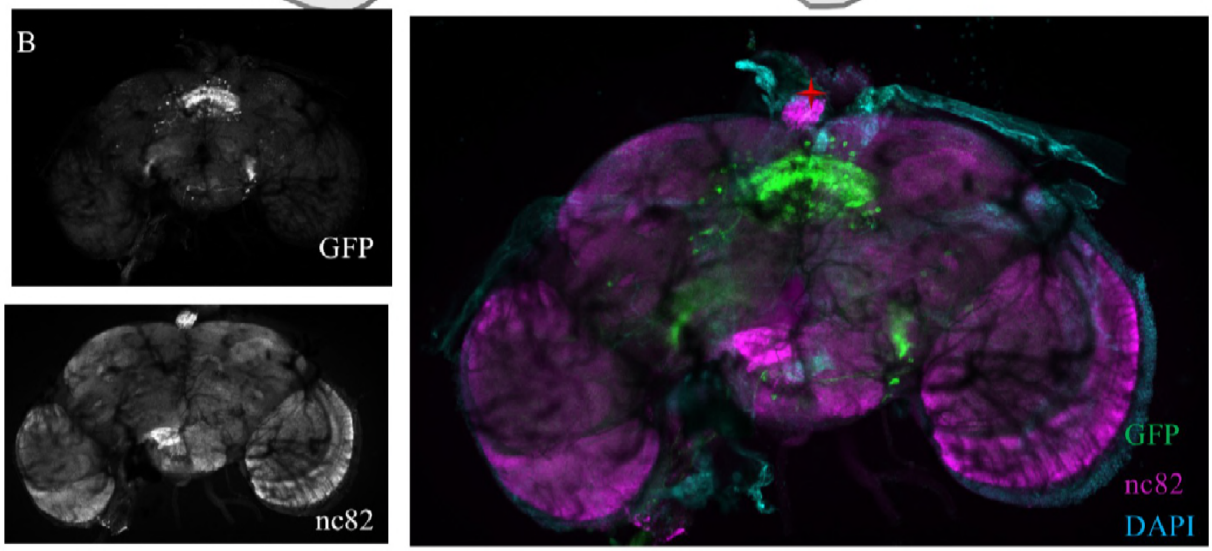
GFP
nc82
GFP
nc82
DAPI

C

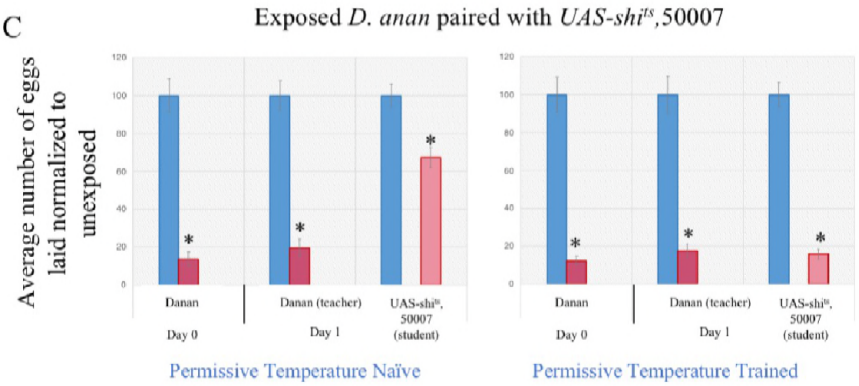
Exposed D. anan paired with UAS-shi^ts,50007
Average number of eggs laid normalized to unexposed
120
100
80
60
40
20
0
*
Danan
Day 0
Danan (teacher)
Day 1
UAS-shi^ts, 50007 (student)
Permissive Temperature Naïve
Permissive Temperature Trained

D

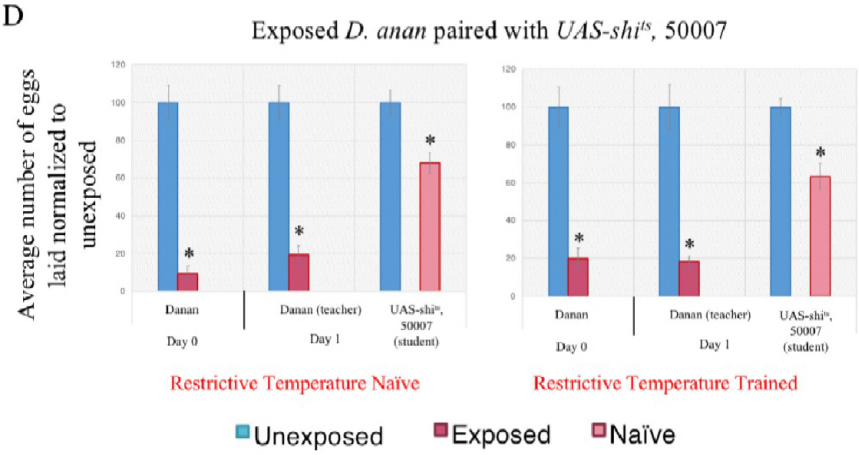
Exposed D. anan paired with UAS-shi^ts, 50007
Average number of eggs laid normalized to unexposed
120
100
80
60
40
20
0
*
Danan
Day 0
Danan (teacher)
Day 1
UAS-shi^ts, 50007 (student)
Restrictive Temperature Naïve
Restrictive Temperature Trained
Unexposed
Exposed
Naïve

Supplementary Figure 10. The fan-shaped body is required for dialect learning shown with 50007 driver.

(A) Cartoon schematic of the region of interest. (B) Confocal image of adult brain where 50007-GAL4 is driving UAS-CD8-GFP, stained with nc82 (magenta) and DAPI (teal). Fly light intensity/distribution score is 3/3 and was the only region of the brain identified. Percentage of eggs laid by exposed flies normalized to eggs laid by unexposed flies is shown. UAS-shi^{ts} crossed to 50007-GAL4 trained by *D. ananassae* at the permissive temperature shows wild-type trained state (C), but at the restrictive temperature shows defective acquisition in the trained state (D). Error bars represent standard error (n = 12 biological replicates) (*$p < 0.05$).

A

D
M
L
V

B

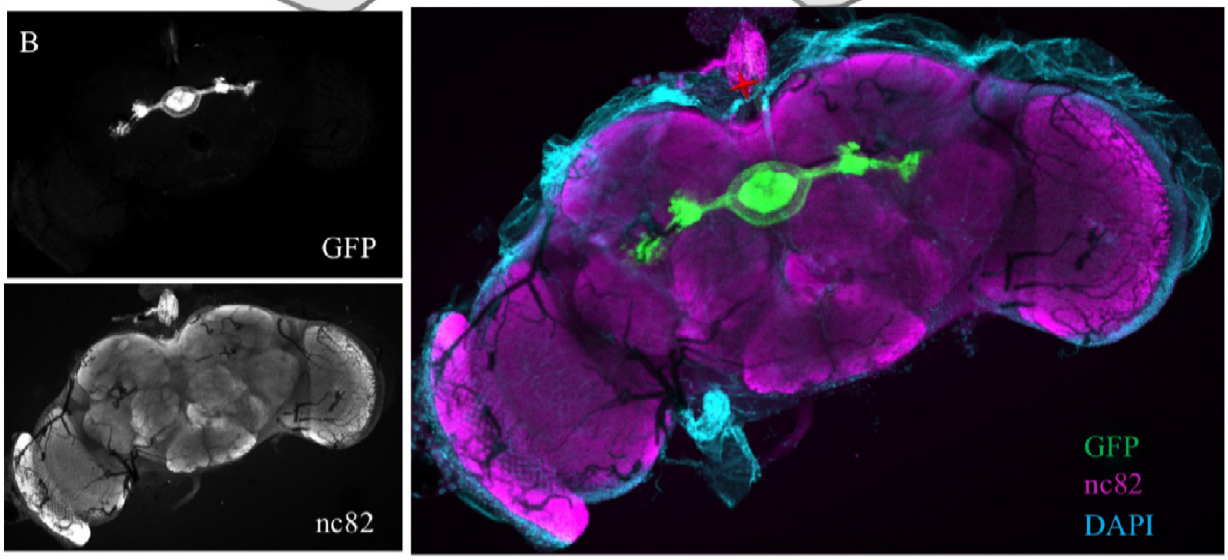
GFP
nc82
GFP
nc82
DAPI

C

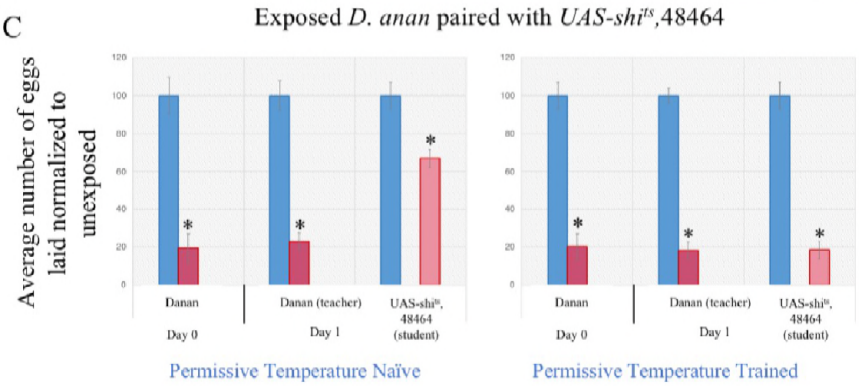
Exposed D. anan paired with UAS-shi^{ts},48464
Average number of eggs laid normalized to unexposed
120
100
80
60
40
20
0
*
Danan
Day 0
Danan (teacher)
Day 1
UAS-shi^{ts}, 48464 (student)
Permissive Temperature Naïve
Permissive Temperature Trained

D

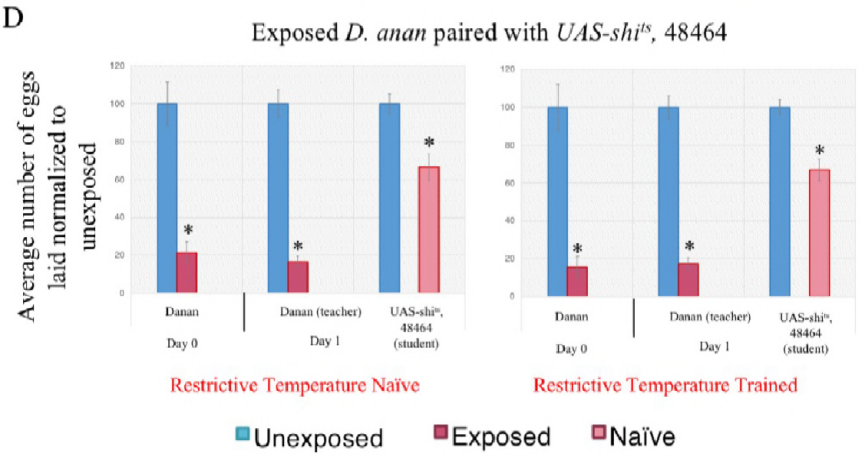
Exposed D. anan paired with UAS-shi^{ts}, 48464
Average number of eggs laid normalized to unexposed
120
100
80
60
40
20
0
*
Danan
Day 0
Danan (teacher)
Day 1
UAS-shi^{ts}, 48464 (student)
Restrictive Temperature Naïve
Restrictive Temperature Trained
Unexposed
Exposed
Naïve

Supplementary Figure 11. The ellipsoid body is required for dialect learning shown with 48464 driver.

(A) Cartoon schematic of the region of interest. (B) Confocal image of adult brain where 48464-GAL4 is driving UAS-CD8-GFP, stained with nc82 (magenta) and DAPI (teal). Fly light intensity/distribution score is 3/5 and was the only region of the brain identified. Percentage of eggs laid by exposed flies normalized to eggs laid by unexposed flies is shown. UAS-shi^{ts} crossed to 48464-GAL4 trained by *D. ananassae* at the permissive temperature shows wild-type trained state (C), but at the restrictive temperature shows defective acquisition in the trained state (D). Error bars represent standard error (n = 12 biological replicates) (*$p < 0.05$).

A

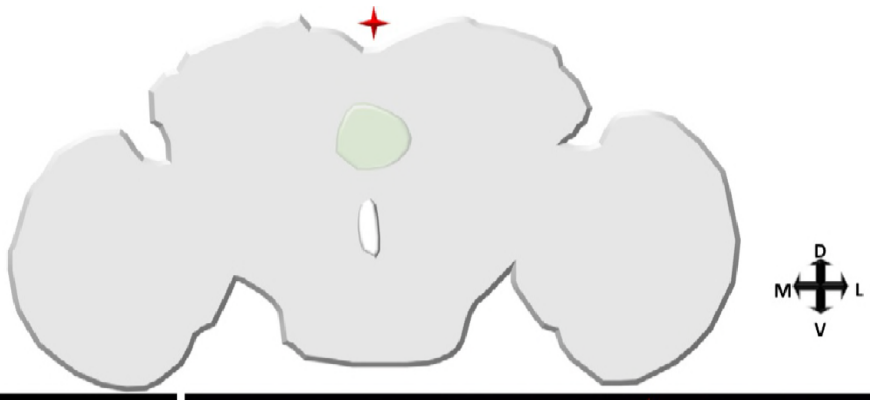
D
M
L
V

B

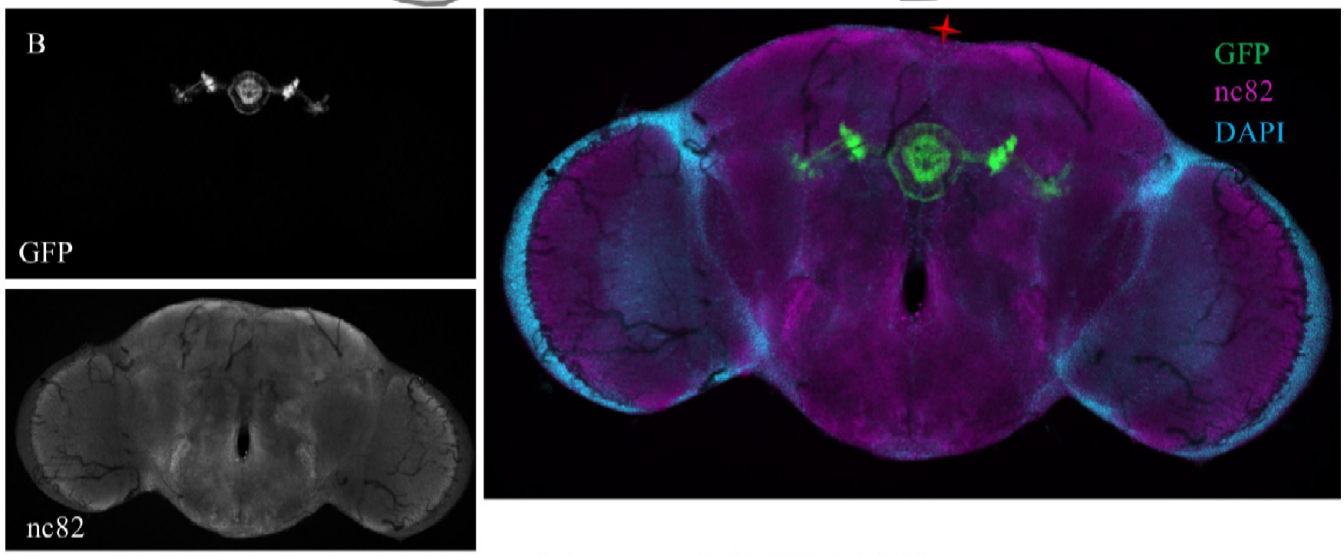
GFP
nc82
GFP
nc82
DAPI

C

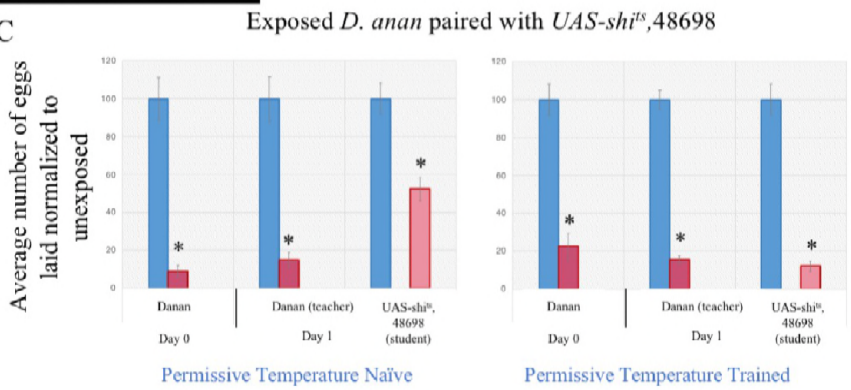
Exposed D. anan paired with UAS-shi^ts,48698
Average number of eggs laid normalized to unexposed
120
100
80
60
40
20
0
*
Danan
Day 0
Danan (teacher)
Day 1
UAS-shi^ts, 48698 (student)
Permissive Temperature Naïve
Permissive Temperature Trained

D

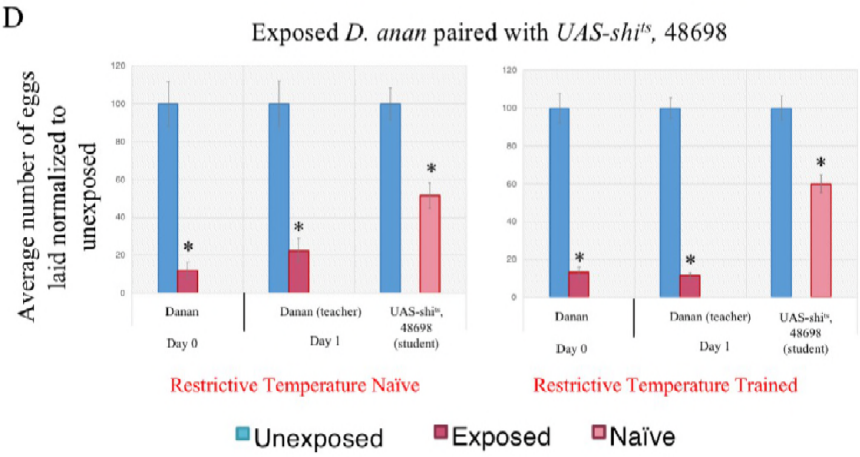
Exposed D. anan paired with UAS-shi^ts, 48698
Average number of eggs laid normalized to unexposed
120
100
80
60
40
20
0
*
Danan
Day 0
Danan (teacher)
Day 1
UAS-shi^ts, 48698 (student)
Restrictive Temperature Naïve
Restrictive Temperature Trained
Unexposed
Exposed
Naïve

Supplementary Figure 12. The ellipsoid body is required for dialect learning shown with 48698 driver.

(A) Cartoon schematic of the region of interest. (B) Confocal image of adult brain where 48698-GAL4 is driving UAS-CD8-GFP, stained with nc82 (magenta) and DAPI (teal). Fly light intensity/distribution score is 5/5 and was the only region of the brain identified. Percentage of eggs laid by exposed flies normalized to eggs laid by unexposed flies is shown. UAS-shi^{ts} crossed to 48698-GAL4 trained by *D. ananassae* at the permissive temperature shows wild-type trained state (C), but at the restrictive temperature shows defective acquisition in the trained state (D). Error bars represent standard error (n = 12 biological replicates) (*$p < 0.05$).

A

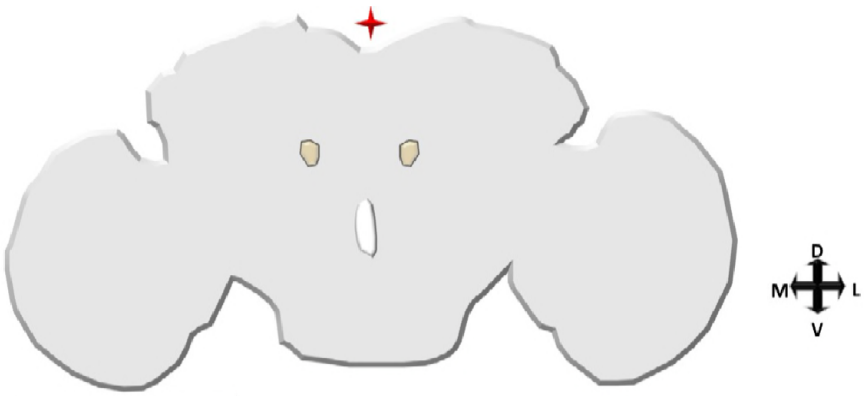
D
M
L
V

B

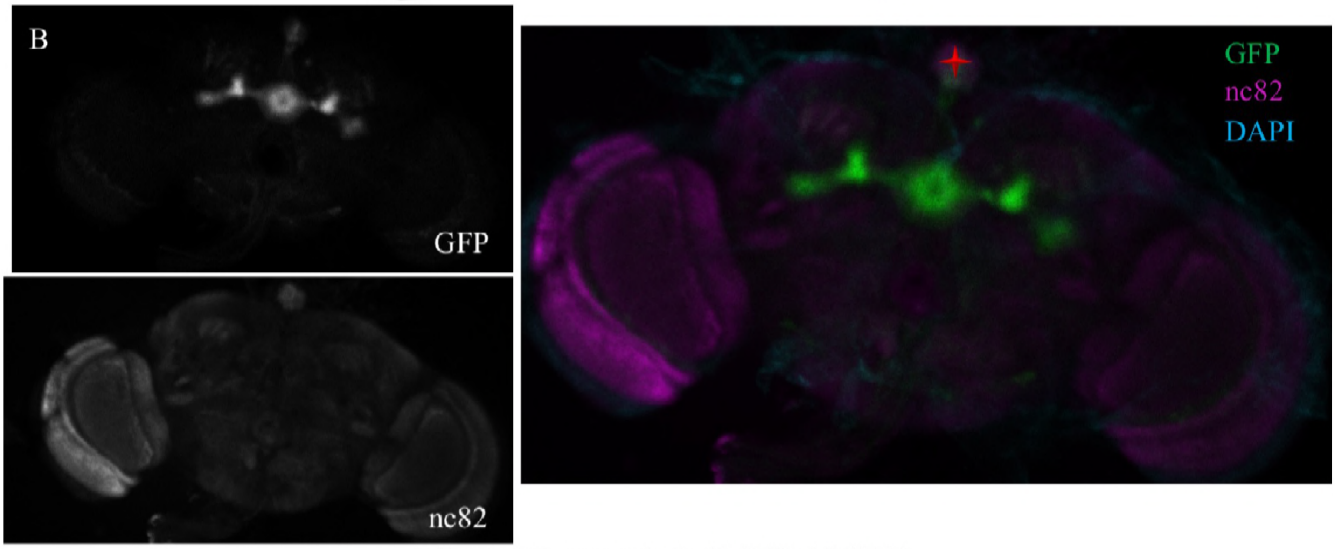
GFP
nc82
GFP
nc82
DAPI

C

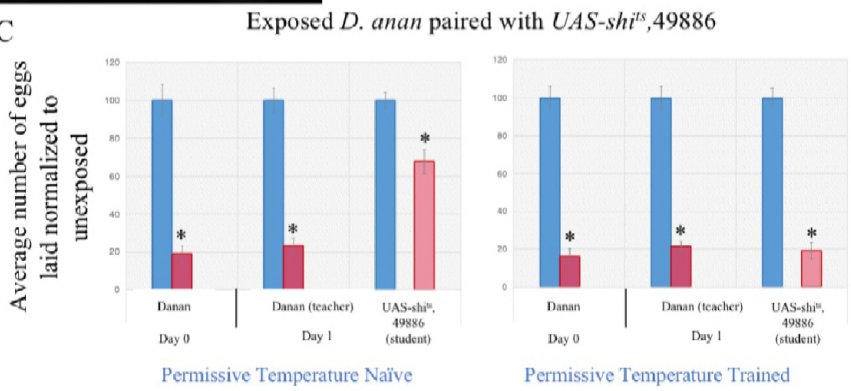
Exposed D. anan paired with UAS-shi^{ts},49886
Average number of eggs laid normalized to unexposed
120
100
80
60
40
20
0
*
Danan
Day 0
Danan (teacher)
Day 1
UAS-shi^{ts}, 49886 (student)
Permissive Temperature Naïve
Permissive Temperature Trained

D

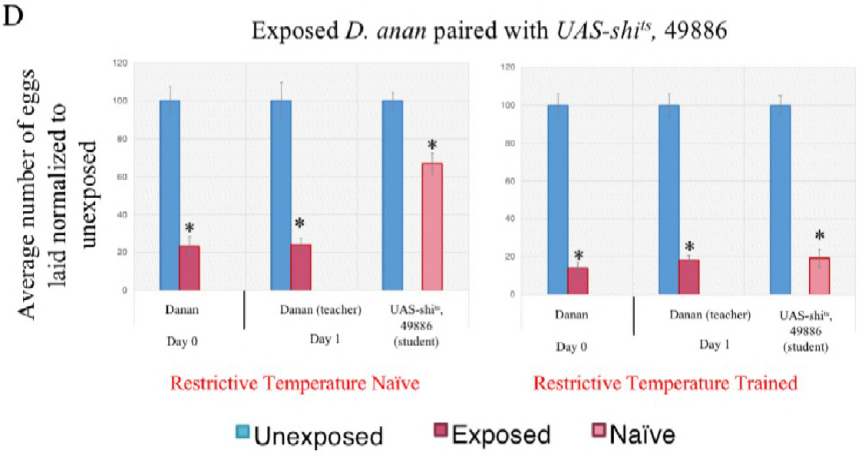
Exposed D. anan paired with UAS-shi^{ts}, 49886
Average number of eggs laid normalized to unexposed
120
100
80
60
40
20
0
*
Danan
Day 0
Danan (teacher)
Day 1
UAS-shi^{ts}, 49886 (student)
Restrictive Temperature Naïve
Restrictive Temperature Trained
Unexposed
Exposed
Naïve

Supplementary Figure 13. The bulb is dispensable for dialect learning shown with 49886 driver.

(A) Cartoon schematic of the region of interest. (B) Confocal image of adult brain where 49886-GAL4 is driving UAS-CD8-GFP, stained with nc82 (magenta) and DAPI (teal). Fly light intensity/distribution score is 5/4 and was the only region of the brain identified. Percentage of eggs laid by exposed flies normalized to eggs laid by unexposed flies is shown. Percentage of eggs laid by exposed flies normalized to eggs laid by unexposed flies is shown. UAS-shi^{ts} crossed to 49886-GAL4 trained by *D. ananassae* at both the permissive temperature (C) and restrictive temperature (D) shows wild-type trained state. Error bars represent standard error (n = 12 biological replicates) (*$p < 0.05$).

A

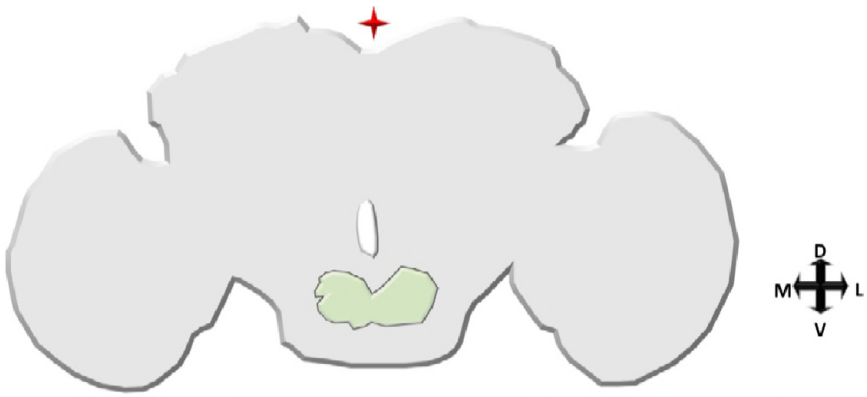
D
M
L
V

B

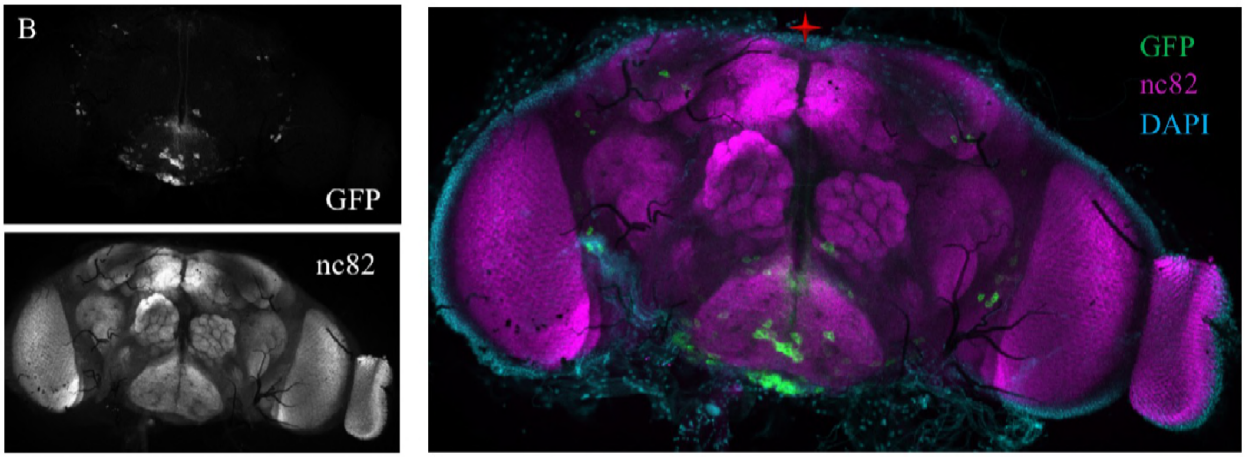
GFP
nc82
GFP
nc82
DAPI

C

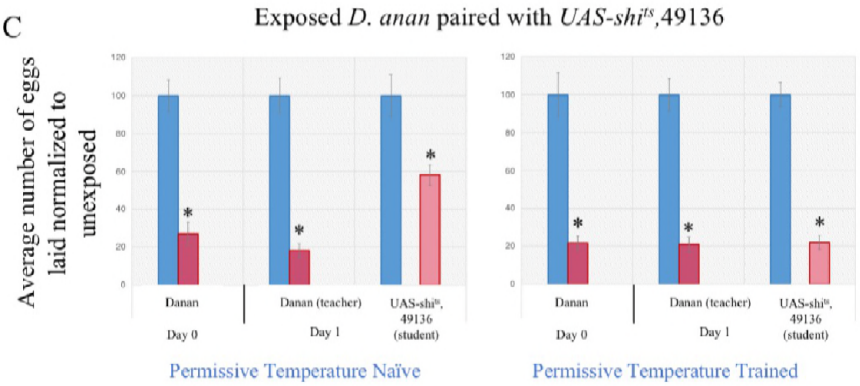
Exposed D. anan paired with UAS-shi^{ts},49136
Average number of eggs laid normalized to unexposed
Danan
Day 0
Danan (teacher)
Day 1
UAS-shi^{ts}, 49136 (student)
Permissive Temperature Naïve
Permissive Temperature Trained

D

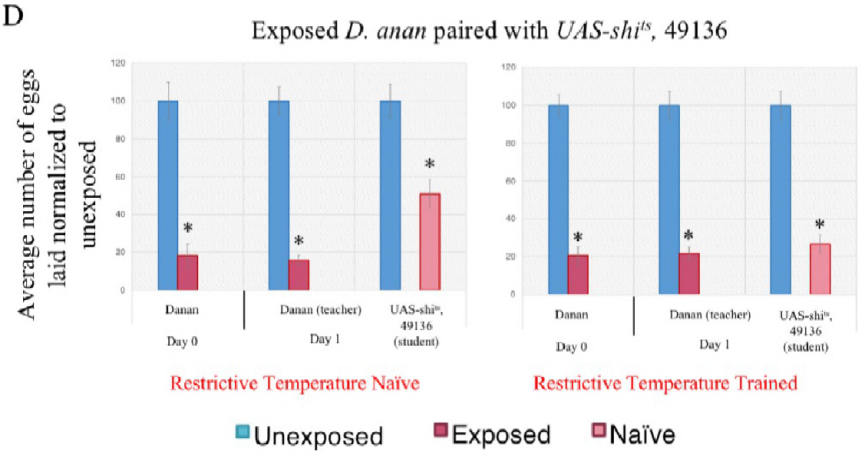
Exposed D. anan paired with UAS-shi^{ts}, 49136
Average number of eggs laid normalized to unexposed
Danan
Day 0
Danan (teacher)
Day 1
UAS-shi^{ts}, 49136 (student)
Restrictive Temperature Naïve
Restrictive Temperature Trained
Unexposed
Exposed
Naïve

Supplementary Figure 14. The prow is dispensable for dialect learning shown with 49136 driver.

(A) Cartoon schematic of the region of interest. (B) Confocal image of adult brain where 49136-GAL4 is driving UAS-CD8-GFP, stained with nc82 (magenta) and DAPI (teal). Fly light intensity/distribution score is 4/4 and was the only region of the brain identified. Percentage of eggs laid by exposed flies normalized to eggs laid by unexposed flies is shown. UAS-shi^{ts} crossed to 49136-GAL4 trained by *D. ananassae* at both the permissive temperature (C) and restrictive temperature (D) shows wild-type trained state. Error bars represent standard error (n = 12 biological replicates) (*$p < 0.05$).

A

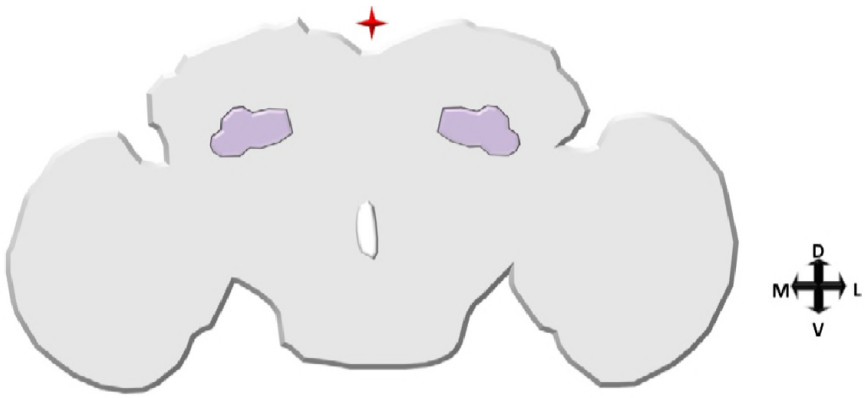
D
M
L
V

B

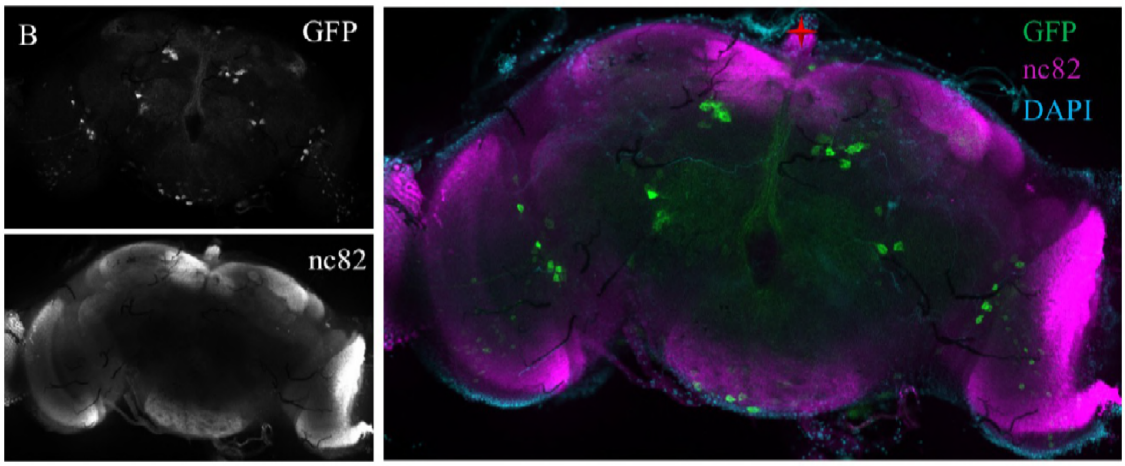
GFP
nc82
GFP
nc82
DAPI

C

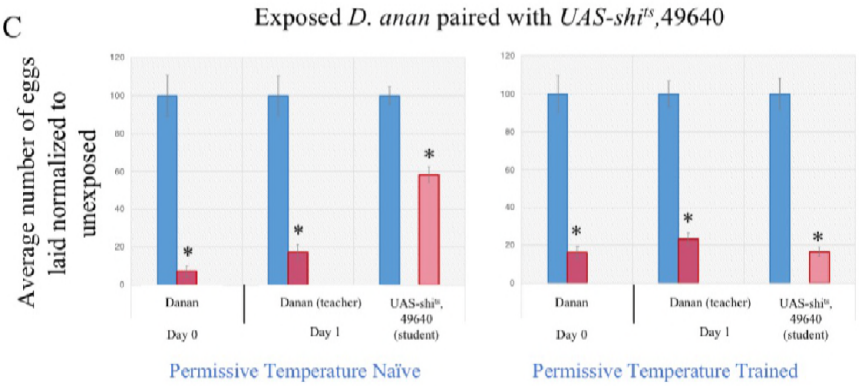
Exposed D. anan paired with UAS-shi^ts,49640
Average number of eggs laid normalized to unexposed
Danan
Day 0
Danan (teacher)
Day 1
UAS-shi^ts, 49640 (student)
Permissive Temperature Naïve
Permissive Temperature Trained

D

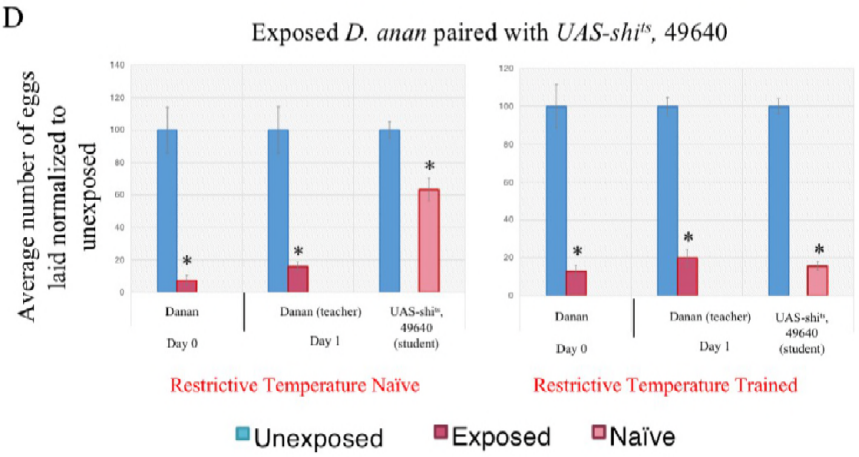
Exposed D. anan paired with UAS-shi^ts, 49640
Average number of eggs laid normalized to unexposed
Danan
Day 0
Danan (teacher)
Day 1
UAS-shi^ts, 49640 (student)
Restrictive Temperature Naïve
Restrictive Temperature Trained
Unexposed
Exposed
Naïve

Supplementary Figure 15. The superior clamp is dispensable for dialect learning shown with 49640 driver.

(A) Cartoon schematic of the region of interest. (B) Confocal image of adult brain where 49640-GAL4 is driving UAS-CD8-GFP, stained with nc82 (magenta) and DAPI (teal). Fly light intensity/distribution score is 3/3 and was the only region of the brain identified. Percentage of eggs laid by exposed flies normalized to eggs laid by unexposed flies is shown. UAS-shi^{ts} crossed to 49640-GAL4 trained by *D. ananassae* at both the permissive temperature (C) and restrictive temperature (D) shows wild-type trained state. Error bars represent standard error (n = 12 biological replicates) (*$p < 0.05$).

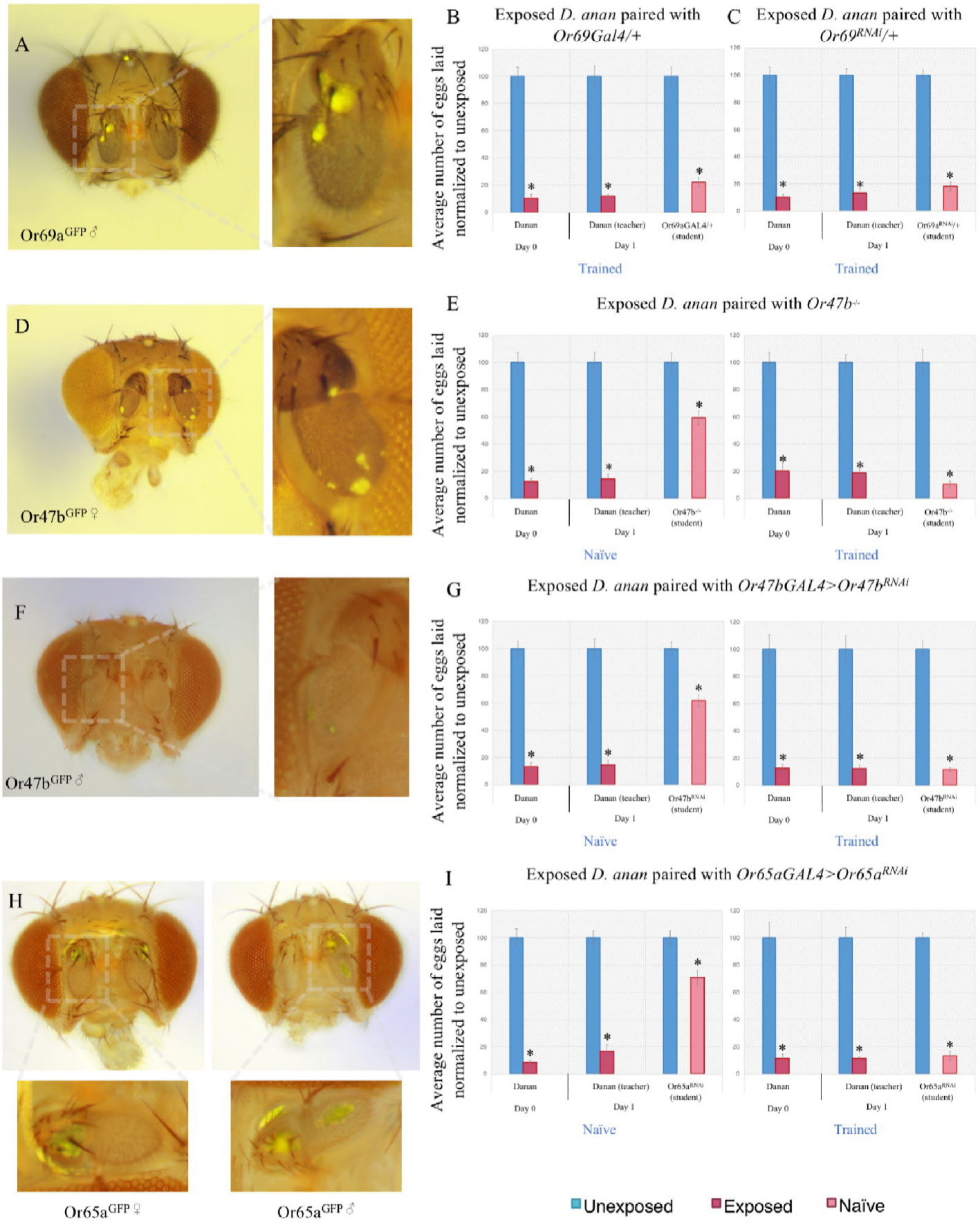
A
Or69a^{GFP} ♂
B
Exposed *D. anan* paired with *Or69Gal4/+*
C
Exposed *D. anan* paired with *Or69^{RNAi}/+*
Average number of eggs laid normalized to unexposed
Danan
Day 0
Danan (teacher)
Day 1
Or69aGAL4/+ (student)
Or69a$^{RNAi/+}$ (student)
Trained
D
Or47b^{GFP} ♀
E
Exposed *D. anan* paired with *Or47b$^{-/-}$*
Or47b$^{-/-}$ (student)
Naïve
F
Or47b^{GFP} ♂
G
Exposed *D. anan* paired with *Or47bGAL4>Or47b^{RNAi}*
Or47b^{RNAi} (student)
H
Or65a^{GFP} ♀
Or65a^{GFP} ♂
I
Exposed *D. anan* paired with *Or65aGAL4>Or65a^{RNAi}*
Or65a^{RNAi} (student)
Unexposed
Exposed
Naïve

Supplementary Figure 16. Further evidence implicating the role of *Or69a* in dialect learning.

(A) Expression of Or69a using the Or69a^{GFP} construct highlighting expression in the antenna in males. Dotted boxes indicate regions of magnification. Percentage of eggs laid by exposed flies normalized to eggs laid by unexposed flies is shown. Or69aGAL4/+ and Or69a^{RNAi}/+ show wild-type trained behavior (B-C). (D) Female expression of Or49b using the Or49b ^{GFP} construct highlighting expression in the antenna. Or49b$^{-/-}$ shows wild-type naïve behavior, and are able to learn the dialect from *D. ananassae* following training (E). Female expression of Or49b using the Or49b ^{GFP} construct highlighting expression in the antenna (F). Or49b^{GAL4} driving Or49b^{RNAi} shows wild-type naïve behavior and can learn the dialect from *D. ananassae* following training (G). Male and female expression of Or65a using the Or65a ^{GFP} construct highlighting expression in the antenna (H). Or65a^{GAL4} driving Or65a^{RNAi} shows wild-type naïve behavior and can learn the dialect from *D. ananassae* following training (I) Error bars represent standard error (n = 12 biological replicates) (*$p < 0.05$).

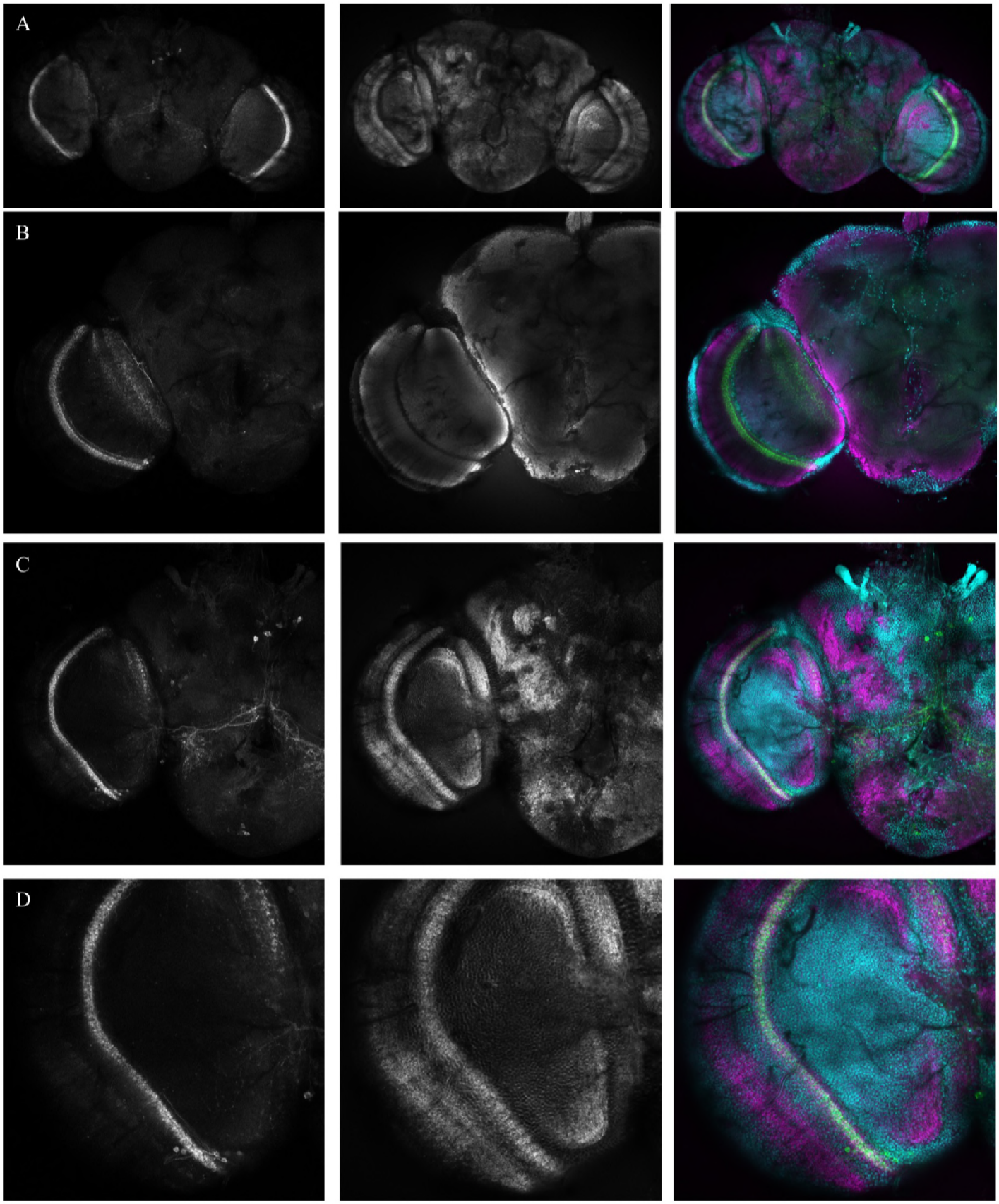

GFP nc82 merge

Supplementary Figure 17. Expression pattern of the L1 line used.

(A-D) Confocal image of adult brain where L1-GAL4 is driving UAS-CD8-GFP, stained with nc82 (magenta) and DAPI (teal).

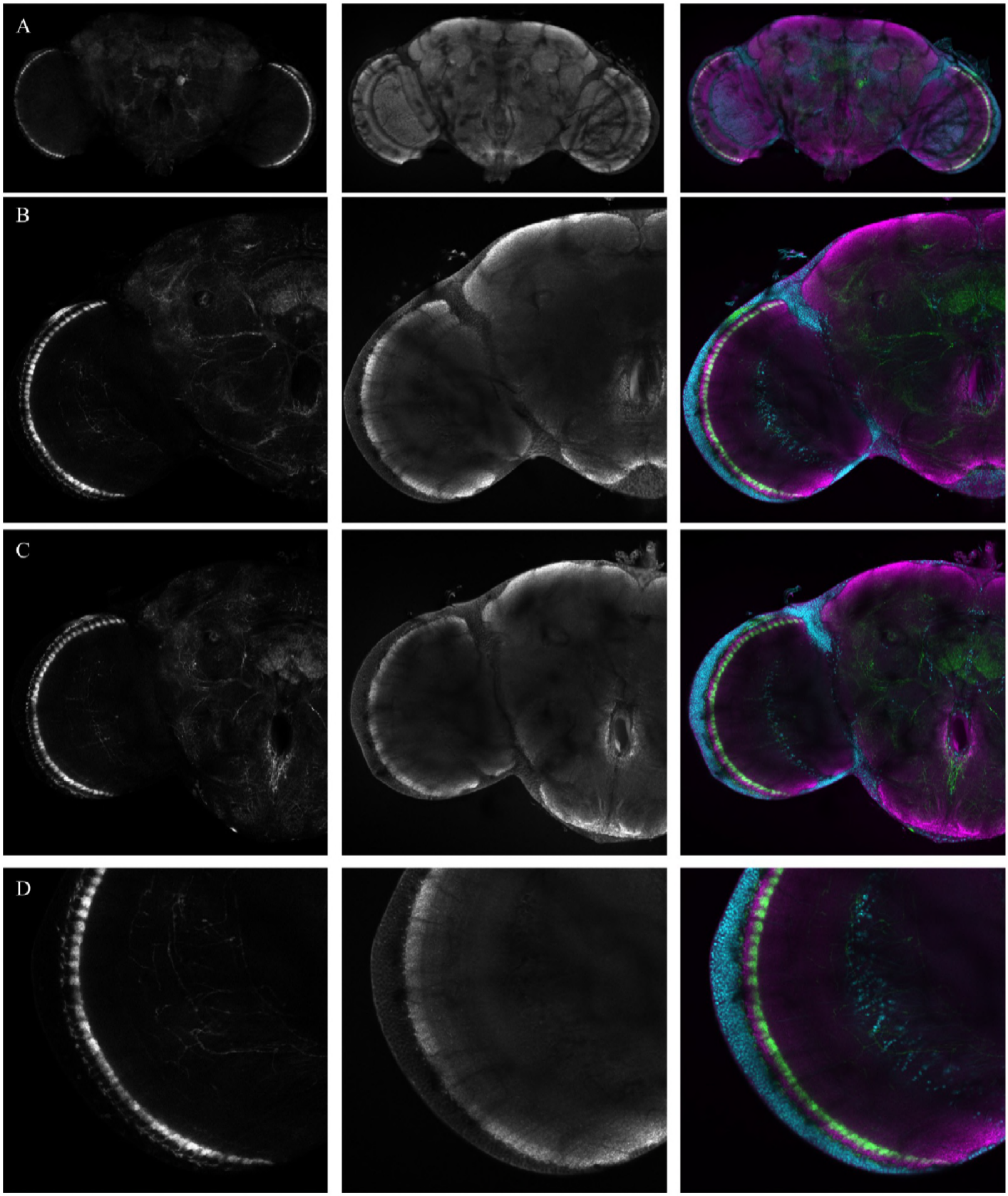

GFP nc82 merge

Supplementary Figure 18. Expression pattern of the L2 line used.

(A-D) Confocal image of adult brain where L2-GAL4 is driving UAS-CD8-GFP, stained with nc82 (magenta) and DAPI (teal).

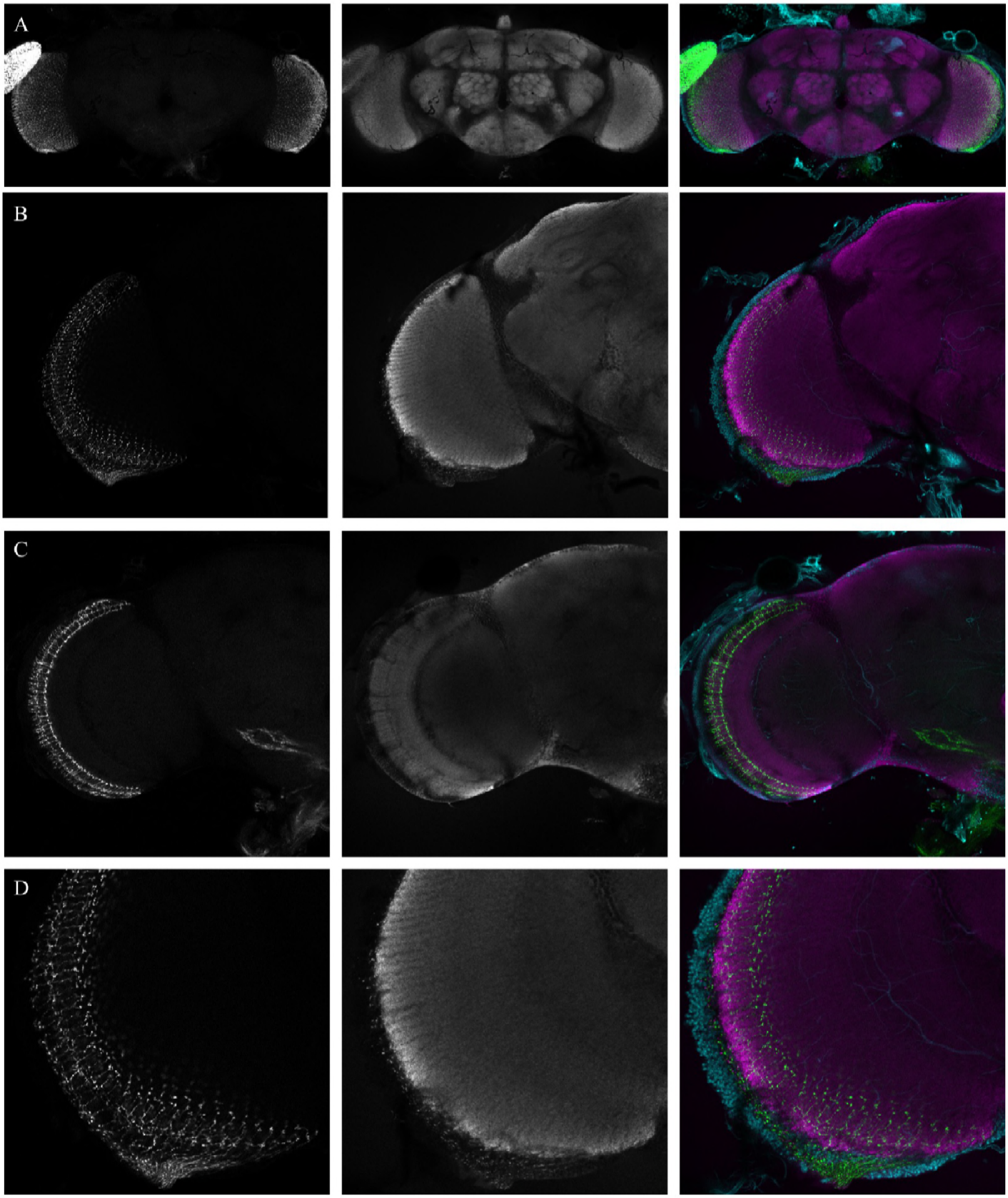
A
B
C
D
GFP
nc82
merge

Supplementary Figure 19. Expression pattern of the $L4^{0987}$ line used.

(A-D) Confocal image of adult brain where $L4^{0987}$-GAL4 is driving UAS-CD8-GFP, stained with nc82 (magenta) and DAPI (teal).

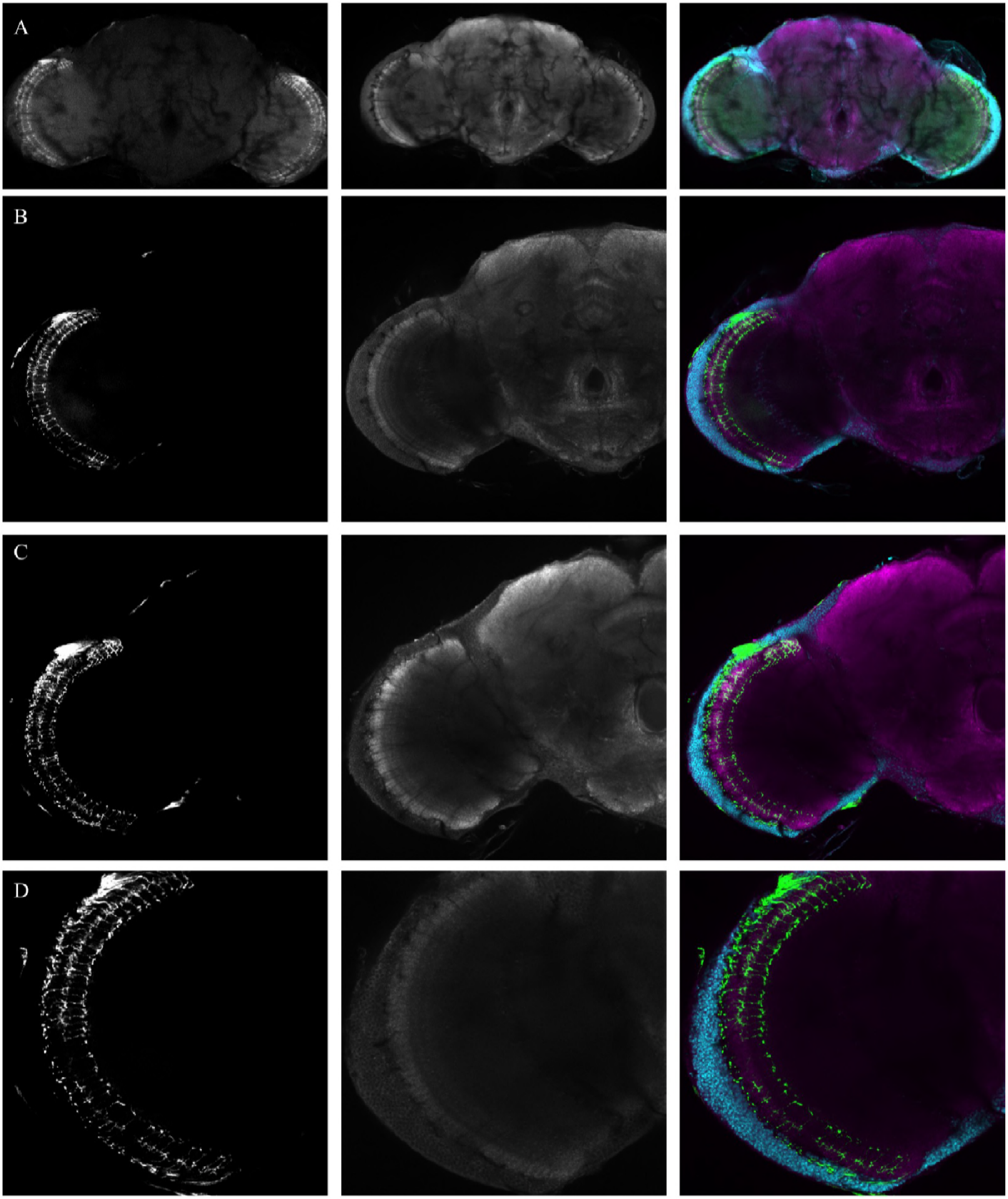

GFP nc82 merge

Supplementary Figure 20. Expression pattern of the splitL4 line used.

(A-D) Confocal image of adult brain where splitL4-GAL4 is driving UAS-CD8-GFP, stained with nc82 (magenta) and DAPI (teal).

A

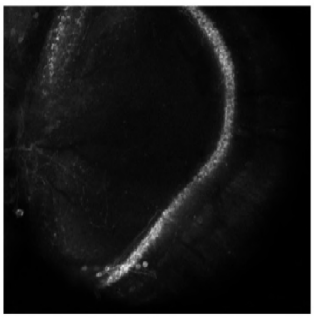

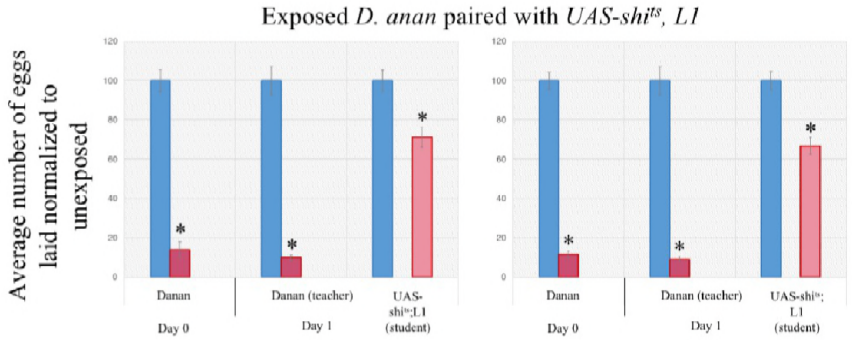

B

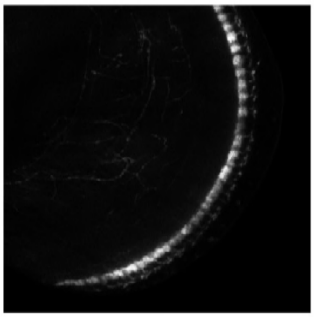

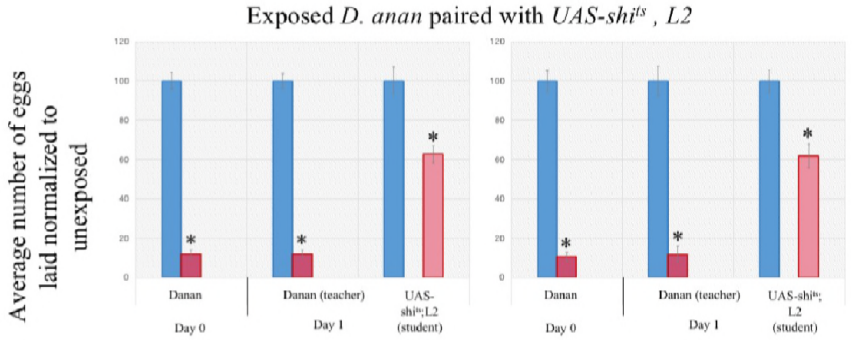

C

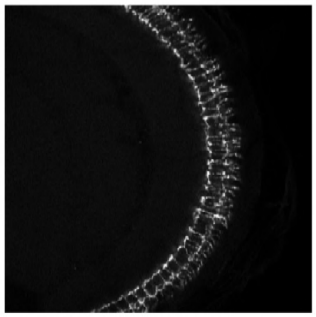

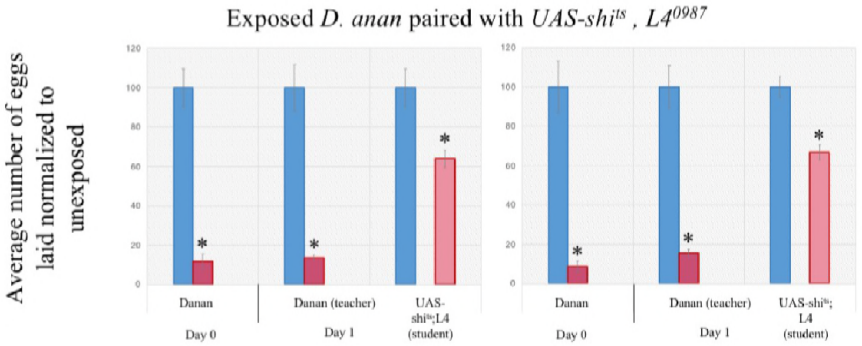

D

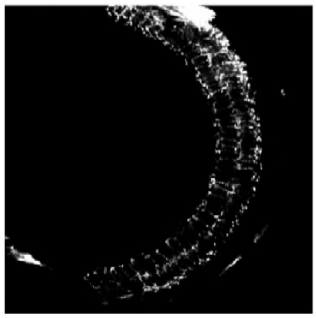

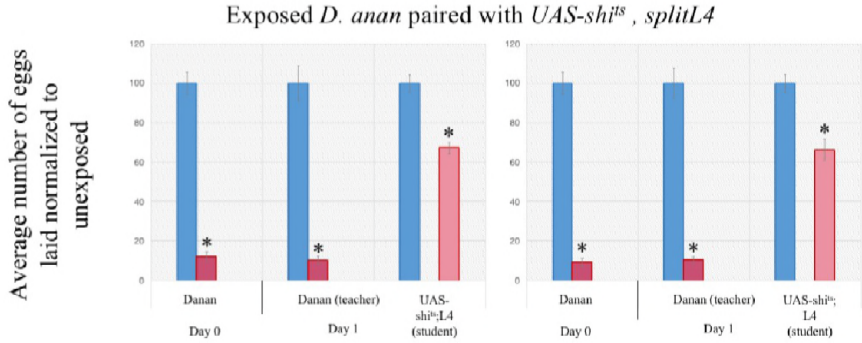

GFP

Restrictive Temperature Naïve

Permissive Temperature Naïve

Unexposed Exposed Naïve

Supplementary Figure 21. Further evidence implicating the role of motion-detecting circuitry in dialect learning using UAS Shi^{ts}.

Dialect learning is performed at either the permissive (22°C) or restrictive (30°C) temperature, while the wasp exposure and social learning period is performed exclusively at the restrictive temperature. Percentage of eggs laid by exposed flies normalized to eggs laid by unexposed flies is shown. (A) UAS-shi^{ts} crossed to *L1-GAL4* in the naïve state at restrictive and permissive temperatures shows wild-type naïve state. Expression pattern of *L1-GAL4* also shown. (B) UAS-shi^{ts} crossed to *L2-GAL4* in the naïve state at restrictive and permissive temperatures shows wild-type naïve state. Expression pattern of *L2-GAL4* also shown. (C) UAS-shi^{ts} crossed to *L4^{0987}-GAL4* in the naïve state at restrictive and permissive temperatures shows wild-type naïve state. Expression pattern of *L4^{0987}-GAL4* also shown. (D) UAS-shi^{ts} crossed to split*L4-GAL4* in the naïve state at restrictive and permissive temperatures shows wild-type naïve state. Expression pattern of split*L4-GAL4* also shown. Error bars represent standard error (n = 12 biological replicates) (*$p < 0.05$).

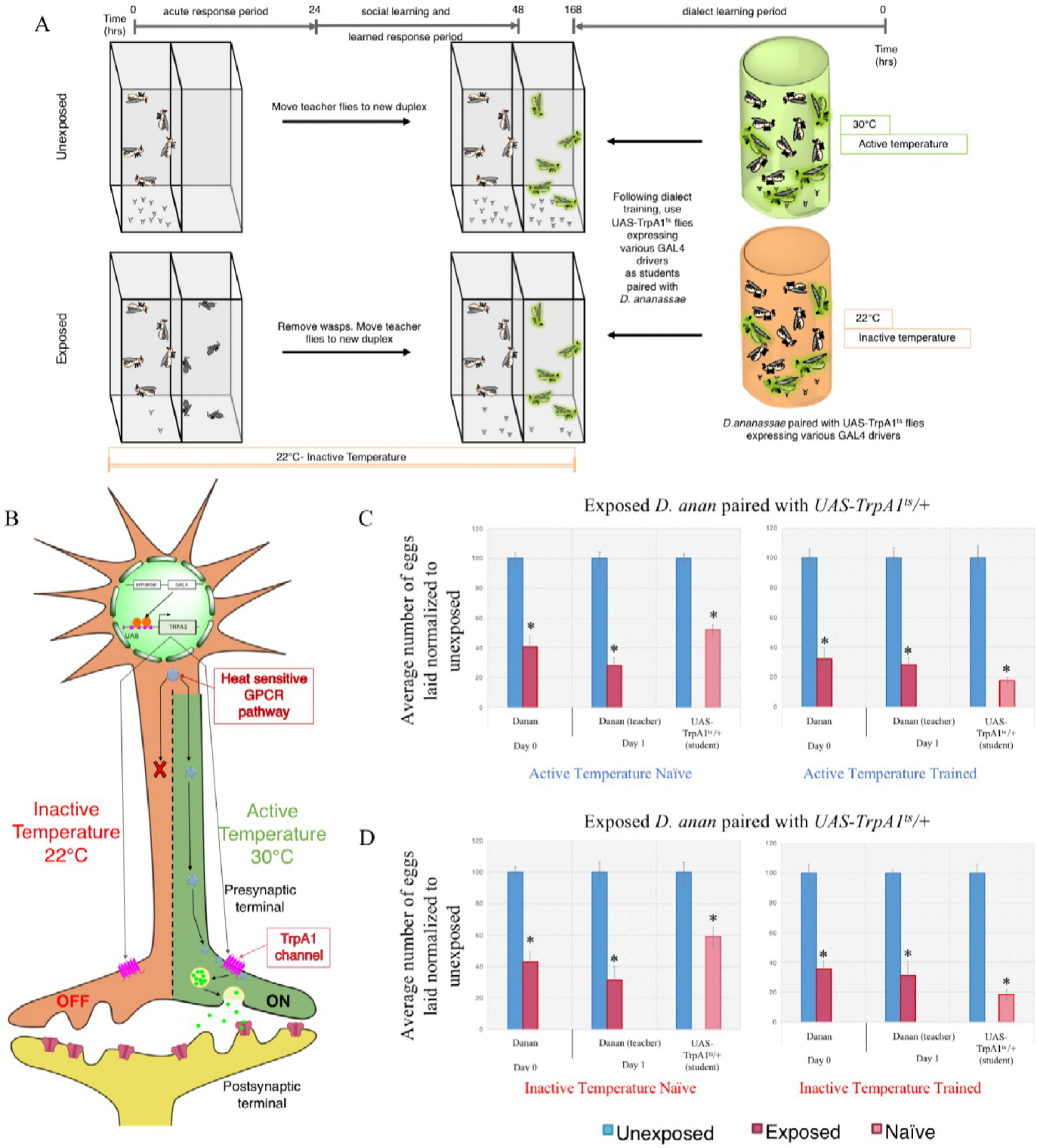
A
Time (hrs)
0
acute response period
24
social learning and
learned response period
48
168
dialect learning period
0
Time (hrs)
Unexposed
Move teacher flies to new duplex
30°C
Active temperature
Following dialect training, use UAS-TrpA1ts flies expressing various GAL4 drivers as students paired with D. ananassae
Exposed
Remove wasps. Move teacher flies to new duplex
22°C
Inactive temperature
D.ananassae paired with UAS-TrpA1ts flies expressing various GAL4 drivers
22°C- Inactive Temperature
B
Heat sensitive GPCR pathway
Inactive Temperature 22°C
Active Temperature 30°C
Presynaptic terminal
TrpA1 channel
OFF
ON
Postsynaptic terminal
C
Exposed D. anan paired with UAS-TrpA1ts/+
Average number of eggs laid normalized to unexposed
Danan
Danan (teacher)
UAS-TrpA1ts/+ (student)
Day 0
Day 1
Active Temperature Naïve
Active Temperature Trained
D
Exposed D. anan paired with UAS-TrpA1ts/+
Inactive Temperature Naïve
Inactive Temperature Trained
Unexposed
Exposed
Naïve

Supplementary Figure 22. Dialect learning can be analyzed using UAS-TrpA1^{ts}.

(A) Standard experimental design using UAS-TrpA1^{ts} in conjunction with various GAL4 drivers. Dialect learning is performed at either the inactive (22°C) or active (30°C) temperature, while the wasp exposure and social learning period is performed exclusively at the restrictive temperature. (B) Schematic of the UAS-TrpA1^{ts} expression in neurons, where the restrictive temperature turns on the neurons of interest in the absence of a given stimulus and the restrictive temperature does not affect these neurons. (C) Percentage of eggs laid by exposed flies normalized to eggs laid by unexposed flies is shown. UAS-TrpA1^{ts} outcrossed to *Canton S* trained by *D. ananassae* at either the permissive temperature (C) or the restrictive temperature (D) show wild-type dialect acquisition in both the naïve and trained states. Error bars represent standard error (n = 12 biological replicates) (*$p < 0.05$).

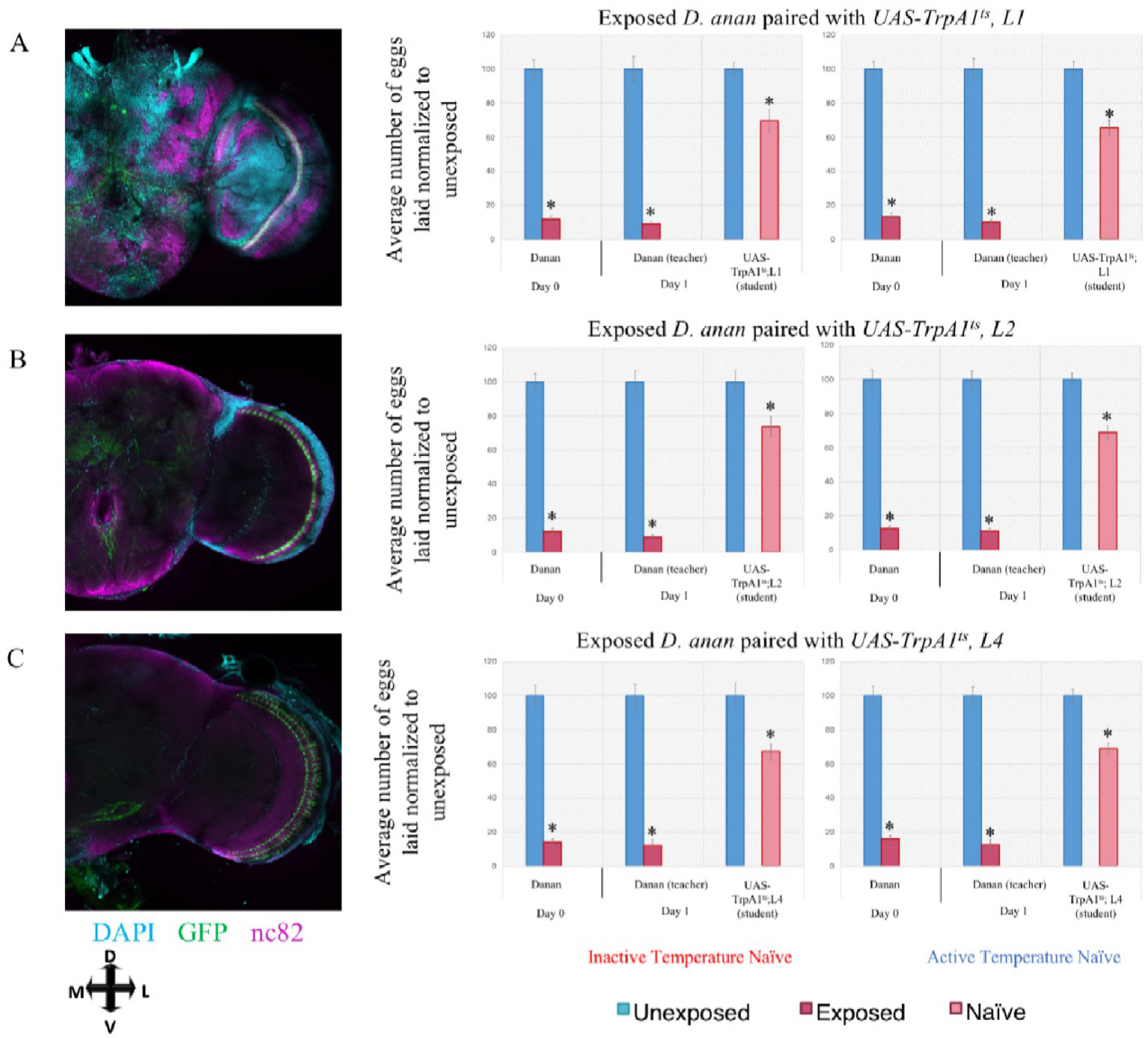
A
B
C
Exposed D. anan paired with UAS-TrpA1ts, L1
Exposed D. anan paired with UAS-TrpA1ts, L2
Exposed D. anan paired with UAS-TrpA1ts, L4
Average number of eggs laid normalized to unexposed
Danan
Danan (teacher)
UAS-TrpA1ts;L1 (student)
UAS-TrpA1ts; L1 (student)
UAS-TrpA1ts;L2 (student)
UAS-TrpA1ts; L2 (student)
UAS-TrpA1ts;L4 (student)
UAS-TrpA1ts; L4 (student)
Day 0
Day 1
Inactive Temperature Naïve
Active Temperature Naïve
Unexposed
Exposed
Naïve
DAPI GFP nc82
D
M
L
V

Supplementary Figure 23. Further evidence implicating the role of motion-detecting circuitry in dialect learning using UAS TrpA1.

Dialect learning is performed at either the active (30°C) or inactive (22°C) temperature exclusively in the dark, while the wasp exposure and social learning period is performed exclusively at the restrictive temperature. Percentage of eggs laid by exposed flies normalized to eggs laid by unexposed flies is shown. (A) UAS-TrpA1^{ts} crossed to *L1-GAL4* in the naïve state at restrictive and permissive temperatures shows wild-type naïve state. Expression pattern of *L1-GAL4* also shown. (B) UAS-TrpA1^{ts} crossed to *L2-GAL4* in the naïve state at restrictive and permissive temperatures shows wild-type naïve state. Expression pattern of *L2-GAL4* also shown. (C) UAS-TrpA1^{ts} crossed to *L4*^{0987}*-GAL4* in the naïve state at active and inactive temperatures shows wild-type naïve state. Expression pattern of *L4*^{0987}*-GAL4* also shown. Error bars represent standard error (n = 12 biological replicates) (*$p < 0.05$).

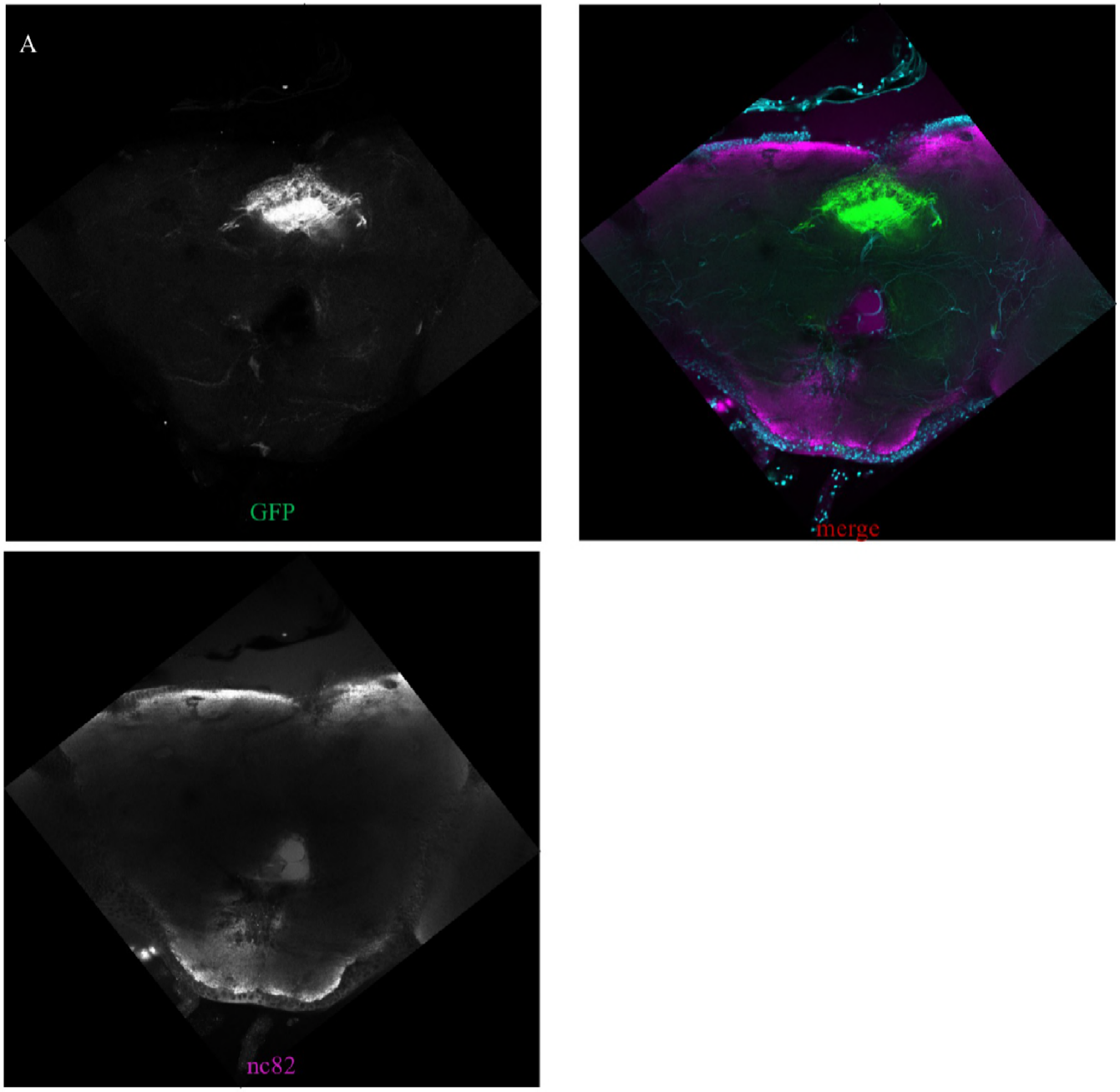
A
GFP
merge
nc82

Supplementary Figure 24. Expression pattern of the fan-shaped body driver line 39906.

(A) Confocal image of adult brain where 39906 is driving UAS-CD8-GFP, stained with nc82 (magenta) and DAPI (teal).

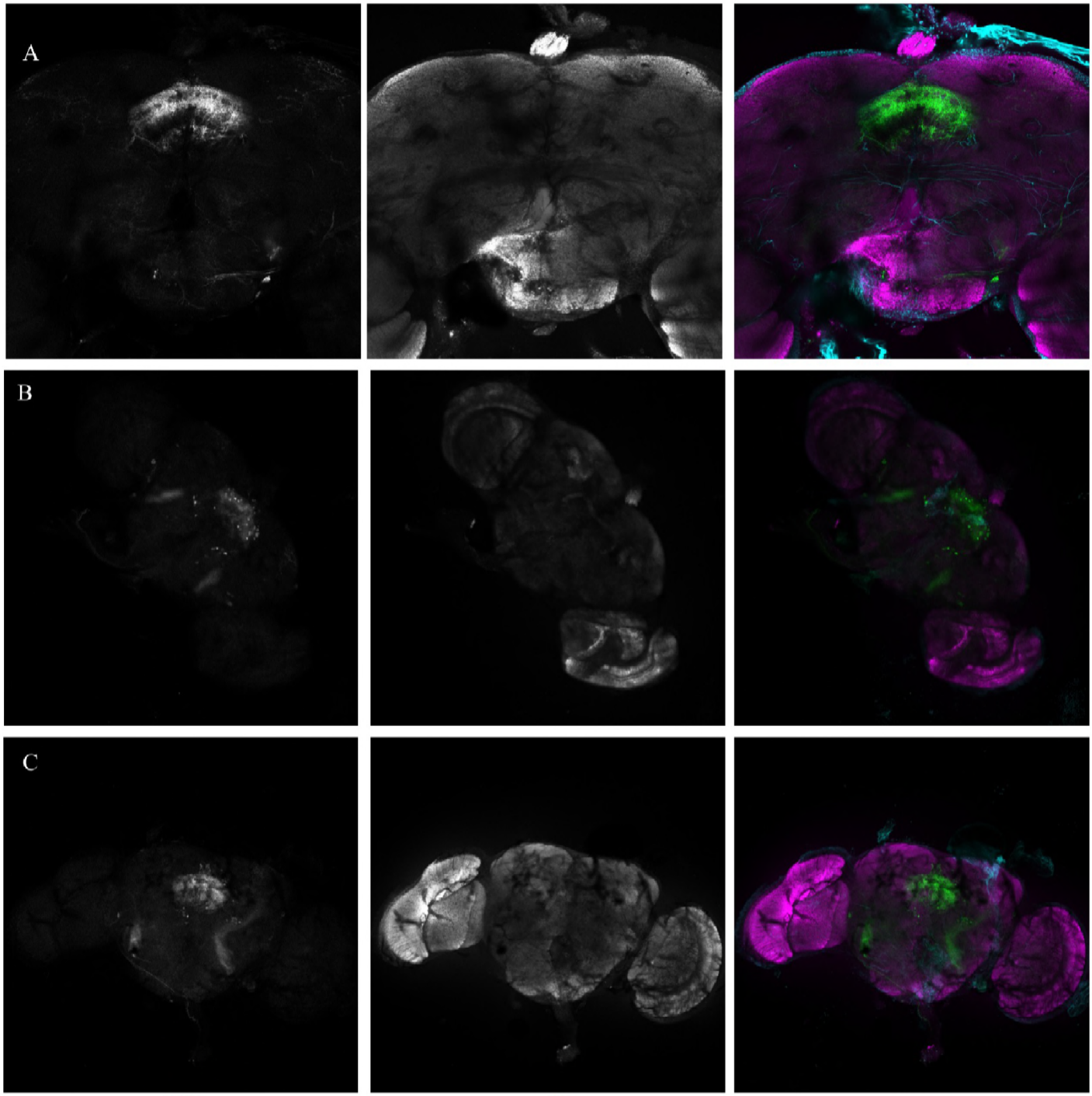
A
B
C
GFP
nc82
merge

Supplementary Figure 25. Expression pattern of the fan-shaped body driver line 50007.

(A-C) Confocal image of adult brain where 50007 is driving UAS-CD8-GFP, stained with nc82 (magenta) and DAPI (teal).

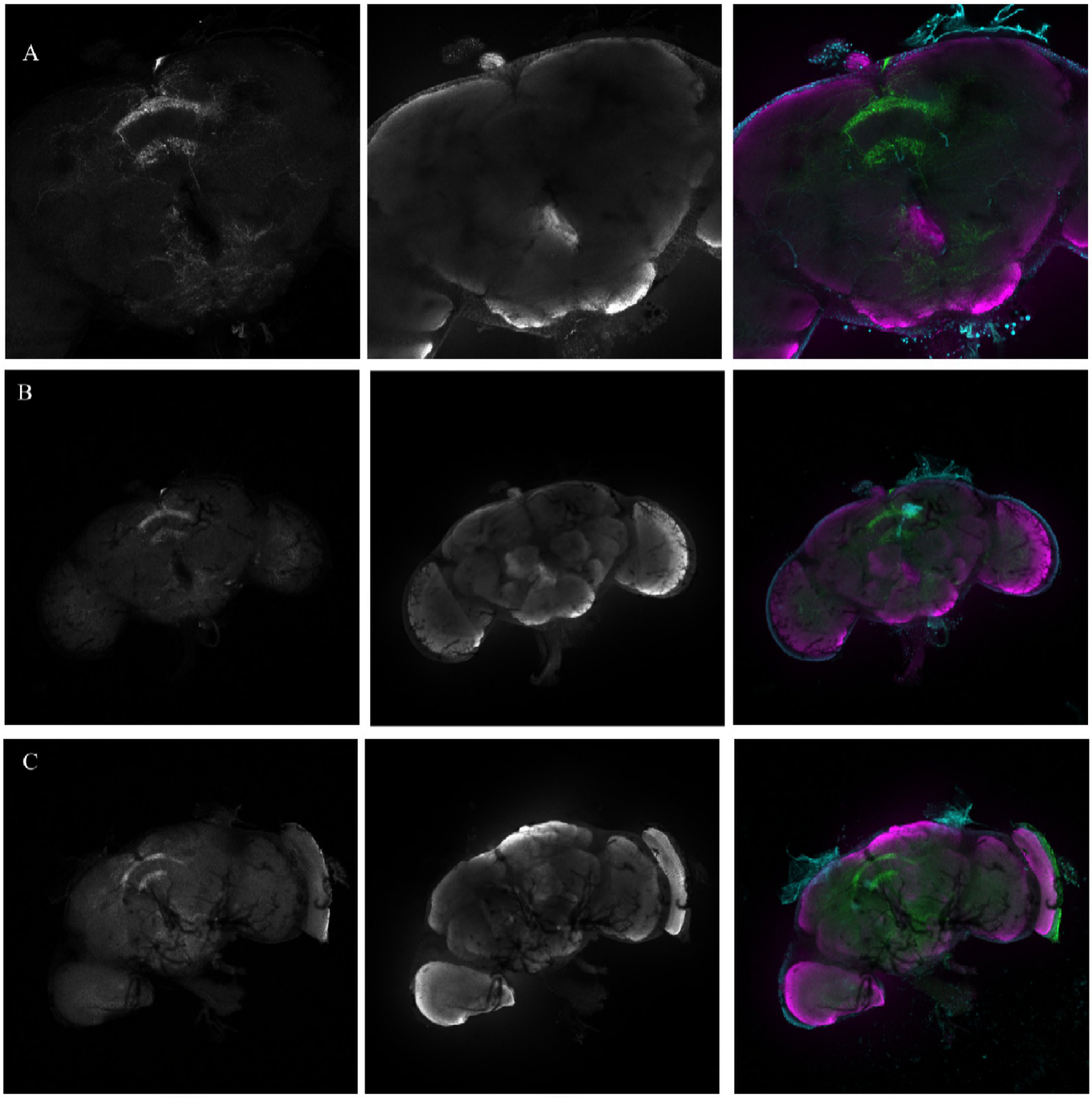
A
B
C
GFP
nc82
merge

Supplementary Figure 26. Expression pattern of the fan-shaped body driver line 40553.

(A-C) Confocal image of adult brain where 40553 is driving UAS-CD8-GFP, stained with nc82 (magenta) and DAPI (teal).

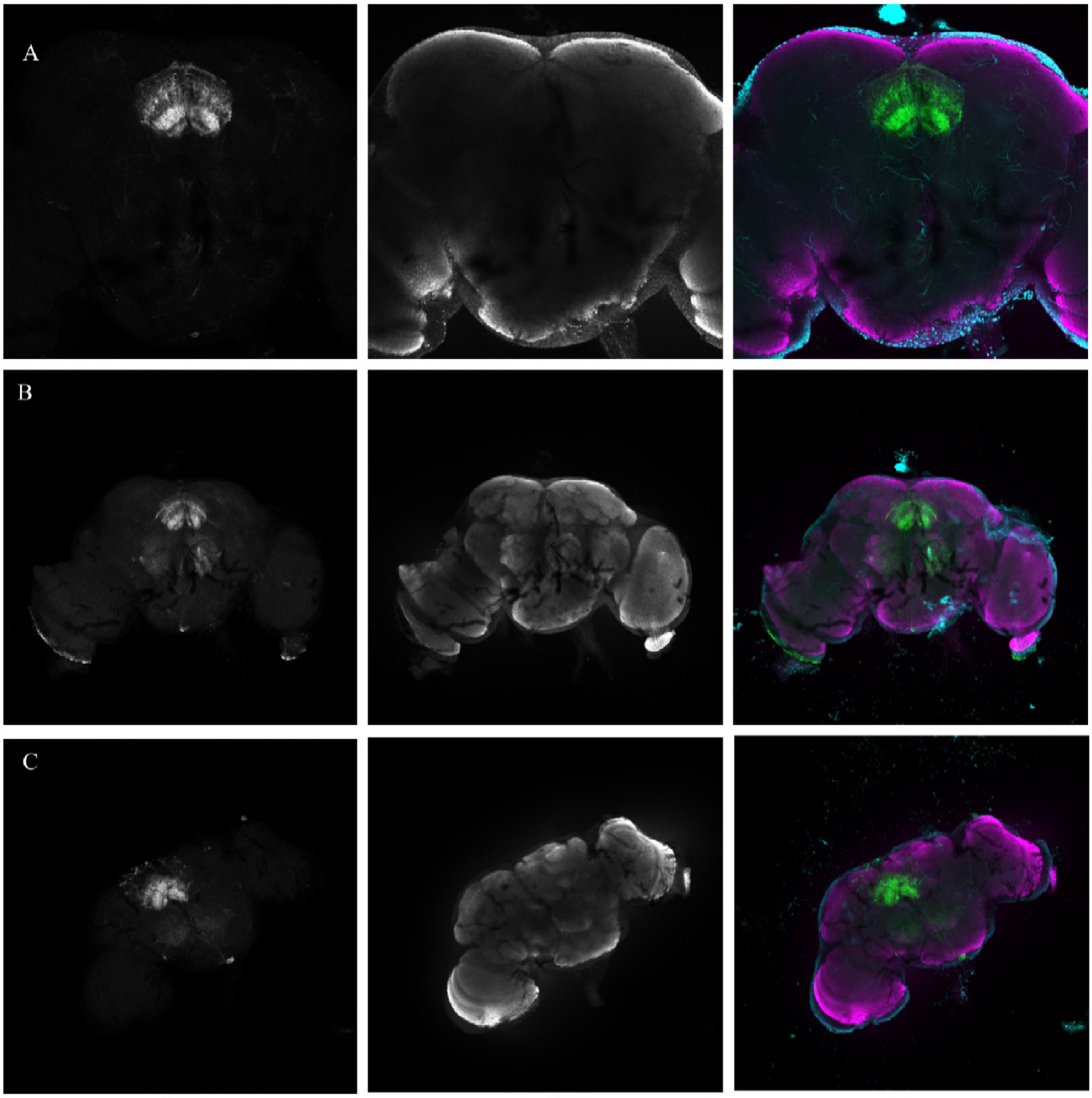
A
B
C
GFP
nc82
merge

Supplementary Figure 27. Expression pattern of the fan-shaped body driver line 38712.

(A-C) Confocal image of adult brain where 38712 is driving UAS-CD8-GFP, stained with nc82 (magenta) and DAPI (teal).

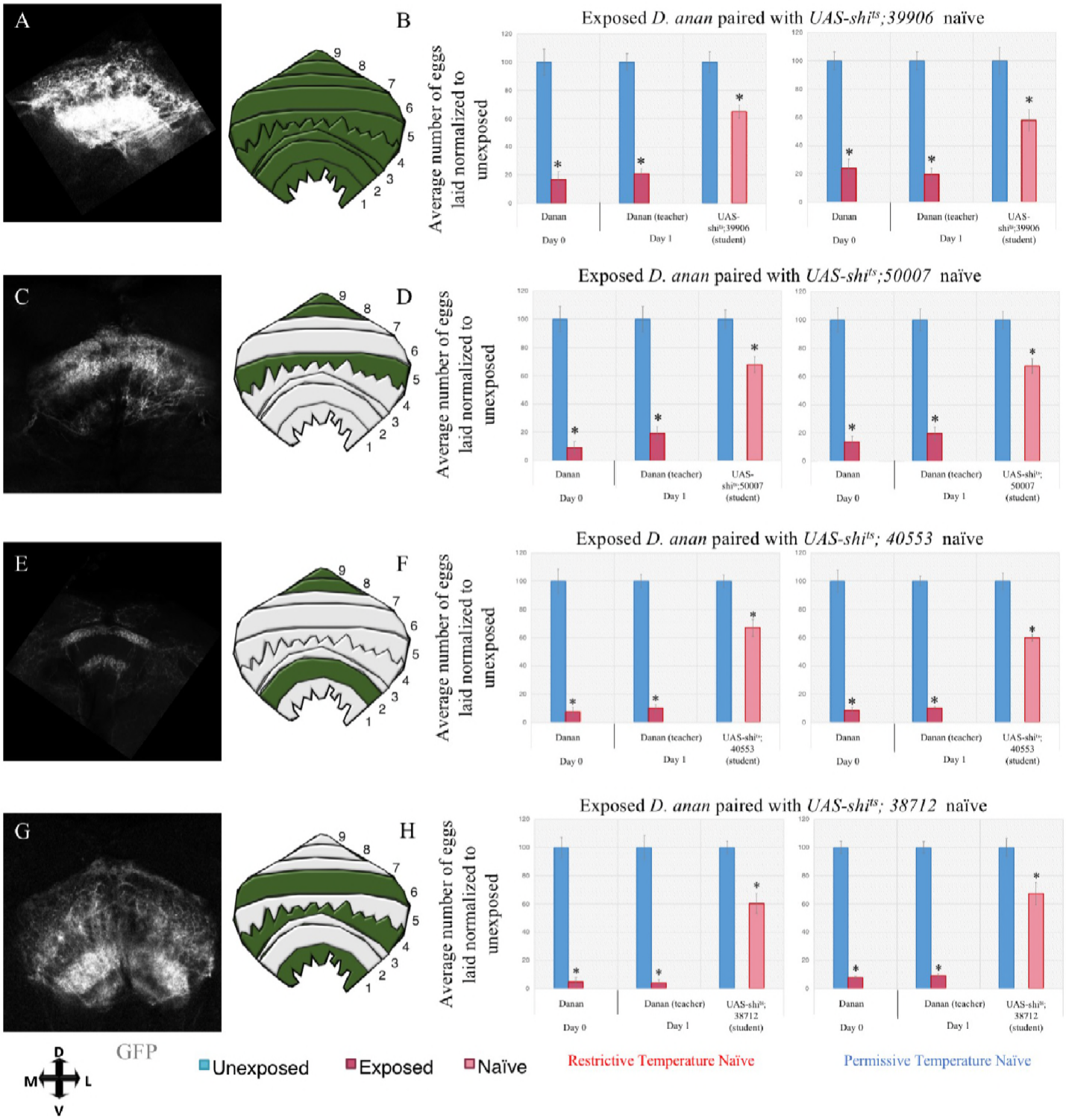
A
B
Exposed D. anan paired with UAS-shi^{ts};39906 naïve
Average number of eggs laid normalized to unexposed
Danan
Danan (teacher)
UAS-shi^{ts};39906 (student)
Day 0
Day 1
C
D
Exposed D. anan paired with UAS-shi^{ts};50007 naïve
UAS-shi^{ts};50007 (student)
E
F
Exposed D. anan paired with UAS-shi^{ts}; 40553 naïve
UAS-shi^{ts}; 40553 (student)
G
H
Exposed D. anan paired with UAS-shi^{ts}; 38712 naïve
UAS-shi^{ts}; 38712 (student)
GFP
D
M
L
V
Unexposed
Exposed
Naïve
Restrictive Temperature Naïve
Permissive Temperature Naïve

Supplementary Figure 28. Further evidence indicating that Region 5 of the fan-shaped body is necessary for dialect learning.

Dialect learning is performed at either the permissive (22°C) or restrictive (30°C) temperature, while the wasp exposure and social learning period is performed exclusively at the restrictive temperature. Percentage of eggs laid by exposed flies normalized to eggs laid by unexposed flies is shown. (A) Expression and schematic of expression pattern of the *39906* FSB driver shows pan-FSB marking. (B) UAS-shi^{ts} crossed to *39906* trained by *D. ananassae* at the permissive and restrictive temperature shows wild-type untrained state. (C) Expression and schematic of expression pattern of the *50007* FSB driver shows expression in regions 5, 8, and 9. (D) UAS-shi^{ts} crossed to *50007* trained by *D. ananassae* at the permissive and restrictive temperature shows wild-type naïve state. (E) Expression and schematic of expression pattern of the *40553* FSB driver shows expression in regions 2, 8, and 9. (F) UAS-shi^{ts} crossed to *40553* trained by *D. ananassae* at the permissive and restrictive temperature shows wild-type untrained state. (G) Expression and schematic of expression pattern of the *38712* FSB driver shows expression in regions 1, 4, and 6. (H) UAS-shi^{ts} crossed to *38712* trained by *D. ananassae* at the permissive and restrictive temperature shows wild-type naïve state. Error bars represent standard error (n = 12 biological replicates) (*$p < 0.05$).

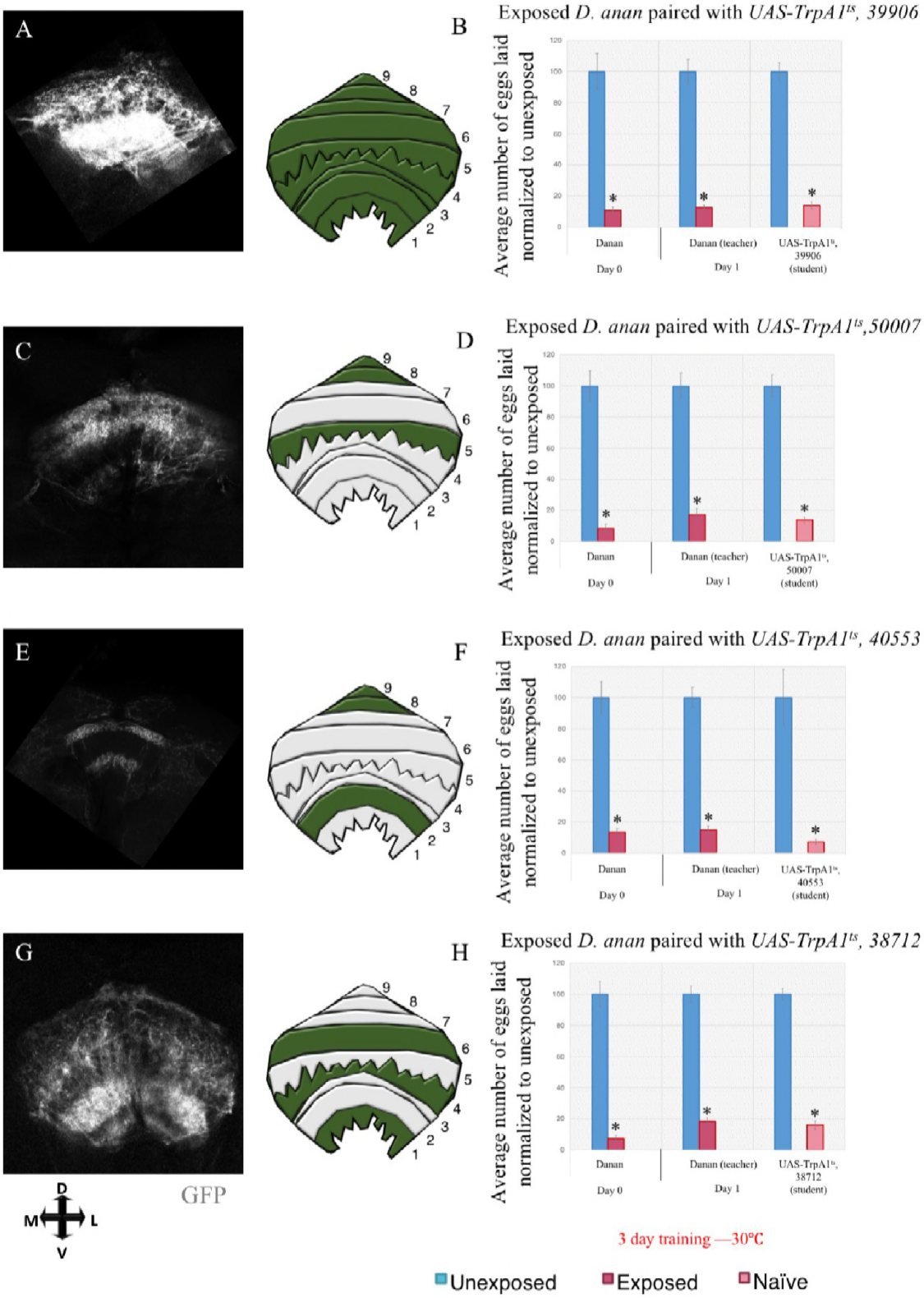
A
B
Exposed D. anan paired with UAS-TrpA1ts, 39906
Average number of eggs laid normalized to unexposed
Danan
Danan (teacher)
UAS-TrpA1ts, 39906 (student)
Day 0
Day 1
C
D
Exposed D. anan paired with UAS-TrpA1ts,50007
Danan
Danan (teacher)
UAS-TrpA1ts, 50007 (student)
E
F
Exposed D. anan paired with UAS-TrpA1ts, 40553
Danan
Danan (teacher)
UAS-TrpA1ts, 40553 (student)
G
H
Exposed D. anan paired with UAS-TrpA1ts, 38712
Danan
Danan (teacher)
UAS-TrpA1ts, 38712 (student)
GFP
D
M
L
V
3 day training —30°C
Unexposed
Exposed
Naïve

Supplementary Figure 29. Further evidence indicating that Region 5 of the fan-shaped body is sufficient for dialect learning.

Dialect learning for this experiment series is performed for 3 days at the active (30°C) temperature, while the wasp exposure and social learning period is performed exclusively at the restrictive temperature. Percentage of eggs laid by exposed flies normalized to eggs laid by unexposed flies is shown. (A) Expression and schematic of expression pattern of the *39906* FSB driver shows pan-FSB marking. (B) UAS-shi^{ts} crossed to *39906* trained by *D. ananassae* for 3 days at the permissive temperature shows wild-type trained state. (C) Expression and schematic of expression pattern of the *50007* FSB driver shows expression in regions 5, 8, and 9. (D) UAS-shi^{ts} crossed to *50007* trained by *D. ananassae* for 3 days at the permissive temperature shows wild-type trained state. (E) Expression and schematic of expression pattern of the *40553* FSB driver shows expression in regions 2, 8, and 9. (F) UAS-shi^{ts} crossed to *40553* trained by *D. ananassae* for 3 days at the permissive temperature shows wild-type trained state. (G) Expression and schematic of expression pattern of the *38712* FSB driver shows expression in regions 1, 4, and 6. (H) UAS-shi^{ts} crossed to *38712* trained by *D. ananassae* for 3 days at the permissive temperature shows wild-type trained state. Error bars represent standard error (n = 12 biological replicates) (*$p < 0.05$).

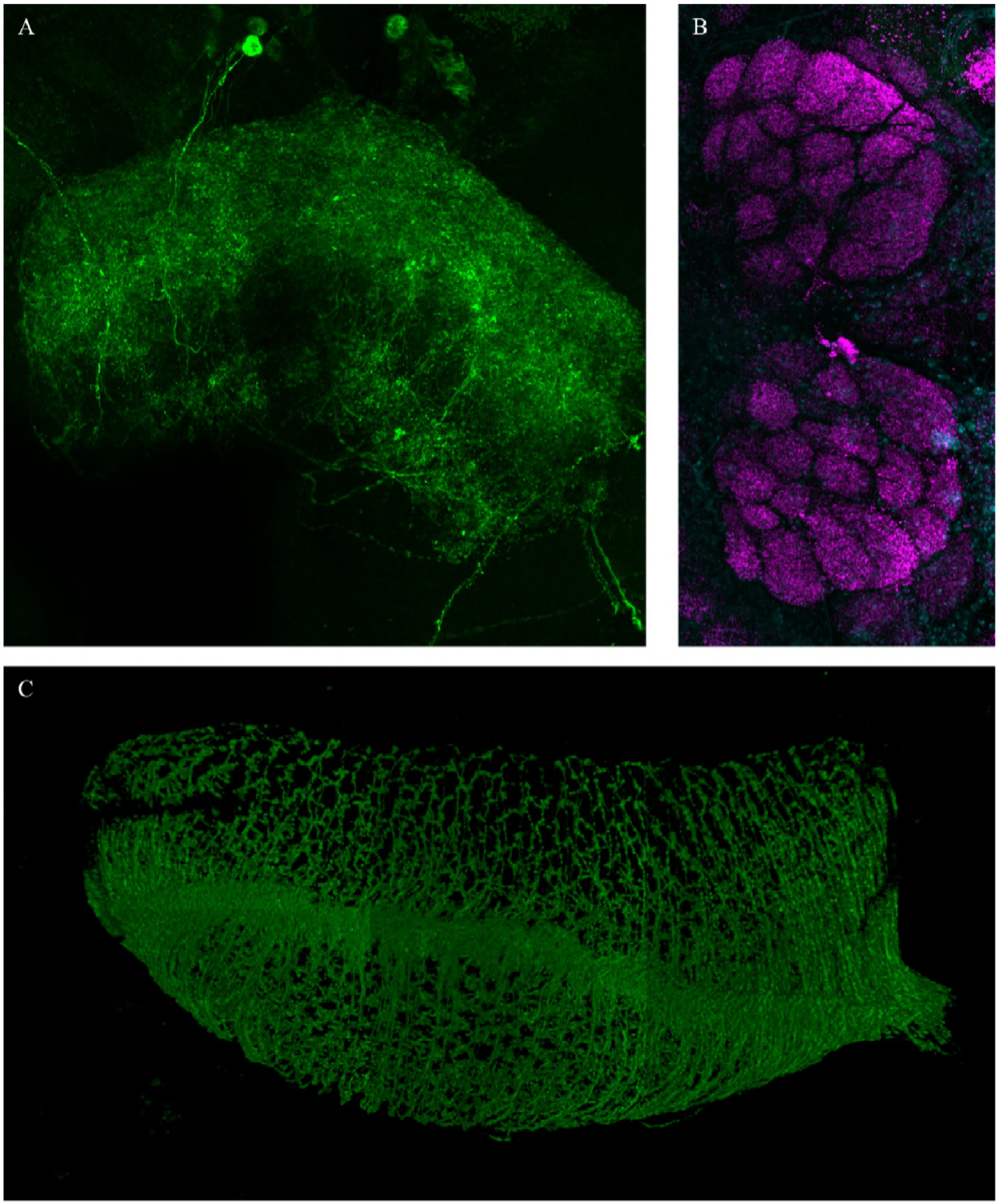
A
B
C

Supplementary Figure 30. Super resolution microscopy of key brain regions in dialect learning.

(A) Z-stack maximum intensity project super resolution image of driver line 50007 in conjunction with UAS-CD8-GFP. (B) Z-stack maximum intensity project super resolution image of the antennal lobe stained with nc82. (C) Z-stack maximum intensity project super resolution image of driver line $L4^{0987}$ in conjunction with UAS-CD8-GFP.

SUPPLEMENTARY TABLE LEGENDS

Supplementary Table 1. Name, genotype, acquisition location, and stock identification number (if applicable) are shown.

Gene/Allele	Genotype	Acquisition location	ID #
CS (WT control)	-	n/a	n/a
D. ananassae	-	Drosophila species stock center	14024-0371.13
L1 GAL4	w[+] (I); L1[c202a]Gal4 / (Cyo) (isoD1)	Marion Silies--European Neuroscience Institute	n/a
L2 GAL4	w[+] (I); L2[21Dhh]-Gal4 / TM6B (isoD1)	Marion Silies--European Neuroscience Institute	n/a
L4 GAL4	w (I); L4 [0987]-GAL4 / (CyO) (isoD1)	Marion Silies--European Neuroscience Institute	n/a
splitL4 GAL4	w (I); L4 [0987]-GAL4-F32.1-A30-dw (II); 0980-D33.1-A2-dw (III) (isoD1)	Marion Silies--European Neuroscience Institute	n/a
Or69a-GFP	w[*]; P{w[+mC]=Or69aA-Mmus\Cd8a.GFP}3	Bloomington Drosophila Stock Center	52636
Or65a-GFP	w[*]; P{w[+mC]=Or65a-Mmus\Cd8a.GFP}2	Bloomington Drosophila Stock Center	52631
Or47b-GFP	y[1] w[*]; P{w[+mC]=Or47b-CD2.M}3/TM3, Sb[1]	Bloomington Drosophila Stock Center	9915
Or47b-/-	y[1] w[*]; Mi{y[+mDint2]=MIC}Or47b[MI05132]	Bloomington Drosophila Stock Center	38008
Or47b[RNAi]	y[1] v[1]; P{y[+t7.7] v[+t1.8]=TRiP.JF02586}attP2	Bloomington Drosophila Stock Center	27274
Or47b[GAL4]	w[*]; P{w[+mC]=Or47b-GAL4.7.467}15.6	Bloomington Drosophila Stock Center	9984
Or69a-/-	y[1] w[*]; Mi{y[+mDint2]=MIC}Or69a[MI00896]	Bloomington Drosophila Stock Center	32714
Or69a[GAL4]	w[*]; P{w[+mC]=Or69a-GAL4.F}81.3	Bloomington Drosophila Stock Center	9999
Or65a[RNAi]	y[1] v[1]; P{y[+t7.7] v[+t1.8]=TRiP.JF02763}attP2	Bloomington Drosophila Stock Center	27683
Or65a[GAL4]	w[*]; P{w[+mC]=Or65a-GAL4.F}72.5	Bloomington Drosophila Stock Center	9993
Or69a[RNAi]	y[1] sc[*] v[1]; P{y[+t7.7] v[+t1.8]=TRiP.HMC05836}attP40	Bloomington Drosophila Stock Center	64962
UAS-TrpA1[ts]	w[*]; P{y[+t7.7] w[+mC]=UAS-TrpA1(B).K}attP16	Bloomington Drosophila Stock Center	26263
optic lobe-GAL4	w[1118]; P{y[+t7.7] w[+mC]=GMR10B01-GAL4}attP2	Bloomington Drosophila Stock Center	49234
optic lobe-GAL4	w[1118]; P{y[+t7.7] w[+mC]=GMR17F12-GAL4}attP2	Bloomington Drosophila Stock Center	48779
mushroombody-GAL4	w[1118]; P{y[+t7.7] w[+mC]=GMR13F02-GAL4}attP2	Bloomington Drosophila Stock Center	48571
mushroombody-GAL4	w[1118]; P{y[+t7.7] w[+mC]=GMR16A06-GAL4}attP2	Bloomington Drosophila Stock Center	48709
antenna lobe-GAL4	w[1118]; P{y[+t7.7] w[+mC]=GMR21C11-GAL4}attP2	Bloomington Drosophila Stock Center	47898
antenna lobe-GAL4	w[1118]; P{y[+t7.7] w[+mC]=GMR19H04-GAL4}attP2	Bloomington Drosophila Stock Center	48865
lateral horn-GAL4	w[1118]; P{y[+t7.7] w[+mC]=GMR10G01-GAL4}attP2	Bloomington Drosophila Stock Center	48270
fanshapedbody-GAL4	w[1118]; P{y[+t7.7] w[+mC]=GMR75G12-GAL4}attP2	Bloomington Drosophila Stock Center	39906
fanshapedbody-GAL4	w[1118]; P{y[+t7.7] w[+mC]=GMR38E07-GAL4}attP2	Bloomington Drosophila Stock Center	50007
fanshapedbody-GAL4	w[1118]; P{y[+t7.7] w[+mC]=GMR89E07-GAL4}attP2	Bloomington Drosophila Stock Center	40553
fanshapedbody-GAL4	w[1118]; P{y[+t7.7] w[+mC]=GMR58F03-GAL4}attP2	Bloomington Drosophila Stock Center	38712
ellipsoidbody-GAL4	w[1118]; P{y[+t7.7] w[+mC]=GMR11F03-GAL4}attP2	Bloomington Drosophila Stock Center	48464
ellipsoidbody-GAL4	w[1118]; P{y[+t7.7] w[+mC]=GMR15F02-GAL4}attP2	Bloomington Drosophila Stock Center	48698
bulb-GAL4	w[1118]; P{y[+t7.7] w[+mC]=GMR32B03-GAL4}attP2	Bloomington Drosophila Stock Center	49886
prow-GAL4	w[1118]; P{y[+t7.7] w[+mC]=GMR25G04-GAL4}attP2	Bloomington Drosophila Stock Center	49136
superiorclamp-GAL4	w[1118]; P{y[+t7.7] w[+mC]=GMR30F03-GAL4}attP2	Bloomington Drosophila Stock Center	49640
UAS-shi[ts]	w[*]; P{w[+mC]=UAS-shi[ts1].K}3	Bloomington Drosophila Stock Center	44222
CD8-GFP	UAS-CD8-GFP/Cyo	Mani Ramaswami	n/a

SUPPLEMENTARY MOVIE LEGENDS

Supplementary Movie 1. Expression pattern of the $L4^{0987}$ line in whole brain.

Super resolution confocal movie of adult Drosophila brain where $L4^{0987}$ GAL4 is driving UAS-CD8-GFP, stained with DAPI (teal) and nc82 (magenta).

Supplementary Movie 2. Expression pattern of the $L4^{0987}$ line in optic lobe.

Super resolution confocal movie of adult Drosophila brain where $L4^{0987}$ GAL4 is driving UAS-CD8-GFP, stained with DAPI (teal) and nc82 (magenta).

Supplementary Movie 3. Expression pattern of the fan-shaped body driver line 50007.

Super resolution confocal movie of adult Drosophila brain where 50007 is driving UAS-CD8-GFP, stained with DAPI (teal).

Supplementary Movie 4. Expression pattern of the fan-shaped body driver line 50007 in a magnified region.

Super resolution confocal movie of adult Drosophila brain where 50007 is driving UAS-CD8-GFP, stained with DAPI (teal).

SUPPLEMENTARY FILE LEGENDS

Supplementary Table 1. Raw egg counts and p values for figures used in this study. Each tab corresponds to a given panel series. Within tab contains the genotype of construct(s) used, raw egg counts, and p-values.